EFFECT OF THE HISTIDINE E7 AMINO ACID IN THE SULFHEME FORMATION OF THE HEMOGLOBIN I FROM LUCINA PECTINATA

by

Elddie Marie Román-Morales

A thesis submitted in partial fulfillment of the requirements for the degree of

MASTER OF SCIENCE
in
CHEMISTRY

UNIVERSITY OF PUERTO RICO
MAYAGÜEZ CAMPUS
2008

Approved by:

_____	_____
Marisol Vera, Ph.D. Member, Graduate Committee	Date
_____	_____
Robert Ríos, Ph.D. Member, Graduate Committee	Date
_____	_____
Juan López-Garriga, Ph.D. President, Graduate Committee	Date
_____	_____
Nilda E. Aponte, Ph.D. Office of Graduate Studies Representative	Date
_____	_____
Francis Patrón, Ph.D. Chairperson, Department of Chemistry	Date

Abstract

Sulfhemoglobin is a non-functional derivative of hemoglobin known to be produced by exposure to sulfa drugs, air pollution and others. It is formed by the reaction between H_2O_2, H_2S and the heme group in the presence of oxygen with the corresponding specific addition of sulfur to the pyrrole B of the heme. It is characteristic spectroscopic absorption is observed around 620nm. The intermediates in the reaction are the heme Fe ^{IV}=O ferryl species, known as Compound I and II. This complex is of immense importance in the medical community because it is one of the main forms of nonfunctional hemoglobin that produces anemia. This derivative is commonly observed in most hemeproteins with the exception of HbI, HbII, and HbIII, hemeproteins, from the clam *Lucina pectinata*. Studies performed over the years with these Hb's and H_2S in the presence of O_2 showed no formation of the sulfheme complex. Therefore, it is important to determine the chemical structure of the protein responsible for the formation of sulfhemoglobin. UV-Vis spectroscopic analyses were made on human Hb, HbI, HbII/HbIII, HbI PheE11Val, HbI GlnE7His, HbI PheB10His, HbI PheB10Val protein samples upon reaction with hydrogen sulfide and hydrogen peroxide, using horse heart myoglobin (Mb) as the control. Surprisingly, the only HbI mutant to form the sulfheme complex was HbI GlnE7His variant, evidenced by the formation of the 626nm band. These studies revealed that only heme proteins with histidine in the specific E7 position form the unique sulfheme derivative. However, the sulf$Mb_{(O2)}$ final product may co-exist with a six coordinated high spin species while the SHbI GlnE7His final product could co-exist with a low spin oxy complex, as show by Optical and ^{1}H NMR Spectra. In addition, the results indicated that neither compound I nor compound II play a significant role in the formation of the sulfheme derivative since HbI and HbII/HbIII, which form stable compound I and compound II, respectively, did not form the sulf species. Thus, it is suggested that if any ferryl species is involved in the formation of sulfheme complex, it should be the one where His in the E7 position interacts directly with the bound hydrogen peroxide, as in the hydroperoxy complex.

Resumen

La sulfhemoglobina es un derivado no-funcional de la hemoglobina producido por la exposición a drogas sulfáticas y contaminación ambiental, entre otros. Se forma a través de la reacción entre H_2O_2, H_2S y el grupo hemo con la correspondiente adición específica del azufre al pyrol B del grupo hemo. Su absorción espectroscópica característica se observa alrededor de 620nm. Los intermediarios involucrados en el proceso son las especies ferriles, mejor conocidas como Compuesto I y II. Este complejo es de suma importancia para la comunidad médica debido a que es una causante de anemia. Este derivado se observa comúnmente en la mayoría de las hemoproteinas, con la excepción de las hemoproteinas HbI, HbII y HbIII de la almeja *Lucina pectinata*. A través de los años, estudios de estas proteínas con H_2S en la presencia de oxígeno no demostraron la formación del complejo sulfhemo. Por tanto, es importante conocer la estructura química de la proteína responsable de la formación del complejo sulfhemo. Análisis de UV-Vis fueron realizados con hemoglobina humana, HbI, HbII, HbIII, y los mutantes: HbI PheE11Val, HbI GlnE7His, HbI PheB10His, HbI PheB10Val a través de la reacción con H_2O_2 y H_2S, utilizando a mioglobina (Mb) como el control. Sorprendentemente, el único mutante que formó el complejo sulfhemo fue HbI GlnE7His, mostrándolo a través de la banda 626nm. Estos estudios revelaron que solamente las hemoproteínas con histidina en la posición específica E7 formaron el complejo sulfhemo. Sin embargo, el producto final de $SMb_{(O2)}$ puede coexistir con una especie sexta coordinada de alto espin mientras que SHbI GlnE7His puede coexistir con un complejo oxy de bajo spin, como fue demostrado por espectroscopía óptica y ^1H RMN. En adición, los resultados indicaron que ni el compuesto I ni el compuesto II juegan un papel importante en la formación del derivado sulfhemo, debido que las hemoproteinas HbI, HbII /HbIII, con el complejo estable compuesto I y II, respectivamente, no formaron el derivado sulfhemo. Debido a que la HisE7 es necesaria para la formación del complejo sulfhemo, si una especie ferril juega un rol importante durante la formación del derivado sulfhemo, entonces es uno donde la HisE7 tiene interacción directa, como observada en el complejo hidroperóxido.

In life,
what sometimes appears to be the end,
it is really a new beginning
To my family, you are my rock, love, happiness, strength and peace

ACKNOWLEDGMENTS

I thank God and my family for their indescribable love and support, my parents, Freddie H. Román Avilés & Elba Iris Morales Medina, my brothers and sisters, Fredito, Humbertito, Iris, Elbita, Hortensia, Blanca and Freddie Alejandro . I wish to thank my mentor and role model, Dr. Juan López-Garriga, for always being there. I also wish to thank my thesis committee members Dr. Marisol Vera, Dr. Robert Ríos and Dr. Enrique Melendez for their guidance and support. Edgardo Jesus Quiñones Cruz for his incomparable love and support; and to my friends, Brenda Ramos, Samirah Mercado, Ruth Pietri, María Rodríguez, Laura Granell, Rosalie Ramos, Rosángela Rivera, Cacimar Ramos, and Héctor Arbelo; you are the true definition of friendship. To the Chemistry Department of the University of Puerto Rico in Mayagüez, and my partners from the laboratory and the Science on Wheels Educational Center. I am very grateful to all of these persons who helped me put together this work. I really appreciate the time and effort that each one spent into the multiple aspects of this study.

I acknowledge the support of the National Science Foundation (NSF) and Graduate and Undergraduate Students Enhancing Science and Technology (GUEST K-12) program for providing financial support.

Table of Contents

List of Tables

List of Figures

CHAPTER 1
Introduction

To stay alive and reproduce, living organisms use and transform energy from the environment. To do that, some obtain energy from nutrients and atmospheric oxygen. The specific globular proteins that transport and store oxygen through the human body are known as hemoglobins and myoglobins. Hemoglobin is a tetrameric protein in charge of the oxygen transportation where as myoglobin, a hemoglobin analogue, is a monomeric protein responsible for oxygen storage (Lehninger, 1993). Vertebrate's hemoglobins have a porphyrin iron complex (heme) as the prosthetic group. The structure of the prosthetic group shown in Figure 1.1, consists of four connected rings, each with a nitrogen atom, coordinated to a central iron atom. The iron atom is coordinated to the protein by a histidine residue called proximal histidine. The last coordination position of the iron, also known as the distal position, is occupied by a ligand, for example oxygen (Silfa, 1997).

Any alterations of the heme group could provoke fatal consequences. For instance, sulfhemoglobinemia is a blood disease that results from the reaction of hemoglobin with endogenous and/or exogenous hydrogen sulfide in the presence of oxygen and/or hydrogen peroxide forming a hemoglobin derivative known as Sulfhemoglobin (La Mar et al, 2000; Berzofsky et al 1971). It is not only found (under several conditions) in humans, but also in various organisms and animals including fish and chicken. Patients suffering from this condition, caused by exposure to high concentration of hydrogen sulfide, suffer a persistent cyanosis with normal blood count

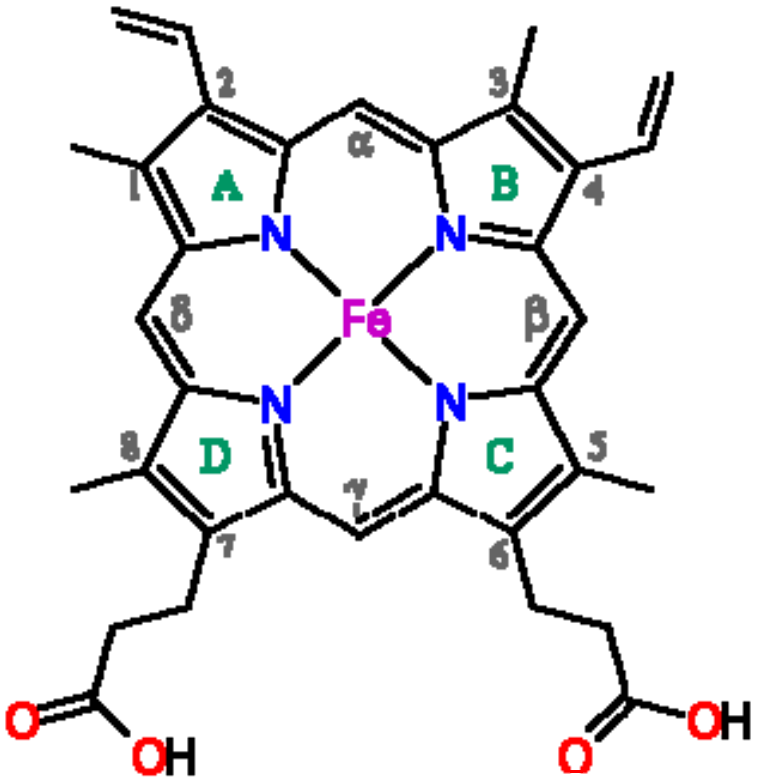

Figure 1.1 Structure of the prosthetic group.

that very often leads to death. This condition does not discriminate on age, therefore it has been found in adults as well as newborn babies and, sadly, its detection is difficult. Clinical methods used to fight this condition are: exposure to high oxygen concentrations, blood transfusions, gastric lavages, and methylene blue treatments. The use of these methods does not assure their survival (Hershman, et al., 1997, Tangerman, et al., 2002, Wu, 1997, Guidotti et al. 1994, Hayes, 1999).

Hydrogen sulfide is a toxic gas that at different concentrations can cause nausea, headaches, loss of appetite, drowsyness, and shortness of breath. It also decreases the body's ability to withstand infection. Eye irritation occurs at hydrogen sulfide concentration of 10 ppm while at 1,000 ppm, it impairs cellular respiration, brain and lungs function. Acute exposure to H_2S causes responses such as hyperpnoea, unconsciousness, apnea, and death (Almeida and Guidotti, 1999). In addition, a new controversial role is also emerging for hydrogen sulfide in the chemistry of biological systems. It has been found that hydrogen sulfide is synthesized endogenously in mammalian tissues and that at very low concentrations it functions as a neuromodulator, a smooth muscle relaxant, and a transmitter of informational signaling between cells (Kashiba et al., 2002, Eto et al., 2002, Kimura, 2002). The hydrogen sulfide has positive and negative effects depending on its concentration and the targeted proteins.

The reactivity of hydrogen sulfide toward hemeproteins to form the sulfheme complex, is known since 1863. Felix Hoppe-Seyler, was not only the first one to observe the absorption spectrum of hemoglobin (Hoppe-Seyler, 1862), but he also discovered that the reaction of hydrogen sulfide with oxyhemoglobin produced a new green hemoglobin derivative with a characteristic absorption band in the red region of the visible spectrum at 620 nm. He named this derivative sulfhemoglobin (Hoppe-Seyler, 1863). The

sulfheme complex has been studied over the years and it also ocurrs in myoglobin (Mb) generating the sulfmyoglobin complex which is analogous to the sulfhemoglobin.

The sulfheme complex derivative is different to the heme-H_2S complex in that the sulfur atom is not bound to the heme iron as the distal ligand. Reduction of sulfhemoglobin (sulfHb) followed by carbon monoxide and oxygen binding to the modified hemeprotein drove this conclusion (Michel, 1938). NMR experiments using ^{35}S demonstrated that only one sulfur atom per heme equivalent was present in the sulfheme complex (Chatfield, 1987). The suggested structure has been described as a chlorin with hydrogen sulfide added only across the β- β double bond of the specifically pyrrole "B" (Berzofsky et al., 1971, Berzofsky et al., 1972, Anderson et al., 1984, Magliozzo and Peisach 1986, Chatfield et al, 1987, Chatfield et al, 1988, Parker et al., 1989, Chatfield and La Mar, 1992).

Preparations of sulfmyoglobin have been found to be heterogeneous by ^1H NMR spectroscopy. ^1H NMR studies on sulfmyoglobin, in all oxidation/spin states, showed that depending on solution conditions, three different forms can be generated, labeled SMbA, SMbB, and SMbC, respectively. Figure 1.2 shows the more stable structures, which are SMbA and SMbC. SMbA is the first sulfheme isomer to form, which leads to the other two sulfheme isomers. It consists of a propyl ring, containing a sulfur atom, bound specifically to the pyrrole "B" of the heme group. The SMbB has a reduced pyrrole, but its structure is uncertain. SMbB does not lead to the SMbC isomer, instead it is considered a final product. SMbC consists of an exocyclic thiolene ring with a

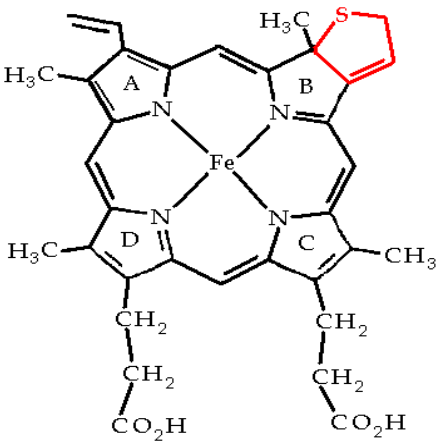

SMbC

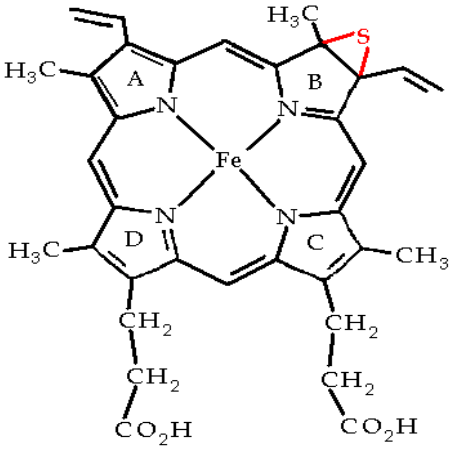

SMbA

Figure 1.2 Structure of the SMbA and SMbC isomers.

saturated 4-vinyl group. The structure of the sulfheme complex was later confirmed by X-Ray Crystallography (Evans et al, 1994) The oxidation/ligation state of the sulfheme species has been found to be reversible. The three isomeric sulfmyoglobin derivatives exhibit significantly different ligand affinity and chemical stability (Chatfield et al 1987, Chatfield et al, 1992).

Moreover, all the known facts regarding the formation of sulfhemoglobin apparently show a correlation with the presence of the ferryl species heme-compound I and II. The ferryl species are known intermediates in the physiological chemical reactions of hemoglobin and myoglobin. They are produced by the reaction of the heme protein with oxygen and/or hydrogen peroxide, however hydrogen peroxide accelerates the reaction. The ferryl species heme-compound I is a π-cation radical $[\text{heme}Fe^{IV}=O]^{\cdot+}$ complex while ferryl species heme-compound II is a $\text{heme}Fe^{IV}=O$ complex.

The sulfheme complex is easily observed in hemoglobin and myoglobin upon the reaction with hydrogen sulfide and oxygen (Berzofsky et al., 1971; Berzofsky et al., 1972; Anderson et al., 1984; Magliozzo and Peisach, 1986; Chatfield et al, 1987; Chatfield et al, 1988; Parker et al., 1989; Chatfield and La Mar, 1992; La Mar et al., 1997). However, other heme proteins such as the one from *Lucina pectinata* (hemoglobin I (HbI), hemoglobin II (HbII), and hemoglobin III (HbIII)) do not form the sulfheme derivatives in the presence of hydrogen sulfide and oxygen. The tropical clam *Lucina pectinata* contains these three hemoglobins with distinct physical-chemical properties. *L. pectinata* is an intriguing organism that lives in sulfide-rich environments and it hosts symbiotic sulfide-oxidizing bacteria that need to be supplied with both hydrogen sulfide and oxygen (Kraus and Wittenberg, 1990, Liberge et al, 2001). The

bacteria use this hydrogen sulfide to fix carbon dioxide into hexose for its food supply. The peculiar monomeric hemoglobin I is the hydrogen sulfide binding protein. The other two hemoglobins (HbII and HbIII), do not bind hydrogen sulfide; instead they deliver oxygen to the clam (Kraus and Wittenberg, 1990; Kraus et al., 1990). The proposed mechanism suggests that HbI reacts with hydrogen sulfide to form a heme Fe(III)-SH_2 low spin complex. Hydrogen sulfide is then transported to the bacteria symbiont and may be released upon formation of the ferrous protein by electron transfer from a still unknown reductant. Hemoglobin I is probably the only heme protein that performs its function in the hydrogen sulfide bound ferric state and in the oxygen bound ferrous state (Kraus and Wittenberg, 1990; Kraus et al., 1990). The X-ray crystal structure of met-aquo HbI (Rizzi et al., 1994) in Figure 1.3, shows that HbI has a histidine in the proximal position to the heme. However, the distal position E7 has a glutamine residue instead of a histidine, just as in elephant myoglobin. Figure 1.3 shows that in addition to the GlnE7 residue, HbI has the unusual PheB10 and the unique PheE11 residue. This aromatic environment may stand as the molecular basis for the very high affinity of HbI for hydrogen sulfide. The peculiar arrangement of phenylalanyl residues at the distal ligand binding site is unusual for hemoglobin and has not been observed before in the globin family. The affinity of hydrogen sulfide for ferric HbI is exceptionally high and is believed to be achieved through fast association (k_{on} = 2.3 x 10^5 $M^{-1}s^{-1}$) and very slow dissociation processes (k_{off} = 0.22 x 10^{-3} s^{-1}). The structural details of the active site of HbI with hydrogen sulfide have been revealed in part by crystal structure analyses of

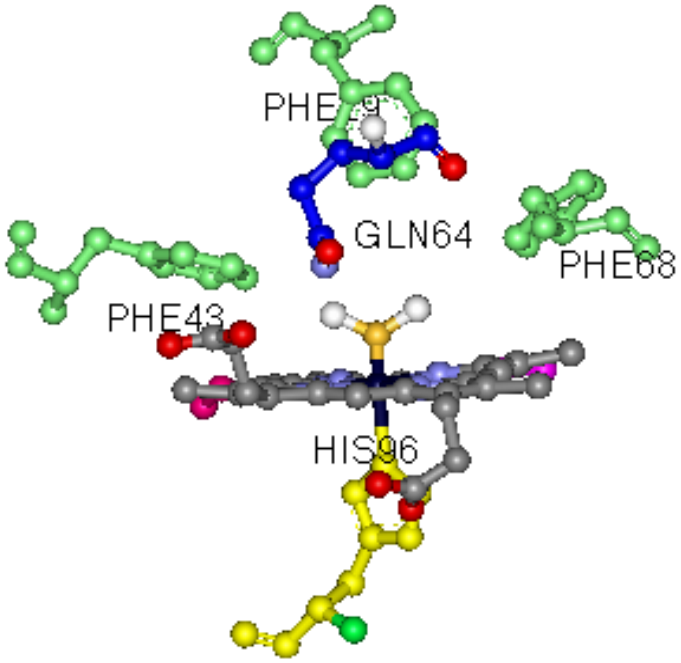

Figure 1.3 Active site of HbI.

HbI-H_2S complexes which suggested the possibility of a hydrogen bond between the heme-H_2S and GlnE7 (Rizzi et al., 1996). This hydrogen bond complex was used to explain the slow dissociation kinetics of the heme-H_2S species (Antommattei et al. 1999; Cerda et al., 1999; De Jesus et al., 2001; De Jesus et al., 2002; De Jesus et al., 2006; Kraus et al., 1990; Kraus et al., 1990; Leon et al., 2004; Lewis et al., 2006; Navarro et al., 1996).

Hemoglobin I shows the ability to stabilize the ferryl (heme Fe^{IV}=O) compound I a thousand times more than Mb (De Jesus et al 2001). A hydrogen bond between HisE7 and the ferryl species was suggested in Mb, which leads to the fast ferryl compound II formation. The stabilization of compound I in HbI suggests the lack of a hydrogen bonding interaction between this specie and GlnE7 due to the movement of this residue upon reaction of HbI with hydrogen peroxide. Figure 1.4 shows the hypothetical mechanism of ferryl compound I and II due to the reaction of HbI with hydrogen peroxide. Despite all these significant findings, a comprehensive understanding of the reactivity of the individual ferryl compound I and ferryl compound II with molecules, such as hydrogen sulfide, to produce sulfhemoglobin or sulfmyoglobin has not been established yet.

It is important to take advantage of the ability of HbI from *L. pectinata* to stabilize, through its unusual heme pocket configuration, the ferryl compound I a thousand times more than Mb. Understanding the structure and dynamics of the sulfheme derivative formation through the reactivity of Mb toward H_2O_2 and H_2S with those of the hemoglobins (HbI, HbII, and HbIII) from *Lucina pectinata* will lead us to understand the role of the ferryl species in the sulfheme formation. This will allow us to

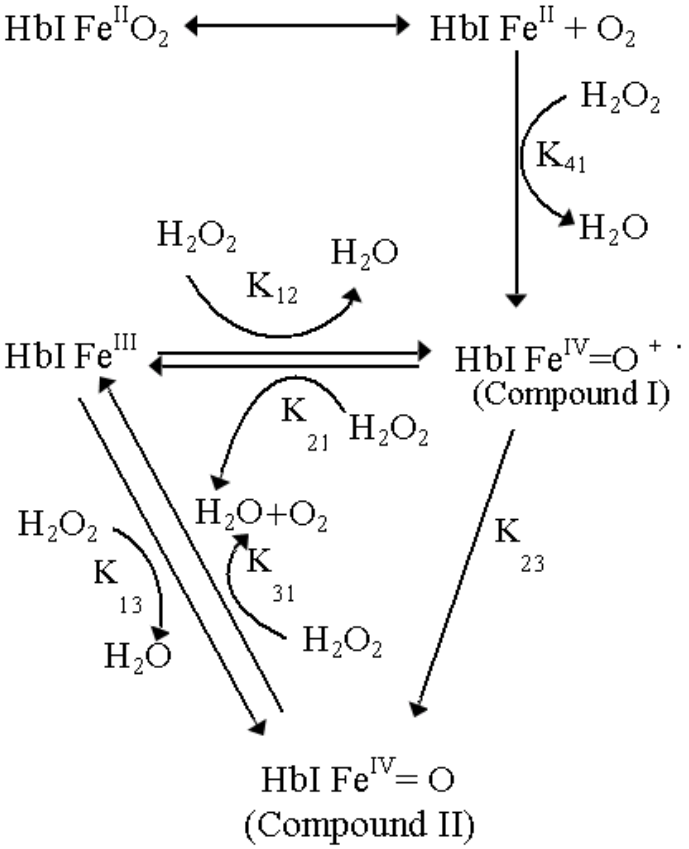

Figure 1.4 Hypothetical mechanism of ferryl compound I and II due to the reaction of HbI with hydrogen peroxide

apply this approach to a series of site directed HbI mutants, which will reveal how the active site structure influences the reaction with hydrogen sulfide, in the presence of hydrogen peroxide to form the sulfheme derivative.

The results will provide structural information about the chlorin and its environment upon its association in SulfHbI. ^{1}HNMR studies can clarify the interaction of a chlorin type arrangement with a H_2S group covalently bound to the "B" porphyrin-pyrrole β-β double bond. Also the data will allow to determine how the chemical nature of the active site amino acids affects the sulfchlorin properties and the possible metal-ligand coordination of the sulfheme complex. This will lead to the development of direct strategies for converting the inactive sulf-heme derivatives back to active, O_2 binding, native forms, possible resulting in treatment for various related human conditions.

CHAPTER 2
Materials and Methods

The desired hemeproteins from the clam *Lucina pectinata* were obtained by the procedures described in the literature (Read et. al. 1962; Krauss et. al. 1990; Navarro et. al. 1996), with some slight modifications. The procedur basically consists of four steps: extraction, homogenization, centrifugation and filtration of the material.

2.1 Extraction

Between 60 to 120 clams were collected from the sulf-rich muds at the Joyuda, Cabo Rojo, Puerto Rico. They were transported in seawater to the laboratory. After opening the clams, a purple-reddish organ known as ctenidia, was carefully dissected and immediately placed in a 4˚C ice-cold 10mM HEPES (N-2-hydroxyethylpiperazine-N'-2-ethanesulfonic acid), 5mM EDTA (ethylenediaminetetraacetic acid), and 1mM dithiothreitol buffer solution with a 7.5pH.

To homogenize the tissue, a CYCLONE I.Q. homogenizer SENTRY microprocessor of the Virtis Company was used at 6,000-14,000 rpm. After homogenization a solution of 1M triethanolamine was added to the mixture to maintain a 7.5 pH. Subsequently, the mixture was bubbled with carbon monoxide for about 15 minutes to maintain the sample stayed in the ferrous state.

To separate the insoluble particles of the tissue from the hemeproteins, the mixture was centrifuged at 19,000 rpm for 1 hour at 4˚C, using a BECKMAN J2-HS centrifuge with a JA-20 rotor from Bioanalytical Instruments. After centrifugation, the brown-reddish precipitant discarded. The bright reddish supernatant was then filtered

using a 0.45 μm WHATMAN filter. All the aextraction procedures were performed at 4˚C.

2.2 Purification of the Hemeproteins (HbI, HbI mutants)

The techniques used for the protein purification are based one of size and ionic properties differences, as described in the literature (Krauss et al. 1990; Silfa et al. 1997), utilizing an AKTA Fast Performance Liquid Chromatography Instrument from Amersham Bioscience. The FPLC was equipped with an UV-Vis lamp and a Frac-950 collector.

2.3 Size Exclusion Chromatography (wild type sample)

5mL of the bright reddish filtered protein mixture were passed through a Size Exclusion Chromatography HiLoad^{TM} 26/60 Superdex^{TM} 200 pre grade column from Amersham Bioscience with a matrix of dextran, covalently bound to highly cross-linked agarose. The proteins are separated by their differences in molecular size when passed through the gel filtration column, using a 7.5 pH buffer solution of 50mM Phosphate and 0.5mM EDTA at a flow rate of 1.5 mL/min under 0.3 MPa pressure.

The resulting elution profile fractions were collected in a Frac-950 fraction collector. Figure 2.1 shows the elution profile, where the first two proteins to exit the column were obtained in a mixture due to the similar molecular sizes. These proteins were HbII and HbIII with molecular sizes of 17,476 and 18,068 Dalton, respectively (Sanoget et. al. 2000). The second elution was also a mixture, which was retained in the column due to the smaller molecular sizes. It contained HbI, with a molecular size of 14,862 Dalton and a protein, rich in cysteine. In order to determine and select the best fractions for both mixtures, HbI/Cys and HbII/HbIII, photometric chromatogram at

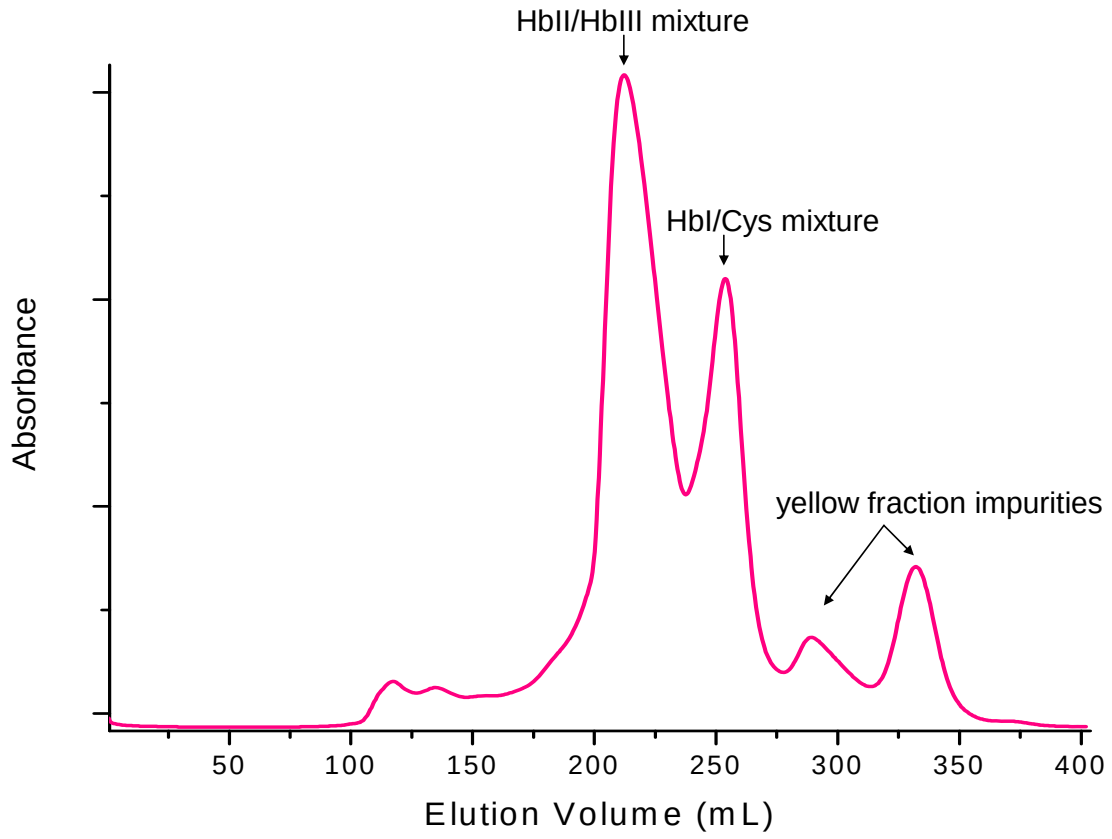

Figure 2.1 Elution profile of the Size Exclusion Chromatography at 280nm for the separation of HbI from HbII and HbIII.

280nm wavelength was done using a UV-Vis lamp in the FPLC instrument, monitoring the presence of all the proteins. All the FPLC procedures and chromatograms visualizations were controlled using a Unicorn 4.0 Software installed in the FPLC Computer. After all the eluted fractions were collected in the Frac-950 collector, the selection of the desired fraction of protein mixture, was made using the Unicorn 4.0 Software chromatogram which monitores all the molecules by their absorbance and conductivity. Each selected fraction was concentrated separately by pressure filtration at 4˚C, using Nitrogen as the pressure gas and a YM-10 membrane, with a molecular range of 10000 in an AMICON ultrafiltration cell. The solvent for both fractions was changed to 0.1 M sodium phosphate buffer with a 7.0 pH, and stored at approximately 50˚C to assure the stability and lifetime of the hemoglobins.

2.4 Purification of HbI

To separate HbI from the cysteine rich protein, an Ion Exchange Chromatography Technique was used, taking advantage of their different ion charge properties. The cysteine rich protein has a high concentration of a sulfur group, resulting in a protein with negative charge. The elution of the protein from the column results from the constant switch between the buffer solution and the proteins. For that reason, a weak anion exchanger known as DEAE was used. The cysteine rich protein was expected to remain more time within the column, thus resulting in the separation of the HbI from the cysteine rich protein.

A Sephadex A-50 column from Amersham Bioscience was previously equilibrated with an 8.3 pH 0.025 M ammonium bicarbonate buffer at a flow rate of 1.0mL/min until the column reached a pH of 8.3. Before injecting the sample, the sample

solvent was changed to the buffer from the column separation procedure. The protein separation was developed using an AKTA UPC-900 FPLC instrument and a Frac-950 fraction collector, from Amersham Pharmacia Biotech. The photometric chromatograms were obtained using an UV-Vis lamp at 280nm wavelength. Figure 2.2 shows the elution of HbI from the column followed by the elution of the cysteine rich protein. The HbI fraction was concentrated by using a pressure filtration process. This was done at 4˚C using Nitrogen as the pressure gas and a YM-10 membrane with a molecular range of 10000 in an AMICON ultrafiltration cell. The solvent was changed to 0.1 M sodium phosphate buffer with a pH of 7.0.

2.5 Hemoglobin's Mutant Preparation

One way to study and understand the relationship between the structure and function of any molecule is by changing a specific part of molecule structure and observing the change in function, and dynamics of the molecule. For that reason, the use and expression of Site Direct Mutagenesis is very appropriate for the analysis of the structure, function and dynamic relationships within the hemoglobin's heme pocket. As a result, it is possible to determine what part of the structure (which particular amino acid in particular) is responsible for the formation of the sulfheme protein.

The procedure for obtaining a particular HbI mutant consisted of four steps: cloning, large scale expression, lysis, and purification. To understand the relationship between structure, function and dynamics of the sulfheme proteins formation, each amino acid at the E7, B10, E11 positions of the HbI heme pocket was individually and specifically changed to the correspondent amino acid in the Horse Heart Myoglobin.

Horse Heart Myoglobin was used and considered as the control throughout the

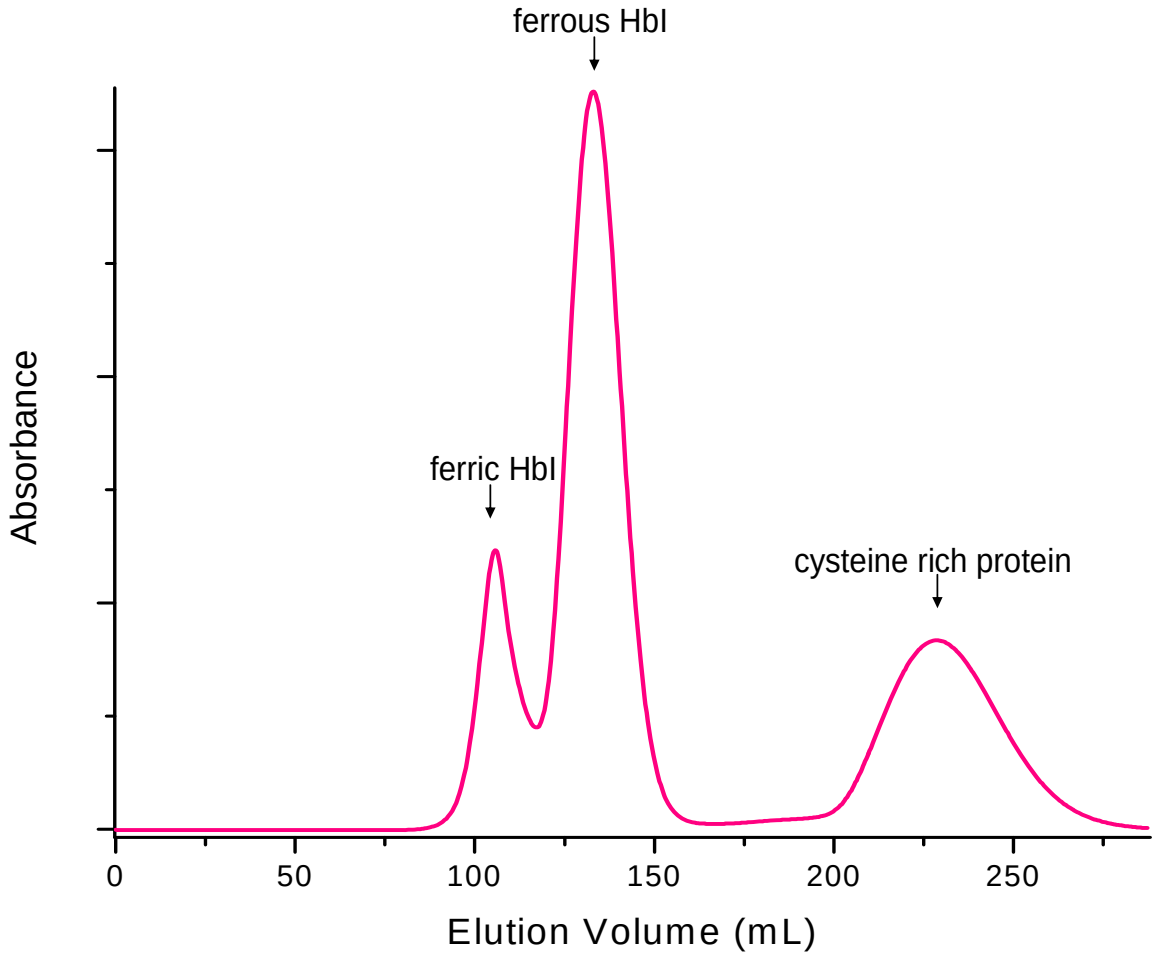

Figure 2.2 Ion Exchange Chromatography elution profile at 280nm for the separation of HbI from the cysteine rich protein.

study. The creation of the HbIPheE11Val, HbIGlnE7His and HbIPheB10His mutants were produced according to Leon et al., 2004. The biomolecular laboratory of Dr. Carmen Cadilla, at the Medical School Canpus of the University of Puerto Rico, provided the *E. coli* Bli5 competent cells with the plasmid of the specific HbI mutant. To assure their lifetime, cultures were prepared immediately and stored in frozen stokes at -80˚C in a 50% sterile glycerol.

2.6 Large Scale Expression of the HbI mutants

The procedures for the Large Scale Expression were applied as reported in the literature (Leon et. al. 2004), with slight modifications. The solutions used for in the fermentation were: 300mL of 50% w/v glucose, 500mL of 1.5 monobasic potassium phosphate, 500mL of 30% w/v ammonium hydroxide, 5mL of 1mM IPTG, 500mL of Terrific Broth Medium with 30µg/mL of chloroamphenical and 70µg/mL of kanamycin, and a solution of 0.17M KH_2PO_4 with 0.72M K_2HPO_4. All solutions, except the ammonium solution, were sterilized at a temperature of 120˚C for 20 minutes. For the fermentation process a Bioflo 110 Modular Benchtop Fermentator was used and prepared with 4L of Tb medium and 15mL of glycerol. The vessel was sealed with the exception of an exhaust to avoid an explosion. The exhaust had at the end, a 0.20µm autoclavable millex vent filter unit from Millipore covered with foil paper to limit the possibility of contamination. After filling the vessel jacket with water, the vessel was placed in a Sanyo Labo Autoclave for sterilization at 121˚C for 1 hour. The glassware and equipment used during this process were cleaned and also sterilized for 20 minutes at 121˚C using a Market Forge Sterilmatic.

The selected frozen stock cells of the specific mutant were transferred 24 hours before the fermentation to a 50mL previously prepared TB medium and incubated at 120-150rpm in a Precision Reciprocal Shaking Bath from Precision Scientific, at 37˚C for 12 hours. After the first 12 hour of incubation, the 50mL cell culture was transferred to 450mL of the TB medium and incubated for another 12 hours under the same conditions. Prior to the fermentation, the vessel was removed from the autoclave, where it was kept to avoid possible contamination.

Five hundred mL of the previously prepared phosphate solution, 30µg/mL chloramphenicol, 70 µg/mL kanamycin, 500 µL antifoam solution and 75mL of 50% w/v glucose were added to the vessel when the desired temperature reached 37˚C. Subsequently, the pH and dissolved oxygen sensors were placed and calibrated according to the Fermentator manual. The software was programmed to maintain a pH of 7.0 and 100% of oxygen in the media. Then 25mL of the media were collected to be use as a reference to subsequently quantify and evaluate cell growth every 30 minutes during the fermentation process measuring the optical density at the 600nm. The 450mL cell culture of the last 12 overnight hours was added to the vessel media to inoculate. Immediately, 3mL aliquot of the inoculated media was collected and an OD_{600} was taken. Another 75mL of the 50% w/v glucose solution were added after inoculation. When bacterial growth reached the lag phase as indicated by measurements of constant growth, 5mL of 1M IPTG were added to induce the protein expression. The solution of 33mg/mL hemin chloride in ammonium hydroxide was also added as needed. The extraction process of the culture from the vessel was initiaded when the measurements of the bacterial growth were constant, known as the lag phase. The culture was collected in a 500mL Beckman

bottle and centrifuged at 4˚C and 4000 rpm for 20 minutes, using a Beckman J2-HS Centrifuge. The supernatant was decanted and discarded; the remaining pellet was store.

2.7 Lysis of the cell

After the large scale expression process, the desired protein was separated from the cytoplasm of the bacteria by lysis or cell breakage. The sterilized buffer used to re-suspend the pellet was Native Binding Buffer (NBB), consisting of 58mM dibasic sodium phosphate, 17mM monobasic sodium phosphate and 68mM sodium chloride. The quantity of NBB necesary to re-suspend the pellet depended on the weight of the pellet; for every 35 g of cells, 90mL of NBB were added. In addition, 1mg of Chicken Egg White Lysozyme was added for every gram of bacteria cell, and incubated for 45 minutes on ice with sporadic stirring. For every 100mL of NBB, 20µL of protease inhibitor were added to minimize the degradation of the protein. Five periods of 75 seconds of 25% intensity sonification, with 45 resting seconds, were applied to break the cell membrane. The lysate was centrifuged at 18000rpm for 1 hour at 4˚C. The pellet was discarded and the supernatant stored.

2.8 Purification of the HbI mutants

To separate the desired HbI mutant from other proteins produced by the bacteria, two chromatographic processes were conducted: affinity and size exclusion chromatography. The previously describe purification process was applied.

2.9 Affinity Chromatography

The affinity method used for the purification of the HbI mutant was based on the interaction between the desired mutant with a metal affinity resin, BV Talon^{TM} from Clonetech. This resin involves a tetradentate chelator of Cobalt (II) in a sepharose bead.

This metal is polyhistidine-tagged selective, therefore binding to the polyhistidine-tagged HbI mutant, thus separating the mutant from other proteins.

A Tricorn 10/100 column from Amersham was utilized for the process. The column was filled with 8-10mL of resin, which made 1column volume (CV) of the total column. Following the instruction manual, the column was equilibrated at a 5.0mL/min flow. It contained 10CV of the 7.0 pH equilibrating buffer (50mM sodium phosphate and 300mM sodium chloride).

To assure the removal of impurities before the column purification, the lysate was centrifuged again at 4˚C and 18000 rpm for 30 minutes and filtered using a 0.45µm syringe filter. To start the purification process, 20mL of the lysate at a 1.0mL/min flow were injected into the column. A wash buffer was used for the removal of all weakly attached proteins in the resin column. This 7.0 pH wash buffer consisted of 50mM sodium phosphate, 300mM sodium chloride and 10mM imidazole. To elute the mutant species from the column, an elution buffer of 50mM sodium phosphate, 300mM sodium chloride and 150mM imidazole at a pH of 7.0 was used. Photometric chromatograms at 280nm wavelength were obtained using an UV-Vis lamp in the FPLC instrument, which monitored the presence of all the proteins.

Protein fraction selection and collection were made using the Unicorn 4.0 Software chromatogram, which monitores all molecules by their absorbance and conductivity. The Figure 2.3 demonstrates the elution profile by Metal Affinity Chromatography at 280nm for the separation of HbI mutant from impurities, where one can observe the elution of the impurities was observed first followed by the desired protein.

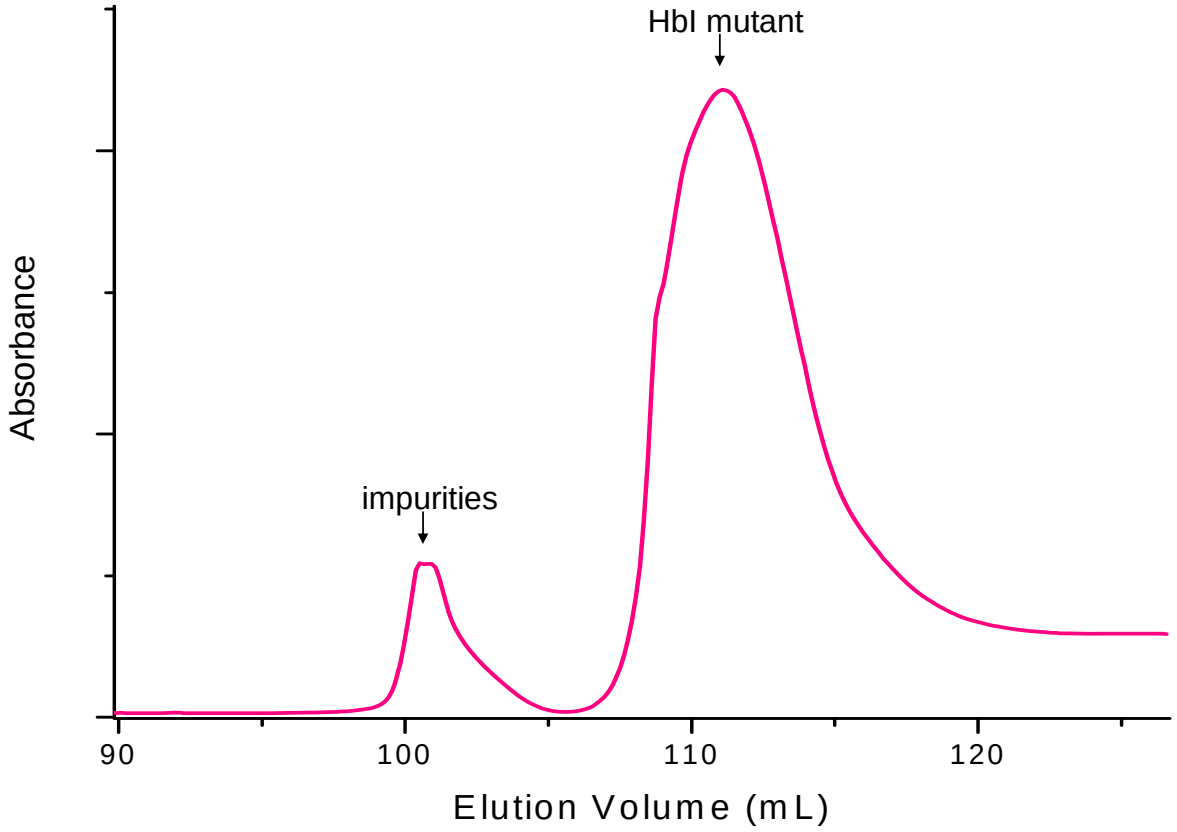

Figure 2.3 Elution profile by Metal Affinity Chromatography at 280nm for the separation of HbI mutant from impurities.

The sample was concentrated and washed with deionized water at 4˚C, by pressure filtration using Nitrogen as the pressure gas and a YM-10 membrane with a molecular range of 10000 in an AMICON ultrafiltration cell. This procedure assured the functionality of the protein by eliminating the imidazole remaining in the sample from the purification buffers. All the mutants with the exception of the HbIGlnE7His mutant, which aggregates in the absence of salts, were washed with 7.0 pH 0.1 M sodium phosphate buffer to maintain the functionality and stability of the mutant. The sample was stored.

2.10 Size Exclusion Chromatography (mutants)

The size exclusion method was conducted for the removal of impurities that may have still been present in the sample. The use of the instrumentation and equipment for this method was as described earlier. The buffer used for the procedure was of 50mM sodium phosphate and 300mM sodium chloride at a pH of 7.0. Figure 2.4 shows the elution profile by Size Exclusion Chromatography at 280nm for the separation of HbI mutant from imidazole and salts impurities, where the elution of the impurities is observed first followed by the elution of the desired protein. After the selection and collection of the fractions, the resulting sample was concentrated and the solvent changed to 7.0 pH 0.1 M sodium phosphate buffer. The sample was stored at approximately 50˚C, to assure the stability and lifetime of the HbI mutant.

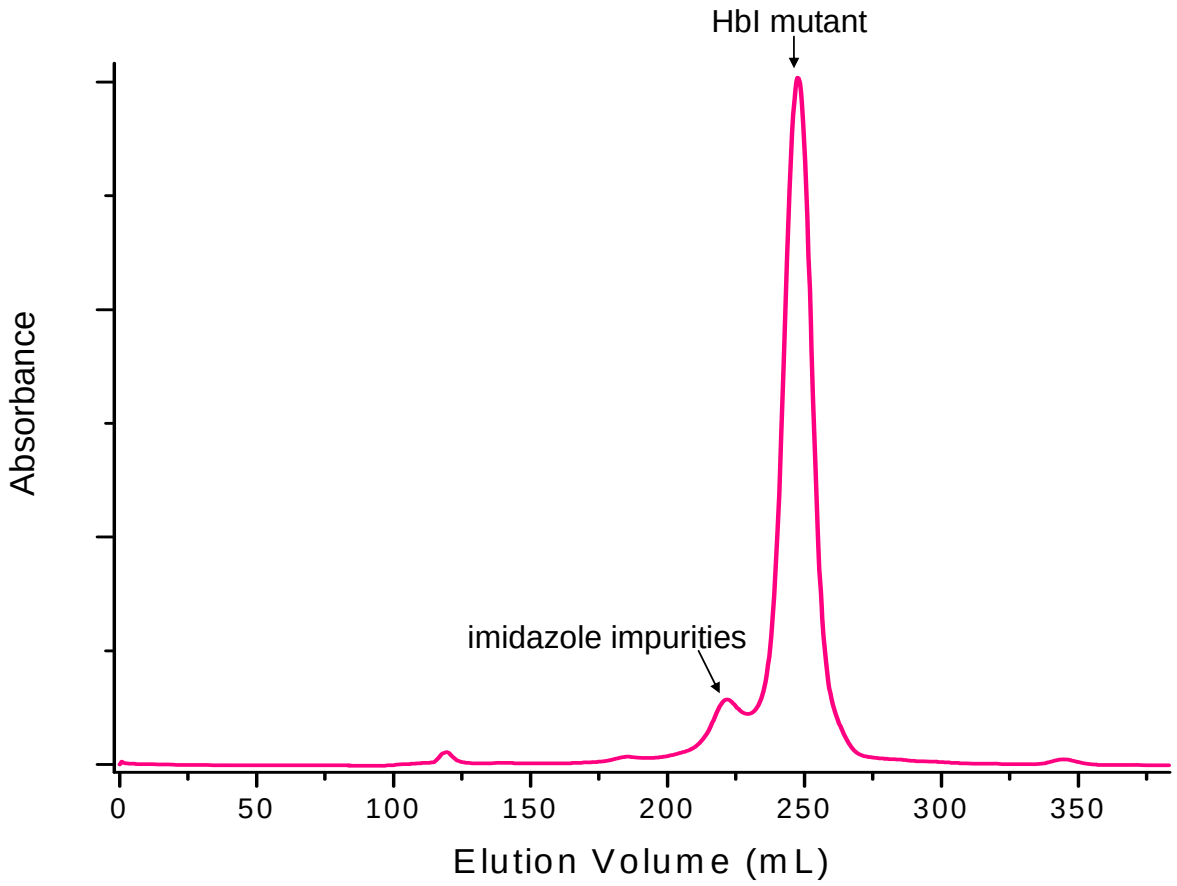

Figure 2.4 Size Exclusion Chromatography elution profile at 280nm for the separation of HbI mutant from imidazole and salts impurities.

2.11 Verification of Sample Purity

The method used for determining the purity of HbI was SDS-PAGE, or sodiumdodecyl sulphate-polyacrylamide gel electrophoresis. It is a qualitative method based on the different rates of migration of proteins with different molecular weight represented by the bands when an electric field is applied. This electrophoresis uses a polyacrylamide gel as a support medium and an anionic denaturalizing detergent, that binds to the proteins increasing their solubility and imparts a negative net charge to them. This net charge facilitates the migration of the molecules through the gel when the electric field is applied, separating them according to their molecular weight. The migration profile provides the heavier molecules on top of the gel, slow migration, and the lighter molecules on the bottom of the gel, more migration.

For a simple evaluation of the purification process and estimation of the proteins molecular weight the resulting bands were compared to these of a SDS-Page standard from Bio-Rad with a molecular range from 6,900 to 194,239 Daltons. The electrophoresis analysis was made using an 8-16% Tris-HCl Ready Gel from Bio-Rad. The samples were prepared by mixing in a Vortex, 20µL of the protein and 10µL of the running buffer solution, which consisted of 0.5 M Tris-HCl at a 6.8 pH, 10% SDS, 1% bromophenol blue as dye marker, Glycerol and β-mercaptoethanol. The mixtures were heated for 5 minutes using a sand bath at 95˚C. Immediately, 16µL of the heated mixture were transferred to the wells in the gel. For the preparation of the standard, 20 µL of the SDS-Page Standard were heated in a sand bath for 1 minute at 32˚C. Then, immediately injected into the first well. The ready gels were previously placed in the vertical trays of the ready gel electrophoresis cell from Bio-Rad, which was filled with running buffer.

The migration of the proteins through the gel was initiated by applying a current of 114 mA and a voltage of 150 V for 45 minutes, using a power supply PAC 3000 from Bio-Rad. When the migration was stopped by discontinuing the applied potential, the gel was carefully removed and stained for 15 minutes with Coomasie Blue G-250, which was then removed by washing with acetic acid solution three times and left in deionized water for a period of 24 hours. After all this procedure, one can clearly observe the presence of bands and determine the purity and absence of contaminant in the protein sample.

2.12 Ultraviolet-Visible Spectroscopy

The UV-Vis spectroscopy gave information about the concentration, complex formation, and purity of the protein sample based on the heme group, using a Shimadzu 2101 PC UV-Vis spectrophotometer. The sulfheme complex formation was followed and verified with the specific maxima absorbance of the Soret and Q bands provided by the complex, as reported by Krauss, 1990. Figure 2.5 shows the optical UV-Vis Spectra characteristic for the metaquo HbI complex, known as the water molecule bound to the ferric state of the iron, with the distinctive Soret band at 407nm and the Q's bands at 505 and 633nm. The sample concentration was determined at the maximum absorption wavelength of the Soret band applying the Beer- Lambert Law: $A=\varepsilon bc$, where A is the maximum absorbance, b is the cuvette pathlength, c is the concentration and ε is the absorptivity coefficient reported in the literature (Krauss et. al. 1990).

2.13 Sample Preparation of the Sulfhemeprotein Complex

The Sulfhemeprotein complex was prepared with the hemeproteins: Horse Heart Mb, HbI, HbII/HbIII mixture, HbIPheE11Val, HbIPheB10Val, HbIGlnE7His and

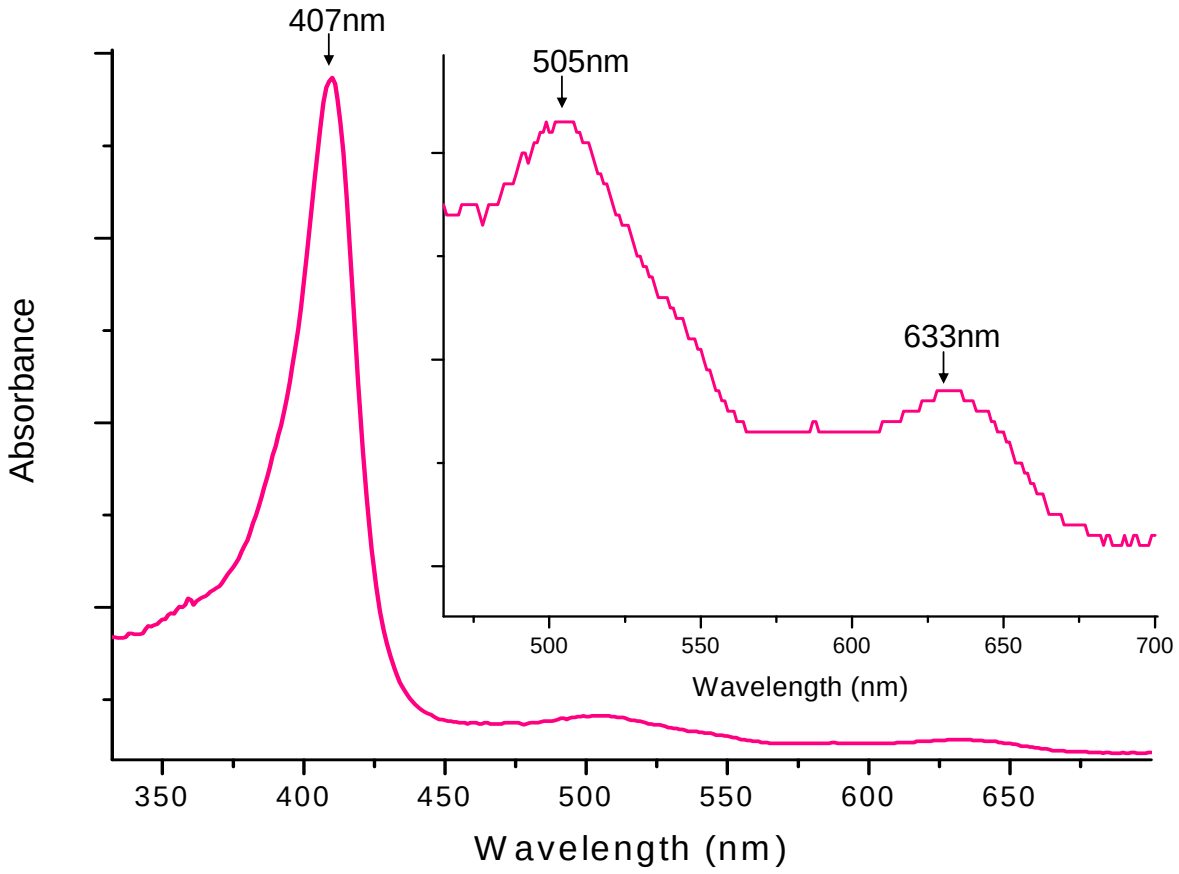

Figure 2.5 Optical UV-Vis Spectrum characteristic for the metaquo HbI complex, with the distinctive Soret band at 407nm and the Q's bands at 505 and 633nm.

HbIPheB10His. The concentration of the protein was determined by UV-Vis, using the reported spectrum properties for each hemeprotein complex.

For the oxy HbI complex, the maximum absorption of the Soret and Q bands are 416, 541, and 576nm, respectively. The Soret and Q bands for oxy Hb II complex are 414, 540, and 576, respectively. Oxy Hb III complex has the same maximum absorption band as Hb II, with the exception of the second Q band that has maximum absorption at 575nm instead of 576nm. For the metaquo HbI complex, the maximum absorption of the Soret and Q bands are 407, 502, and 633nm, respectively. All the HbI mutant complexes have approximately the same spectra properties as the HbI wild type complexes. The Soret and Q bands for the metaquo HbII complex are 403, 502, and 632nm, respectively. Metaquo HbIII complex has the Soret and Q bands at 405, 501, and 630nm, respectively. For the metaquo horse heart Mb complex, the maximum absorption of the Soret and Q bands are 408 and 504nm, respectively.

To obtain the metaquo complex of the hemeproteins, the proteins were titrated with 10% excess of potassium ferrocyanide. The formation was monitored by the maximum absorption displacement of the Soret band to approximately 407nm and the Q bands to 502 and 633. In order to eliminate the excess of potassium ferrocyanide and change the solvent of the sample to: a 100mM Succinic Acid, 100mM Potassium phosphate dibasic and 1mM EDTA solution at a pH of 6.5, a centricon centrifugal filter device with a YM-10 membranes from Amicon were used and centrifuge for periods of 10 minutes in a JA-20 rotor at 8000 and 4˚C. This procedure was performed until all the yellow residue of the potassium ferrocyanide was eliminated. To obtain the oxy complex of the protein, known as the ferrous state with oxygen, a 200mM Na_2S_2O4

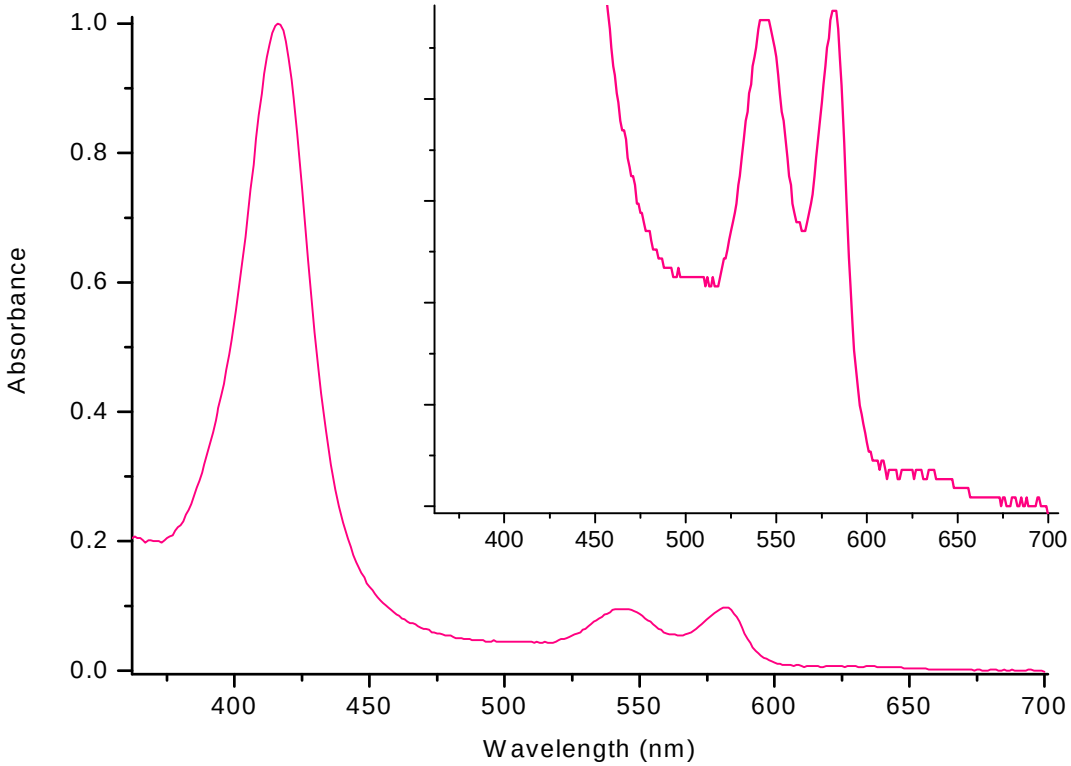

Figure 2.6 Optical UV-Vis Spectrum characteristic for the oxy complex, with the distinctive Soret band at 416nm and the Q's bands at 541 and 576nm.

solution was carefully added to the sample and then purged with oxygen. The complex formation was verified with the UV-Vis Spectrum. Figure 2.6 shows the optical UV-Vis Spectrum characteristic for the oxy complex, with the distinctive Soret band at 416nm and the Q's bands at 541 and 576nm.

The desired experimental concentration of the samples were acquired by centrifuge, as described above, and verified by UV-Vis Spectra. By knowing the sample concentration, the solutions needed for the complex formation could be prepared. They have a concentration relation of 1:5:5. If the Hemeprotein concentration is 1mM, then the hydrogen peroxide and hydrogen sulfide solutions should have a 5mM concentration. The hydrogen peroxide solution was prepared using 30% hydrogen peroxide, purchased from Fisher, and the hydrogen sulfide solution was prepared using the salt sodium sulfide, purchased from Fisher. All solutions were prepared using the 100mM Succinic Acid, 100mM potassium phosphate dibasic and 1mM EDTA solution at a pH of 6.5.

For the anaerobic experiments the sample, the buffer, hydrogen peroxide, and the sodium sulfide salt were each transferred to a small mini-tube and tightly sealed with a rubber septum. They were purged, for 15 minutes, with 99.0% Nitrogen gas from Linde, to remove the oxygen present in the sample.

The concentration relation of 1:5:5 should be maintained throughout all the complex formation procedure. The sample was added to a quartz cuvette and sealed with a rubber septum. When ready, the correspondent μL of the hydrogen peroxide solution were added to the cuvette and after approximately 30 seconds, the corresponding

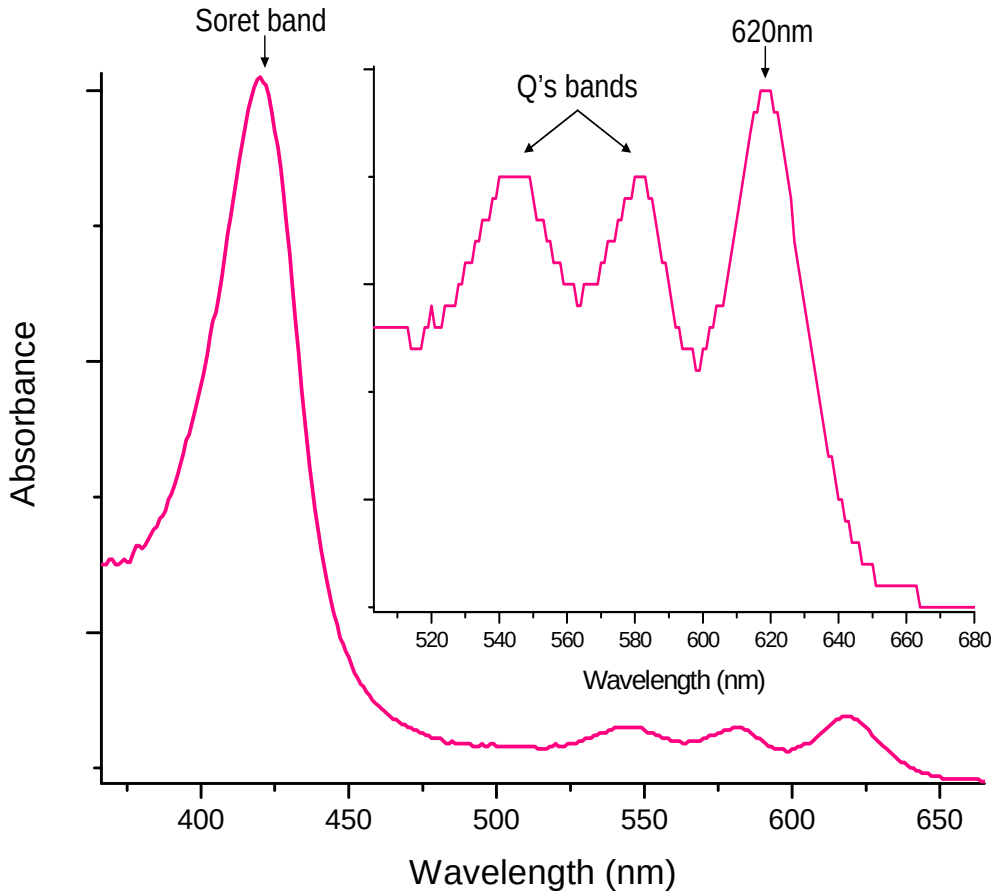

Figure 2.7 Optical UV-Vis Spectrum representing the characteristic absorption band at 620 nm for the sulfheme protein complex.

μL of the hydrogen sulfide solution were added, maintaining the 1:5:5 concentration relation at all times inside the cuvette. The complex formation was monitored by following the presence of the characteristic 620nm maximum absorption using UV- Vis spectrum. Figure 2.7 shows the optical UV-Vis Spectrum, representing the characteristic absorption band of the sulfheme complex at 620nm.

For the NMR experiment, the complex formation procedure was basically the same, with some slight precautions and differences. The hemeprotein used for the NMR experiment was the Mb from the horse heart from Sigma. It was dissolved in the same buffer, but instead of the solvent being dioinized water, it was 100% D_2O, and all the reagents were isotopes with the exception of potassium phosphate monobasic. The NMR experiments required a protein concentration of at least 2 to 4mM. For that reason, when that concentration was reached, the possible subsequent dilution was minimized. Therefore, high concentration solutions of 1M hydrogen sulfide and 1M hydrogen peroxide were prepared to minimize the volume changes affecting the concentration. They were added to the concentrate sample solution, minimizing the dilution of the sample concentration, but still maintaining the 1:5:5 concentration relation during the complex preparation. To eliminate the excess of hydrogen sulfide or hydrogen peroxide, given that it may contribute to the complex degradation and interfere with NMR experiments, the sample was washed 3 times with the deuterated 100mM Succinic Acid, 100mM Potassium phosphate dibasic and 1mM EDTA solution at a pH of 6.5 by centrifuge, as described above. After the centrifuge, approximately 700μL of the sulfmyoglobin was transferred to a 5mm NMR tube from Wilmad (Berzofsky et. al. 1971; La Mar et. al. 2000).

2.14 Nuclear Magnetic Resonance Studies

The Nuclear Magnetic Resonance Spectroscopy provides information about the protons present in the active site that are influenced by the Iron in the heme group, affected by the formation of the complex. NMR can give information about the presence of the sulfheme complex with the possible ligand and oxidation state of the Iron. The spectrum was obtained using a 500MHz Bruker with XWin-NMR 3.0 version software.

2.15 One Dimension Proton-NMR Measurements

The 1D NMR pulse sequence involves an acquisition time, recycling delay and the 90˚ radio-frequency pulse. The 90˚ pulse was calibrated using the length and strength of the radio-frequency pulse at 9.80 μsec and 51.15 dB, respectively. Furthermore, the water frequency signal called O1 was calibrated at 4.70ppm using the acquisition mode of the instrument to perform solvent suppression.

^{1}H spectra were successfully acquired by using a delay time (repetition rate) of $1s^{-1}$ for 128 scans and a free induction decay (FID) of 4096 data points, with various spectral width starting at 34ppm and increasing in a sequential order to 60ppm, 100ppm and 200ppm. These windows allowed to include all resonances and improve resolution for the diamagnetic and paramagnetic envelope in the spectra. The spectra acquisition included variable temperature (VT) experiments (increasing the temperature) at each spectral window collected over the range 5-30°C at pH 6.5 to determine the temperature dependence of heme peripheral groups and detected resonances. Solvent suppression was performed by direct saturation in the relaxation delay period using a presaturation pulse sequence. A decoupler pulse was used to a power level of presaturation for the residual

signal of water. All dimensional data were processed on a PC workstation using the software package MestRe-Nova 5.1.0 Version.

CHAPTER 3
Results and Discussion

3.1 Formation of SulfHeme Protein

Understanding the formation of the sulfheme derivative formation is crucial since it produces the clinical condition known as sulfhemoglobinemia (Tangerman et al., 2002; Guidotti, T.L., 1994; Hayes. L.C., 1999; Wu, et al., 1997). Furthermore, the actual mechanism leading to the formation of this complex is not well understood. It has been suggested that the formation of the sulfheme depends on the presence of hydrogen sulfide and the ferryl species (Berzofsky, J. et al., 1971 and 1972; Andersson et al., 1984; Chatfield et al, 1986, 1987 and 1992; Evans et al., 1994; Magliozzo et al, 1986; Michel, H.O., 1938; Parker et al, 1989).

Hydrogen peroxide, as well as oxygen, produce the ferryl species. However, hydrogen peroxide accelerates the reaction behaving as a catalyst. In the presence of oxygen and hydrogen peroxide, the ferryl species are known to be intermediates in the physiological reactions of hemoglobin and myoglobin. These heme ferryl species involve, the so called compound I, which is a radical cation hemeFe^{IV}=O. Lacking an electron in the heme group, and compound II, which stabilizes the porfirin radical cation by forming the hemeFe^{IV}=O derivative with a radical in the protein. The lifetime of compound I is approximately 60 seconds, while the ferryl species compound II is stable for a longer period of time. They keep doing turnovers until complete degradation of the protein.

Unlike many heme proteins, the reactions of HbI, HbII, and HbIII with hydrogen sulfide, in the presence of oxygen, does not produce the sulfheme derivative despite their

difference in functionality and structure. However, other heme proteins, such as human hemoglobin and myoglobin, the sulfhemecomplex is easily observed under the same conditions. It has been reported that HbI has a stable ferryl species compound I, while HbII has a stable ferryl compound II. Moreover, HbI compound I is nearly one thousand times more stable than Mb compound I. Hence, the differences in H2O2 reactivity towards the formation of compound I and II between Mb, HbI, HbII and HbIII, was used here to study the role of compound I and II in the formation of sulfheme complex (De Jesus et. al. 2001 and 2002; Alayash et al, 1999; Brittain et al., 1997; Egawa et al., 2000; Matsui et al., 1997 and 1999, Nagababu et al., 2000).

Any variation in the heme group, alters the heme electronic structure and as a result, the charge in the density of the central iron changes. The shifts of the UV-Vis bands are influenced by the ligand and oxidation state of the iron. Therefore, the reaction between hydrogen sulfide, hydrogen peroxide and the heme proteins was followed by UV-Vis, monitoring the formation of the sulfderivative at the characteristic 620nm absorption band, which is characteristic of the sulfheme derivatives. Figure 3.1 shows the reaction profile and the UV-Vis spectra of the horse heart myoglobin upon reaction with the hydrogen peroxide and hydrogen sulfide to form the sulfmyoglobin (SMb) complex. Initially, myoglobin is in its metaquo state, having a water molecule bound as a ligand to the iron in its ferric (III) state, which is represented by the green line spectrum. In this state, the characteristic Soret and Q bands are at 409nm, 506nm and 633nm, respectively. The red line spectrumum represents the absorption displacement of the initial reaction between hydrogen peroxide and myoglobin, in the presence of dissolved oxygen.

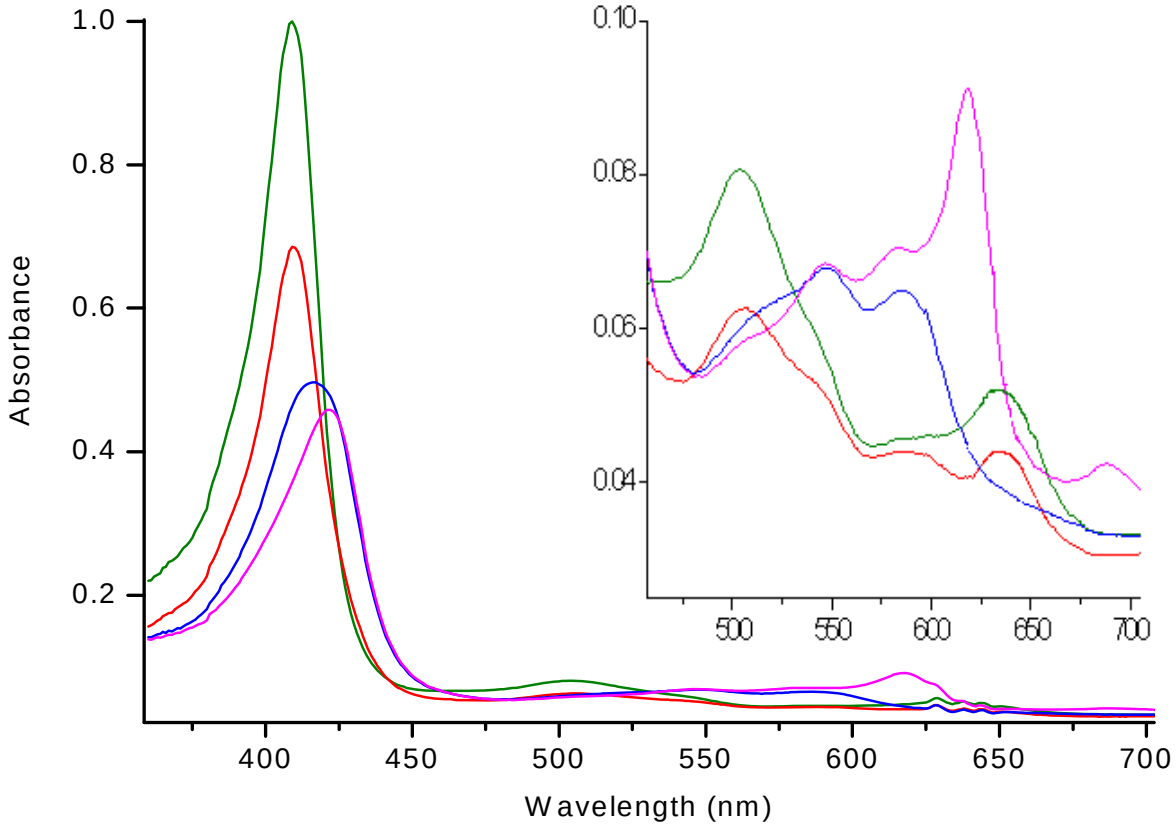

Figure 3.1 UV-Vis Spectrum of the formation of Sulfmyoglobin, starting from horse heart myoglobin. The green line spectrum represents the maximum absorption for met-myoglobin. The immediate reaction between hydrogen peroxide and myoglobin is represented by the red line spectrum, in the presence of dissolved oxygen. The blue line spectrum shows the absorption displacements at approximately 30 to 45 seconds after addition of hydrogen peroxide. The maximum absorption of the sequential addition of hydrogen sulfide is represented by the pink line spectrum, where the characteristic 620nm band of the sulfheme complex is observed.

An immediate, a decrease in the maximum absorption of the Soret and Q bands was observed. After approximately 30 to 45 seconds, the absorption bands were displaced toward the red region of the UV scale, as shown in the by the blue line spectrum. The maximum absorption of the Soret and Q bands were found to be at 418nm, 548nm and 586nm, respectively. The sequential addition of hydrogen sulfide is represented by the pink line spectrum. The maximum absorption of the Soret band shifted to 420nm, which is the characteristic band of the ferryl compound II species, while, the Q bands were essentially unchanged. However, a new band can be observed at 620nm, which is the characteristic absorption for the sulfmyoglobin complex formation. In addition, the distinctive green color was instantly observed. Table 3.1 summarizes the optical absorption displacements for the chemical reaction between the horse heart myoglobin, hydrogen peroxide and hydrogen sulfide, in the presence of dissolved oxygen, leading to the formation of the sulfmyoglobin complex.

Similarly, Figure 3.2 shows the reaction profile and the UV-Vis spectra of human hemoglobin upon reaction with hydrogen peroxide and hydrogen sulfide, in the presence of dissolved oxygen, forming the sulfheme complex. Initially, the human hemoglobin was in its metaquo state, represented by the pink line spectrum. The characteristics Soret and Q bands of the metaquo state can be observed at 406nm, 505nm, and 633nm, respectively. The other two Q bands at 540nm and 576nm are characteristic of the oxy complex. Therefore, the sample was a mixture of the met and oxy complexes, where the met complex was the predominant species. The black line spectrum represents the absorption displacements of the reaction between hydrogen peroxide and human

Table 3.1 Maximum Absorption wavelength (nm) of the UV-Vis Spectrum for the formation of Sulfmyoglobin, starting from horse heart myoglobin

Description	**Soret**	**Q**	**Q**	**Q**	**Q**	**Sulf-complex (color)**
Met Mb	409_{vs}	506_{s}	542_{vw}	580_{vw}	633_{s}	-
Met Mb + H_2O_2	411_{s}	506_{w}	548_{vw}	586_{vw}	633_{w}	-
Met Mb + H_2O_2 – 30 to 45 sec	418_{s}	508_{vw}	548_{w}	586_{w}	No	-
Met Mb + H_2O_2 + H_2S	420_{s}	506_{vw}	548_{w}	586_{w}	No	620_{vs} (green)

The vs, s, w, and vw letters presented in the table represent the absorption behavior of each band: vs = very strong, s = strong, w = weak, and vw = very weak. The (–) line indicates that the band is not applicable. The (No) implies that the band was not detectable. Units are in nanometer (nm).

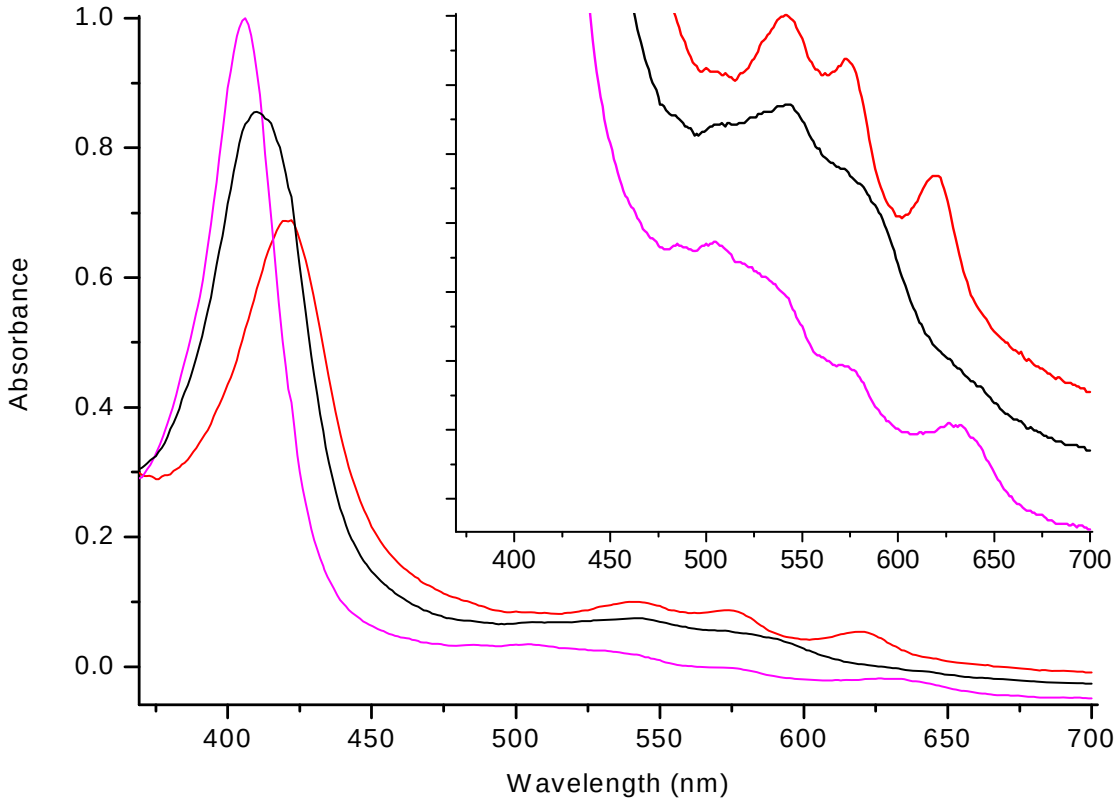

Figure 3.2 UV –Vis Spectra of the reaction for the formation of the Sulfhemoglobin complex, starting from human hemoglobin, in the presence of dissolved oxygen. The pink line spectrum represents the maximum absorption for met-human hemoglobin. The maximum absorptions shifts of the reaction between human hemoglobin and hydrogen peroxide are represented by the black line spectrum. The red line spectrum represents the absorption displacements after the sequential addition of hydrogen sulfide to the sample, where the characteristic 620nm band of the sulfheme complex is present.

hemoglobin. A shift and a decrease in the maximum absorption of the Soret band to 412nm was observed. Two new Q bands were present at 542nm and 583nm, in addition to the very weak 505nm and 633nm bands. The red line spectrum represents the sequential addition of hydrogen sulfide to the sample. The maximum absorption of the Soret band shifted to 422nm, which is the characteristic absorption region of the ferryl compound II. At the same time, the absorptions of the Q bands shifted to 543nm and 576nm. The 620nm absorption band, characteristic of the sulfhemoglobin complex with the unique green color was instantly observed. Regarding this, Table 3.2 summarizes the changes in the Soret and Q bands upon reaction of human hemoglobin with hydrogen peroxide and hydrogen sulfide, in the presence of dissolved oxygen.

On the other hand, Figure 3.3 presents the reaction profile and the UV-Vis spectra upon the reaction of Hemoglobin I with hydrogen peroxide and hydrogen sulfide, in the presence of dissolved oxygen. Initially, HbI was in its metaquo complex, as shown by the pink line spectrum. The characteristic Soret and Q bands of the predominant metaquo state were present at 406nm, 502nm, and 633nm, respectively. The black line spectrum represents the reaction between hydrogen peroxide and HbI. A decrease in the maximum absorption of the Soret and Q bands was observed. The sequential addition of hydrogen sulfide is represented by the red line spectrum. The maximum absorption of the Soret band shifted to 426nm, known as the characteristic band for the hydrogen sulfide complex where the hydrogen sulfide binds to the ferric iron as a ligand. The previous two Q bands disappeared and two new ones appeared at 544nm and 575nm. There was no presence of the green color or the characteristic 620nm absorption band.

Table 3.2 Maximum Absorptions wavwlength (nm) of the UV-Vis Spectra for the formation of Sulfhemoglobin complex, starting from human hemoglobin

Description	**Soret**	**Q**	**Q**	**Q**	**Q**	**Sulf-complex (color)**
Met Human Hb	406_{vs}	505_{vw}	540_{vw}	576_{vw}	633_{w}	-
Met Human Hb + H_2O_2	412_{vs}	505_{vw}	542_{vw}	583_{vw}	633_{vw}	-
Met Human Hb + H_2O_2 + H_2S	421_{s}	505_{vw}	541_{w}	574_{w}	No	620_{w} (green)

The vs, s, w, and vw letters presented in the table represent the absorption behavior of each band: vs = very strong, s = strong, w = weak, and vw = very weak. The (–) line indicates that the band is not applicable. The (No) implies that the band was not detectable. Units are in nanometer (nm).

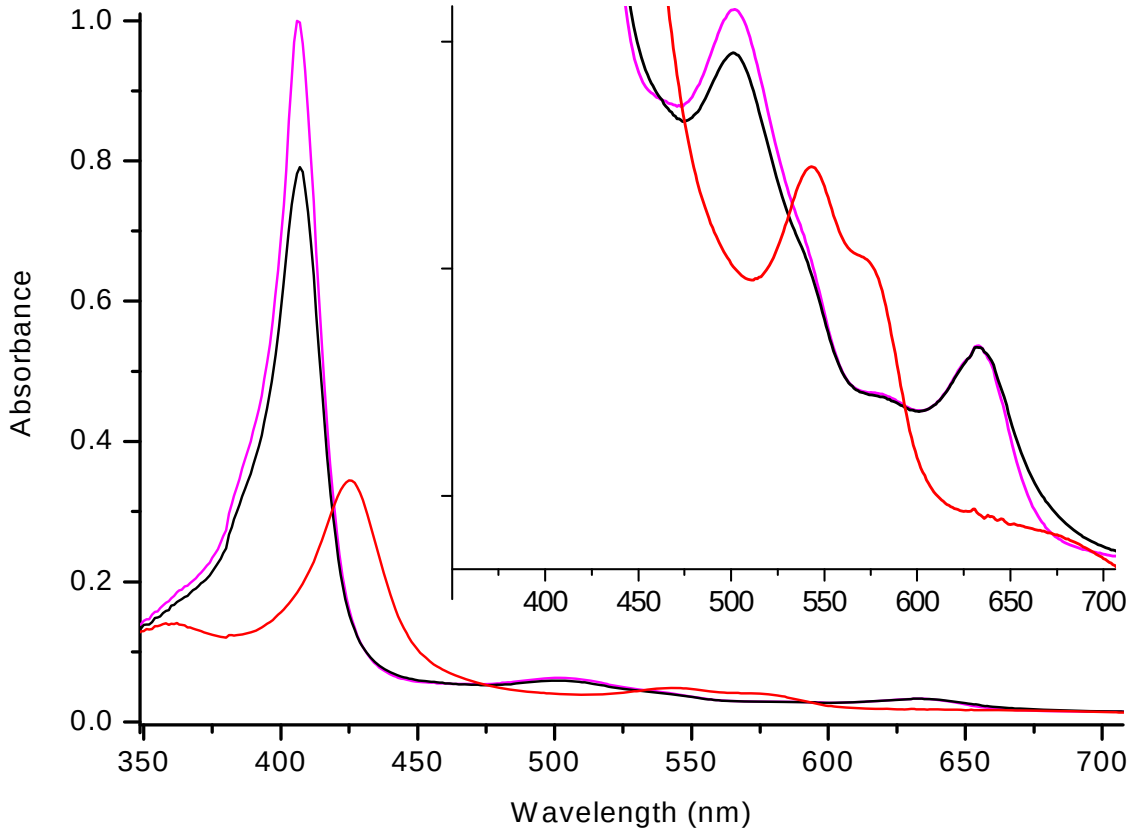

Figure 3.3 UV-Vis Spectra of the reaction of HbI and hydrogen peroxide, in the presence of dissolved oxygen, with the sequential addition of hydrogen sulfide. The pink line spectrum represents the maximum absorption for met-HbI. The absorptions shifts of the reaction between the HbI and hydrogen peroxide are represented by the black line spectrum. The red line spectrum represent the absorption displacements after the sequential addition of hydrogen sulfide, where the characteristic 620nm band for the sulfheme complex was not observed.

Table 3.3 summarizes the changes in the Soret and Q bands as a consequence of the reaction of HbI with hydrogen peroxide and hydrogen sulfide, in the presence of dissolved oxygen.

Likewise, Figure 3.4 shows the absorption of the UV-Vis spectra and the reaction profile upon the chemical reaction between the HbII/HbIII mixture and hydrogen peroxide with the sequential addition of hydrogen sulfide, in the presence of dissolved oxygen. The pink line spectrum represents the met HbII/HbIII complex. The characteristic Soret and Q bands of the metaquo state were present at 406nm, 502nm, and 633nm, respectively. The Tyrosine, in the B10 position at a pH of 6.5, interacted with the heme iron and the bound H_2O ligand producing absorptions at 540nm and 581nm. The black line spectrum represents the reaction between hydrogen peroxide and the HbII/HbIII sample mixture.

A decrease in the maximum absorption of the previously mentioned Soret and Q bands was observed. The Soret and Q bands absorption shifted to 409nm, 541nm, and 576nm. The sequential addition of hydrogen sulfide is represented by the red line spectrum. The maximum absorption of the Soret band shifted to 422nm, which is typical of the ferryl compound II species. The 500nm band disappeared completely and the absorption of the Q bands shifed to 543nm and 576nm. There was no presence of the green color or the characteristic 620nm absorption band. In Table 3.4, the optical absorptions displacements of the chemical reactions between the HbII/HbIII mixture, hydrogen peroxide, and hydrogen sulfide, in the presence of oxygen, are summarized. HbI, HbII and HbIII are present in a natural high sulfur concentration environment. Therefore, in order to maintain their functionality, they have evolved strategies to avoid

Table 3.3 Maximum Absorption wavelength (nm) of the UV-Vis Spectra upon reaction between HbI, hydrogen peroxide and hydrogen sulfide, in the presence of dissolved oxygen.

Description	**Soret**	**Q**	**Q**	**Q**	**Q**	**Sulf-complex**
Met HbI	406_{vs}	502_{w}	540_{vw}	581_{vw}	633_{w}	-
Met HbI + H_2O_2	407_{vs}	502_{w}	540_{vw}	581_{vw}	634_{w}	-
Met HbI + H_2O_2 + H_2S	426_{w}	No	544_{w}	575_{w}	No	No

The vs, s, w, and vw letters present in the table represent the absorption behavior of each band: vs = very strong, s = strong, w = weak, and vw = very weak. The (–) line indicates that the band is not applicable. The (No) implies that the band was not detectable. Units are in nanometer (nm).

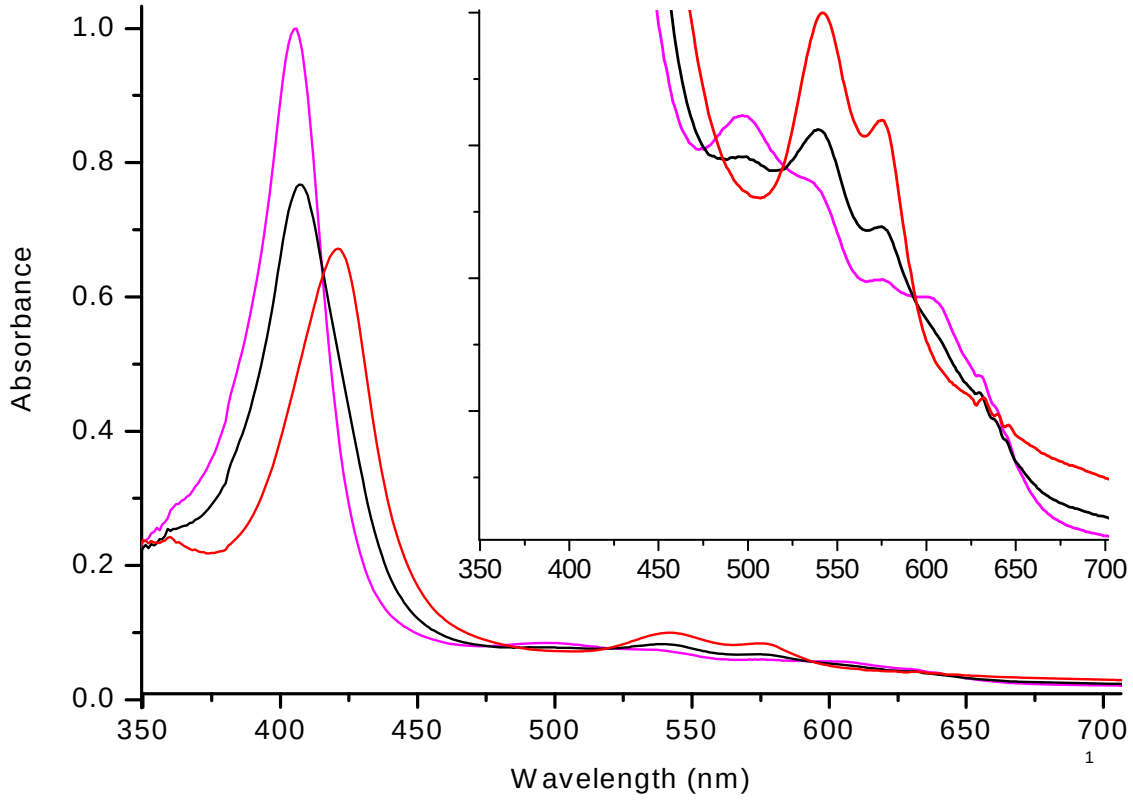

Figure 3.4 UV-Vis Spectra of the reaction of HbII/HbIII sample mixture and hydrogen peroxide, in the presence of dissolved oxygen, with the sequential addition of hydrogen sulfide. The pink line spectrum represents the maximum absorption for met-HbII/HbIII mixture. The absorptions shifts of the reaction between the HbII/HbIII mixture and hydrogen peroxide are represented by the black line spectrum. The red line spectrum represents the absorption displacements after the sequential addition of hydrogen sulfide, where the characteristic 620nm band for the sulfheme complex was not observed.

Table 3.4 Maximum Absorption wavelength (nm)of the UV-Vis Spectra upon reaction between HbII/HbIII mixture, hydrogen peroxide and hydrogen sulfide, in the presence of dissolved oxygen.

Description	**Soret**	**Q**	**Q**	**Q**	**Q**	**Sulf-complex**
Met HbII/HbIII	407_{vs}	500_{w}	540_{vw}	576_{vw}	602_{vw}	-
Met HbII/HbIII + H_2O_2	409_{vs}	500_{vw}	541_{w}	576_{w}	No	-
Met HbII/HbIII + H_2O_2 + H_2S	422_{s}	No	543_{s}	576_{s}	No	No

The vs, s, w, and vw letters present in the table represent the absorption behavior of each band: vs = very strong, s = strong, w = weak, and vw = very weak. The (–) line indicates that the band is not applicable. The (No) implies that the band was not detectable. Units are in nanometer (nm).

sulfderivative formation in the presence of hydrogen sulfide.

The data clearly shows that Mb and human Hb were the only ones to form the sulfheme complex. Berzofsky et al, 1971, proposed that a ferryl species in the presence of hydrogen sulfide was responsible for the sulfheme formation. Table 3.5, shows the stability of the ferryl species, for human Hb, horse heart Mb, HbII/HbIII and HbI and their capabilities for the sulfheme formation. Mb, human Hb, HbII, and HbIII have an unstable ferryl compound I but a stable ferryl compound II. If compound II was responsible for the sulfheme formation, then HbII and HbIII would have formed the sulfheme complex, as Mb and human Hb, but this derivative was not observed. This shows that compound II is not responsible for the formation of the sulfheme derivative. On the other hand, HbI has the ferryl compound I stable. If compound I was responsible for the sulfheme formation, HbI would have formed the sulfheme complex, as Mb and human Hb, but the derivative was not observed either. This implies that compound I is not responsible for the formation of the sulfheme derivative. Therefore, the data suggests that the heme pocket amino acids may be responsible or can play an important role in the formation of the sulfheme complex.

3.2 Unique role of HisE7 in the sulfheme proteins formation

The amino acids in the active site of the heme pocket are known to play an important role in the functional properties of the heme proteins. They participate in the selective cooperative ligand binding process and its stability. Any modification in the chemical properties of the amino acids can alter the chemical properties of the active site and therefore, the functionality of the protein (Antommattei et al., 1999; Cerda et al.,

Table 3.5 Comparison of the Ferryl species stability versus the sulfheme complex formation for Human Hb, horse heart Mb, HbII/HbIII, and HbI.

Protein	**Sulfheme Complex**	**Stability**	
		Compound I	**Compound II**
Human Hb	X		X
Horse heart Mb	X		X
HbI		X	X
HbII/HbIII			X

The (X) implies were the complex was observed

1999; De Jesus et al., 2001, 2002 and 2006; Krauss et al., 1990; Leon et al., 2004; Lewis et al., 2006; Navarro et al., 1996; Rizzi et al., 1994 and 1996; Rosado et al., 2001). Since amino acids in the heme pocket play an essential part in the properties of the chemical reactions of the heme protein, it was vital to learn if they were in part responsible for sulfheme complex formation. This would lead us to the comprehension and understanding of the mechanism for the sulfheme complex formation. Figure 3.5 shows the corresponding amino acids in the active site of Mb, HbI and HbII. Myoglobin has valine (Val), leucine (Leu), Phenylalanine (Phe),and histidine (His) in the E11, B10, CD1, and E7 positions. Human hemoglobin has the same active site as Mb. However, HbII has phenylalanine (Phe), tyrosine (Tyr), phenylalanine (Phe), and glutamine (Gln) in the E11, B10, CD1, and E7 positions. HbI, on the other hand, has phenylalanine (Phe), phenylalanine (Phe), phenylalanine (Phe), and glutamine (Gln) in the E11, B10, CD1, and E7 positions.

Taking advantage of the amino acid difference in the active site between these heme proteins, site direct mutagenesis technique was employed in the HbI active center to monitor the influence of a specific amino acid in the sulfheme complex formation. Single amino acid replacement were performed in the HbI distal site so as to mimic Mb heme-pocket, since sulfheme complex was observed in this protein.

The HbI mutants used were HbI PheE11Val, HbI GlnE7His, HbI PheB10His, and HbI PheB10Val. Initially, the amino acid Phenylananine in the E11 position of HbI was changed to Valine in the E11 position, as in Mb. Figure 3.6 shows the structure of Phe and Val, where Phe is a big, neutral, non polar aromatic amino acid. However, Val is a small, neutral, non polar aliphatic amino acid. Regarding this, Figure 3.7 represents the

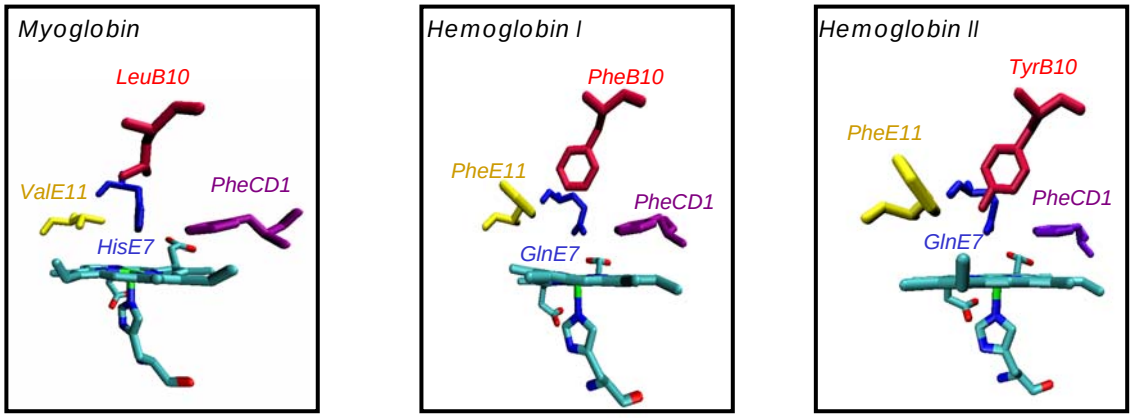

Figure 3.5 Amino acids in the active site of horse heart Mb, HbII and HbI.

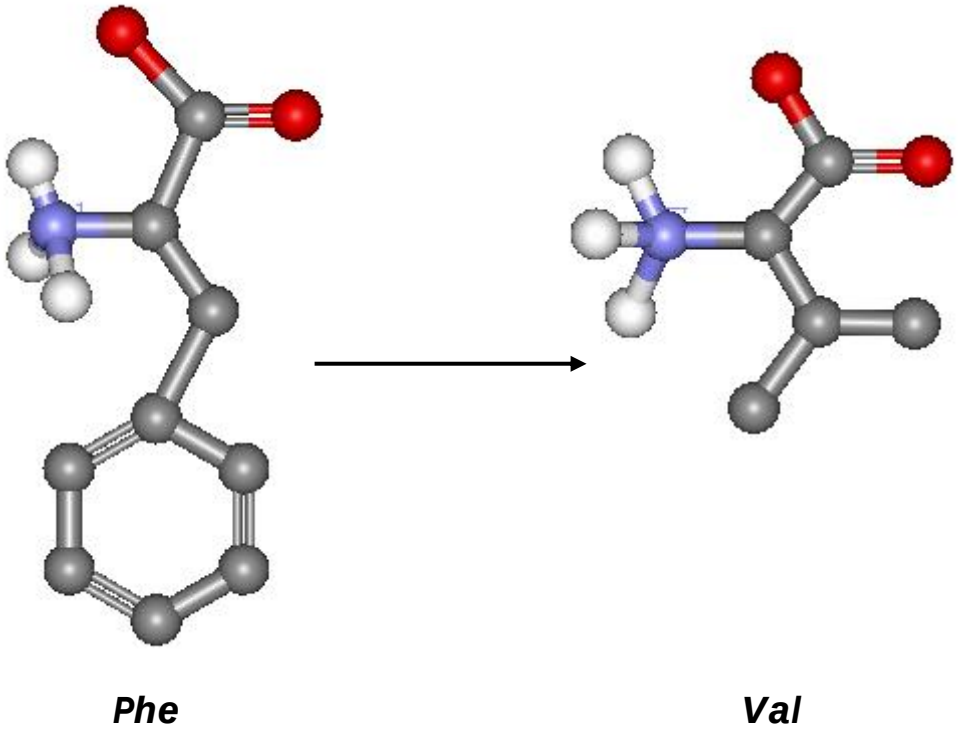

Figure 3.6 Structure of Phe and Val.

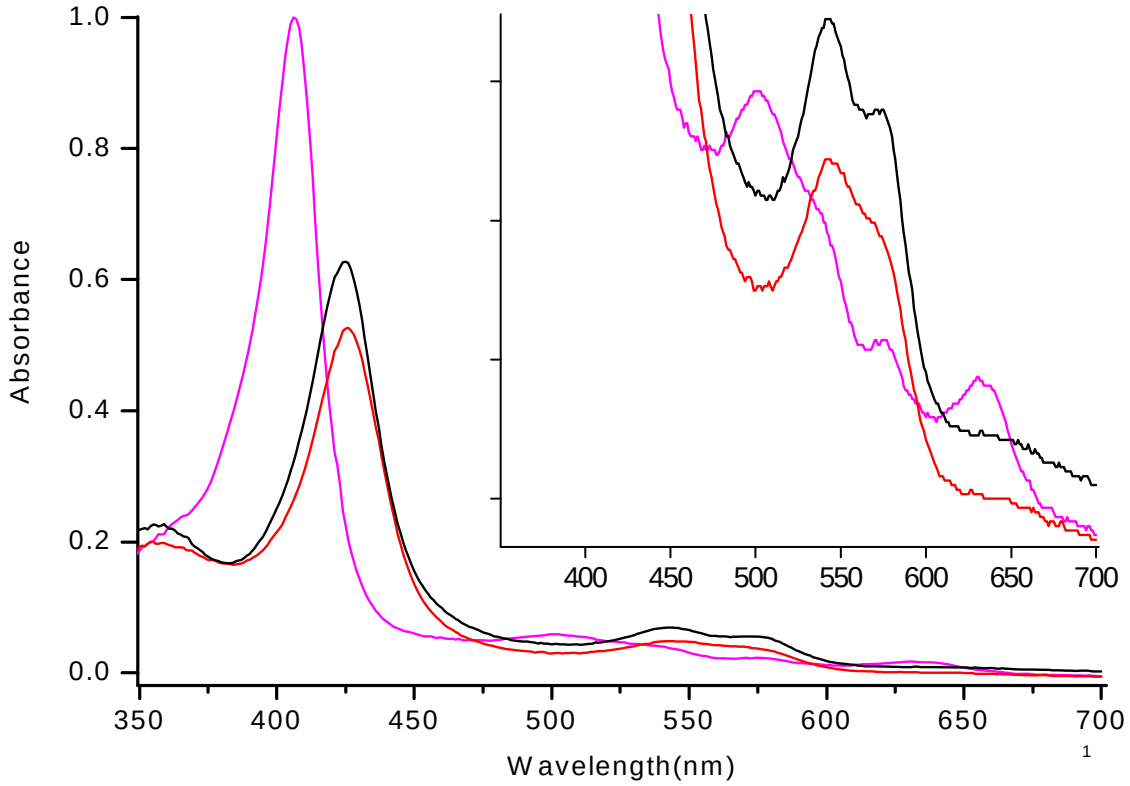

Figure 3.7 UV-Vis Spectra of the reaction of HbI PheE11Val mutant and hydrogen peroxide, in the presence of dissolved oxygen, with the sequential addition of hydrogen sulfide. The pink line spectrum represents the maximum absorption for met- HbI PheE11Val mutant. The absorptions shift of the reaction between HbI PheE11Val mutant and hydrogen peroxide are represented by the black line spectrum. The red line spectrum represents the absorption displacements after the sequential addition of hydrogen sulfide, where the characteristic 620nm band for the sulfheme complex was not observed.

reaction profile of the UV-Vis spectra of HbI PheE11Val mutant with hydrogen peroxide and hydrogen sulfide, in the presence of dissolved oxygen. The pink line spectrum represents the met- HbI PheE11Val mutant. The characteristic absorptions for the metaquo complex were observed at 407nm, 502nm, and 633nm. Also, additional Q bands were present at approximately 540nm and 576nm absorptions. This indicates that complex had a mixture of its high and low states. The black line spectrum represents the absorption displacement of the reaction between the mutant and hydrogen peroxide, in the presence of dissolved oxygen.

Instantly, there was a decrease in the maximum absorption and a shift of the Soret band to 424nm, the absorption region characteristic for the presence of the ferryl species, especially ferryl compound II. The Q bands shifted to 542nm and 575nm with a very weak 633nm band. The sequential addition of hydrogen sulfide to the sample is represented by the red line spectrum. The maximum absorption of the Soret band shifted to 426nm, which is characteristic of the hydrogen sulfide complex. The Q bands remained practically the same with absorptions at 544nm and 575nm. It is important to notice that the presence of the unique green color and the characteristic sulfheme 620nm band were not observed. Table 3.6 contains the optical absorption shifts of the Soret and Q bands for the chemical reaction between HbI PheE11Val mutant, hydrogen peroxide and hydrogen sulfide. The data clearly shows that Valine in the E11 position plays no role in the sulfheme complex formation. The results also indicated that the steric effect of PheE11 is not a factor that may limit the formation of the sulfHbI species.

Table 3.6 Maximum Absorption wavelength (nm) of the UV-Vis Spectra upon reaction between HbI PheE11Val mutant, hydrogen peroxide and hydrogen sulfide, in the presence of dissolved oxygen.

Description	**Soret**	**Q**	**Q**	**Q**	**Q**	**Sulf-complex**
Met HbI PheE11Val	407_{vs}	502_{w}	540_{vw}	576_{vw}	633_{w}	-
Met HbI PheE11Val + H_2O_2	424_{s}	No	542_{s}	575_{s}	633_{vw}	-
Met HbI PheE11Val + H_2O_2 + H_2S	426_{s}	No	544_{w}	575_{w}	633_{vw}	No

The vs, s, w, and vw letters present in the table represent the absorption behavior of each band: vs = very strong, s = strong, w = weak, and vw –=very weak. The (–) line indicates that the band is not applicable. The (No) implies that the band was not detectable. Units are in nanometer (nm).

Similarly, the amino acid Gln in the E7 position of HbI was changed to His in the E7 position, as in Mb. Figure 3.8 shows the structure of Gln and His, where Gln is a very polar uncharged amino acid with a capacity to form hydrogen bond. On the other hand, His is a basic positive charge amino acid with the capacity to accept or donates protons to form an ionic bond. Regarding this, Figure 3.9 demonstrates the absorption of the UV-Vis spectra for the reaction of the HbI GlnE7His mutant and hydrogen peroxide with the sequential addition of hydrogen sulfide, in the presence of dissolved oxygen. The pink line spectrum represents the met- HbI GlnE7His mutant. The characteristic Soret and Q bands for the metaquo complex are at 409nm, 500nm, and 632nm. The other two Q bands with absorptions at 536nm and 575nm indicate that complex has a mixture of its high and low states. The black line spectrum represents the addition of hydrogen peroxide to the sample. Immediately, a shift and a decrease in the maximum absorption of the Soret band to 414nm was observed. The Q bands shifted to 540nm and 576nm. The red line spectrum represents the sequential addition of hydrogen sulfide to the sample. A shift and a decrease in the maximum absorption of the Soret band to 419nm was observed, characteristic of the presence of the ferryl species. The absorptions of the Q bands shifted to 542nm and 575nm. Interestingly, the unique green color and the sulfheme band at 626nm were observed. In Table 3.7, the optical absorption shifts of the Soret and Q bands, for the chemical reaction between HbI GlnE7His mutant, hydrogen peroxide and hydrogen sulfide are summarized.

To verify the formation of the sulfheme complex, a more concentrated HbI GlnE7His mutant sample was used in order to obtain a more define sulfheme band. A 0.88mM HbI GlnE7His mutant sample was used.

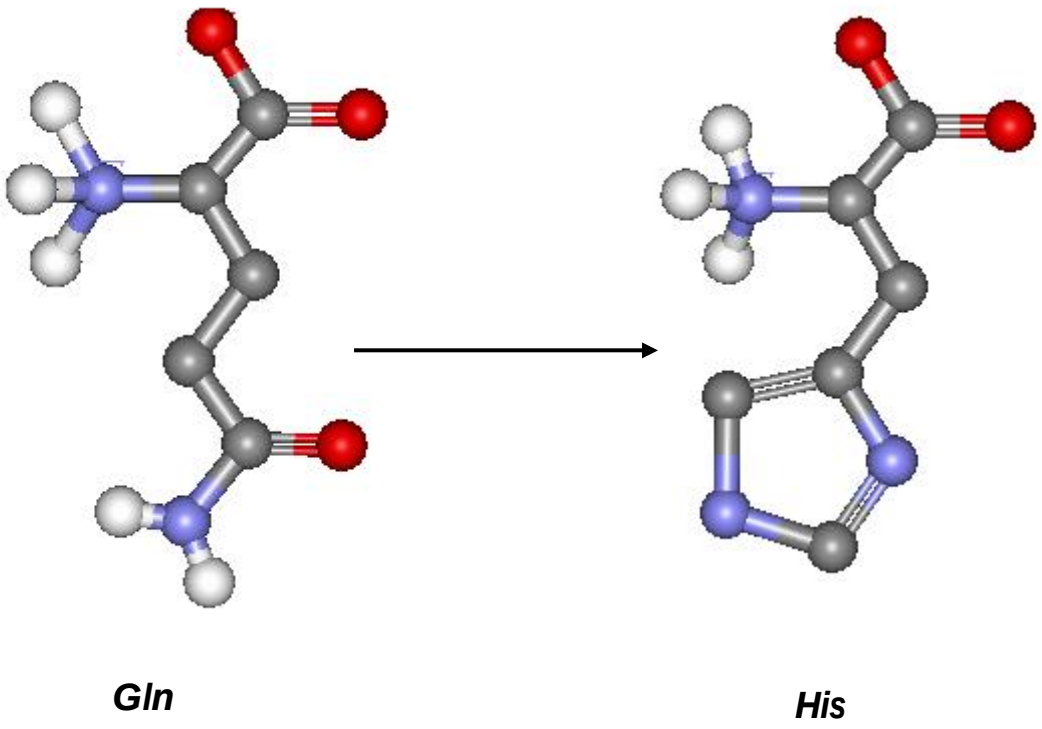

Figure 3.8 Structure of the glutamine and histidine amino acids.

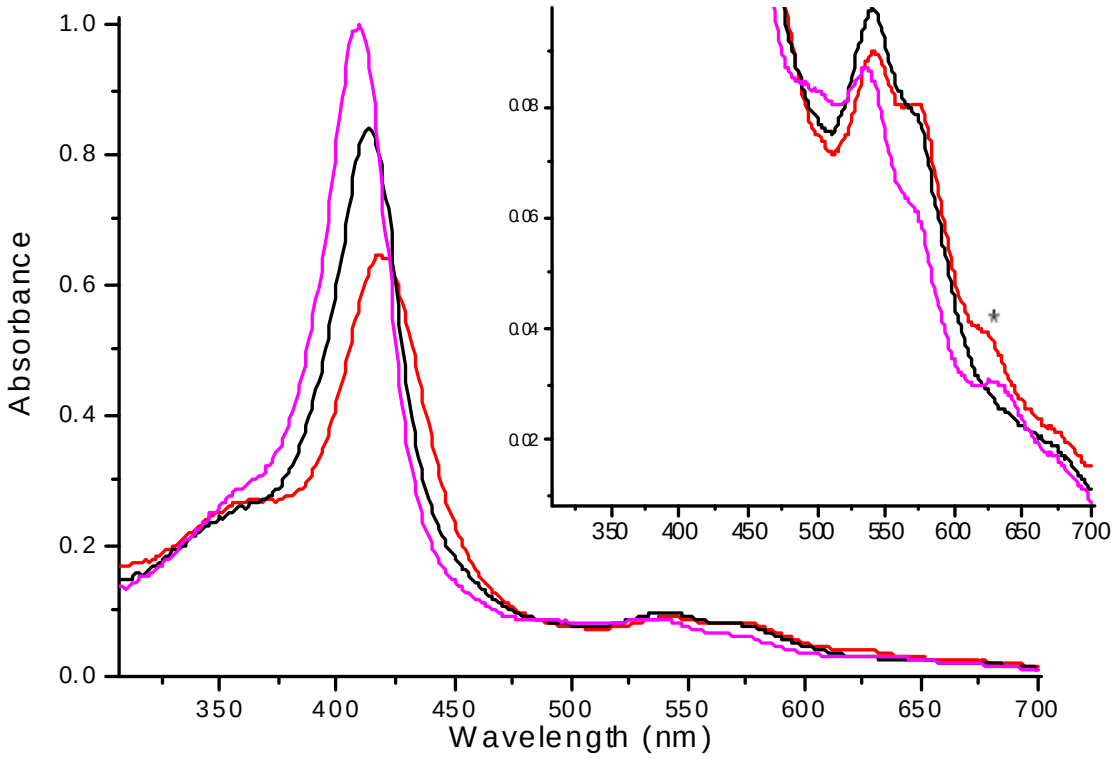

Figure 3.9 UV-Vis Spectra of the formation of sulfhemoglobin, starting from HbI GlnE7His mutant. The pink line spectrum represents the maximum absorption for met-HbI GlnE7His mutant. The maximum absorptions of the reaction between hydrogen peroxide and the mutant were represented by the black line spectrum. The red line spectrum represents the absorption displacements of the sequential addition of hydrogen sulfide, where the characteristic sulfheme band was observed at 626nm.

Table 3.7 Absorptions wavelengths (nm) of the UV-Vis Spectra for the Sulfhemoglobin complex formation upon the reaction between HbI GlnE7His mutant, hydrogen peroxide and hydrogen sulfide, in the presence of dissolved oxygen.

Description	**Soret**	**Q**	**Q**	**Q**	**Q**	**Sulf-complex (color)**
Met HbI GlnE7His	409_{vs}	500_{vw}	536_{s}	575_{vw}	632_{w}	-
Met HbI GlnE7His + H_2O_2	414_{vs}	No	540_{s}	576_{vw}	No	-
Met HbI GlnE7His + H_2O_2 + H_2S	419_{s}	No	542_{s}	575_{s}	No	$626_{vw\ (green)}$

The vs, s, w, and vw letters present in the table represent the absorption behavior of each band: vs = very strong, s = strong, w = weak, and vw = very weak. The (–) line indicates that the band is not applicable. The (No) implies that the band was not detectable. Units are in nanometer (nm).

Regarding this, Figure 3.10 demonstrates the absorption of the UV-Vis spectra of the reaction profile between HbI GlnE7His mutant and hydrogen peroxide with the sequential addition of the hydrogen sulfide, in the presence of dissolved oxygen. The pink line spectrum represents the met- HbI GlnE7His mutant, which is smilar to that of Figure 3.9, the characteristic Soret and Q bands for the metaquo complex are at 409nm, 500nm, and 632nm. The other two Q bands with absorptions at 534nm and 575nm indicate that the complex had a mixture of its high and low spin states. The black line spectrum represents the addition of hydrogen peroxide to the sample. A shift and a decrease in the maximum absorption of the Soret band to 413nm was observed. The Q bands shifted to 540nm and 574nm. The red line spectrum represents the sequential addition of the hydrogen sulfide to the sample. A shift and a decrease in the maximum absorption of the Soret band to 414nm were observed with shifts of the Q bands to 542nm and 575nm. The unique green color and the sulfheme band at 622nm were also observed. Therefore, it is concluded that histidine plays an essential role in the formation of the sulfheme complex. Apparently, for the sulfheme complex to form, histidine needs to be in the active site of the protein. Table 3.8, summarizes the optical absorption for the chemical reaction between HbI GlnE7His mutant, hydrogen peroxide, and hydrogen sulfide.

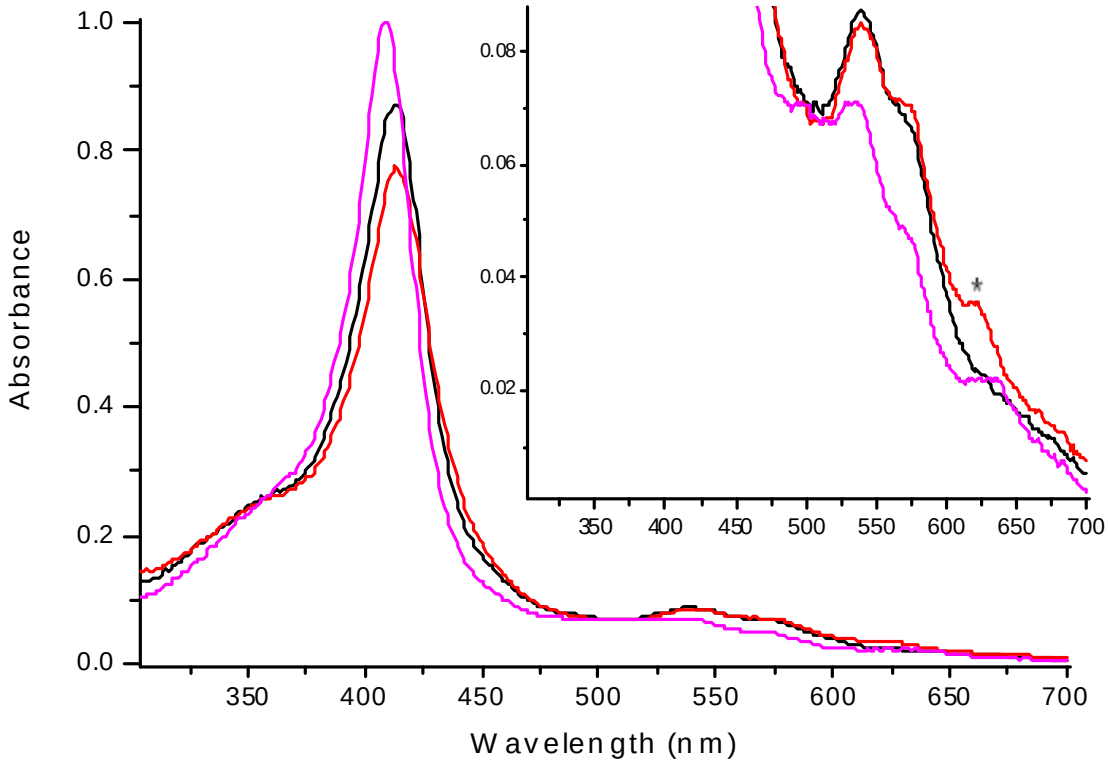

Figure 3.10 UV-Vis Spectra of the formation of sulfhemoglobin, starting from HbI GlnE7His mutant. The pink line spectrum represents the maximum absorption for met-HbI GlnE7His mutant. The maximum absorptions shifts from the reaction between the mutant and hydrogen peroxide were represented by the black line spectrum. The red line spectrum represents the absorption displacements after the sequential addition of hydrogen sulfide, where the characteristic 622nm band for the sulfheme complex was observed.

Table 3.8 Absorptions wavelengths (nm) of the UV-Vis Spectra for the Sulfhemoglobin complex formation upon reaction between HbI GlnE7His mutant, hydrogen peroxide and hydrogen sulfide, in the presence of dissolved oxygen.

Description	**Soret**	**Q**	**Q**	**Q**	**Q**	**Sulf-complex (color)**
Met HbI GlnE7His	409_{vs}	500_{vw}	534_{w}	575_{vw}	633_{w}	-
Met HbI GlnE7His + H_2O_2	413_{vs}	No	540_{w}	574_{vw}	No	-
Met HbI GlnE7His + H_2O_2 + H_2S	414_{vs}	No	542_{w}	575_{vw}	No	$622_{vw\ (green)}$

The vs, s, w, and vw letters present in the table represent the absorption behavior of each band: vs = very strong, s = strong, w = weak, and vw = very weak. The (–) line indicates that the band is not applicable. The (No) implies that the band was not detectable. Units are in nanometer (nm).

To confirm this hypothesis, Phe in the B10 position of HbI was changed to His. Figure 3.11 shows the structure of Phe and His, where Phe is a non polar aliphatic amino acid whiles His is a positive charge amino acid with the capacity to accept or donates a proton to form ionic bonds. Regarding this, Figure 3.12 represents the reaction profile of the UV-Vis Spectra of HbI PheB10His mutant with hydrogen peroxide, in the presence of dissolved oxygen, and the sequential addition of hydrogen sulfide to the sample. The pink line spectrum represents the met-HbI PheB10His mutant. The characteristic absorption of the met complex was observed at 409nm, 633nm, and a broad band from 495nm to 533nm. The broad band and the 565nm Q band indicate that the complex has a mixture of its high and low spin state. The black line spectrum represents the addition of hydrogen peroxide to the sample. A shift and a decrease in the maximum absorption of the Soret band to 410nm was observed. The Q bands decreased, but maintained the same absorption. The red line spectrum represents the sequential addition of hydrogen sulfide to the sample. A shift and a decrease in the maximum absorption of the Soret band to 424nm was observed, a region which is characteristic for the presence of the ferryl compound II. The Q bands absorptions shifted to 542nm and 574nm. The unique green color or the characteristic band for the sulfheme formation were not observed. In Table 3.9, the optical absorptions for the chemical reaction between HbI PheB10His, hydrogen peroxide and hydrogen sulfide are summarized. These results confirmed that Histidine plays an essential role in the sulfheme complex formation, but it needs to be specifically in the E7 position, since the formation of the sulfheme complex was only observed with the HbI GlnE7His mutant.

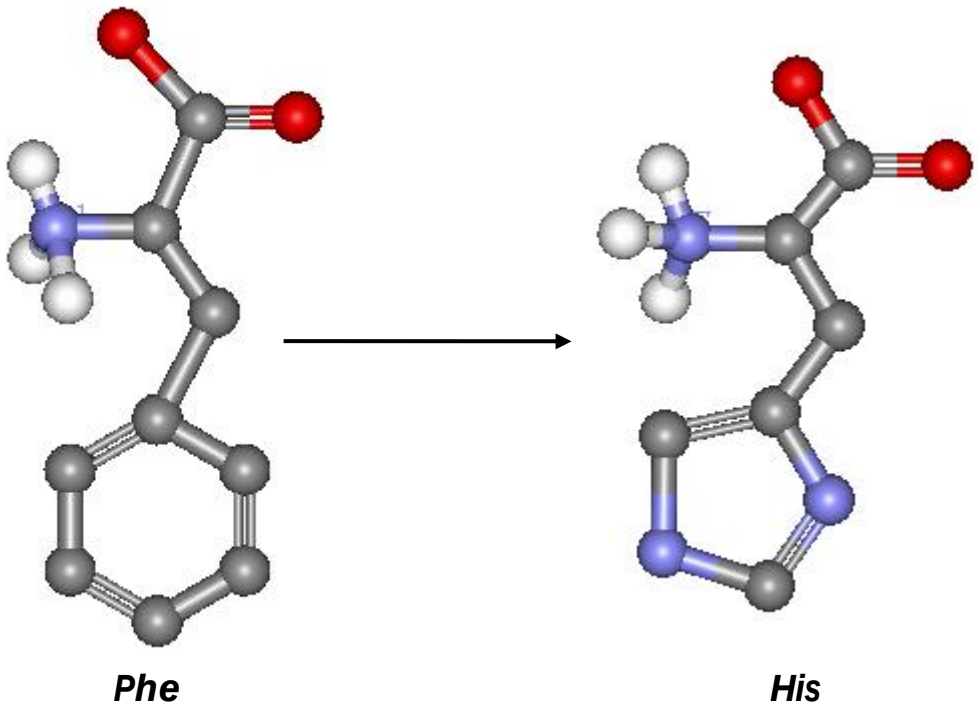

Figure 3.11 Structure of the phenylananine and histidine amino acids.

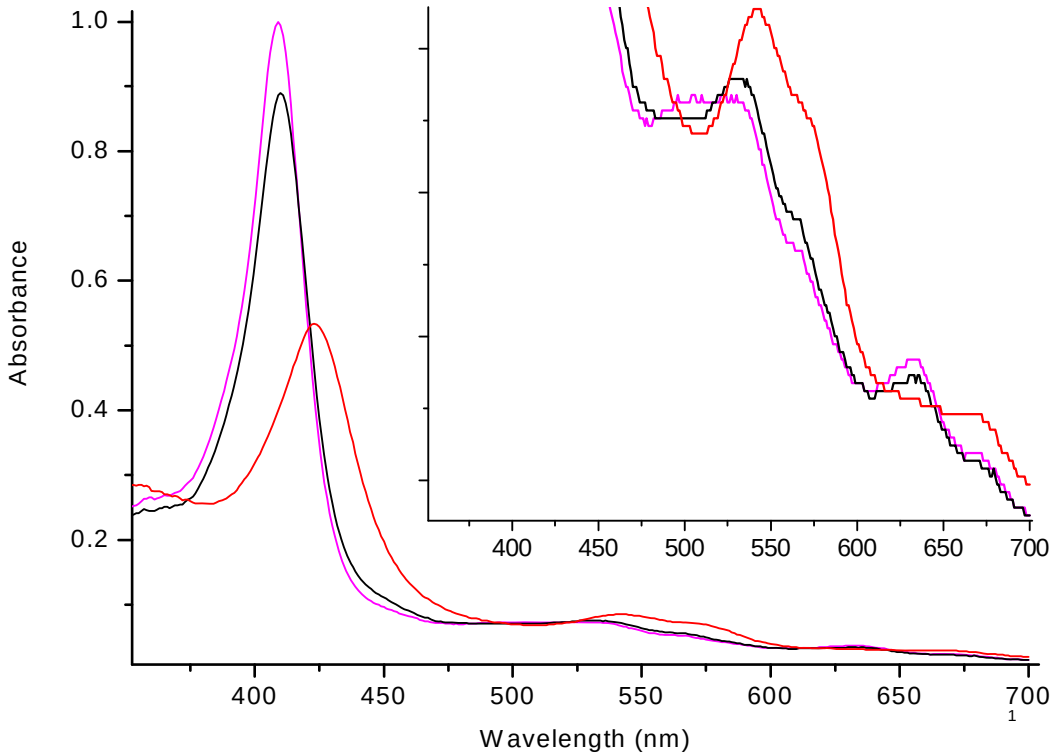

Figure 3.12 UV-Vis Spectra of the reaction of HbI PheB10His mutant and hydrogen peroxide, in the presence of dissolved oxygen, with the sequential addition of hydrogen sulfide. The pink line spectra represent the maximum absorption for met- HbI PheB10His mutant. The absorptions shifts of the reaction between the HbI PheB10His mutant and hydrogen peroxide are represented by the black line spectrum. The red line spectrum represent the absorption displacements after the sequential addition of hydrogen sulfide, where the characteristic 620nm band for the sulfheme complex was not observed.

Table 3.9 Absorption wavelengths (nm) of the UV-Vis Spectra upon reaction between HbI PheB10His mutant, hydrogen peroxide and hydrogen sulfide, in the presence of dissolved oxygen.

Description	**Soret**	**Q**	**Q**	**Q**	**Sulf-complex**
Met HbI PheB10His	409_{vs}	$495\text{-}533_{w}$	565_{vw}	633_{w}	-
Met HbI PheB10His + H_2O_2	410_{vs}	531_{w}	565_{vw}	633_{w}	-
Met HbI PheB10His + H_2O_2 + H_2S	424_{s}	542_{s}	575_{w}	No	No

The vs, s, w, and vw letters present in the table represent the absorption behavior of each band: vs = very strong, s = strong, w = weak, and vw = very weak. The (–) line indicates that the band is not applicable. The (No) implies that the band was not detectable. Units are in nanometer (nm).

Recent research by Pietri, R et al, 2008 (private communication) has demonstrated that the HbI PheB10Val and HbI GlnE7His mutants have the same reduction behavior in the presence of hydrogen sulfide excess. Thus, to discard a possible role or influence of this reduction process to the sulfheme formation, the HbI PheB10Val mutant was analyzed in the presence of hydrogen peroxide, hydrogen peroxide and oxygen. Figure 3.6 shows the structure of the valine and histidine residues, where Val is a non polar aliphatic amino acid whiles His is a positive charge amino acid. Consequently, Figure 3.13 shows the UV-Vis spectra of the reaction HbI PheB10Val mutant with hydrogen peroxide, in the presence of dissolved oxygen, and the sequential addition of hydrogen sulfide to the sample. The pink line spectrum represents the met-HbI PheB10Val mutant. The characteristic absorption of the met complex was observed at 410nm, 633nm, and a broad band from 491nm to 528nm. The broad band and the 565nm Q band indicate a mixture of the high and low spin states of the complex. The black line spectrum represents the addition of hydrogen sulfide to the sample, in the presence of oxygen. A shift and a decrease in the maximum absorption of the Soret band to 415nm was observed. The Q bands shifted to 538nm, 573nm with a very weak band at 633nm. The red line spectrum represents the reaction after 20 minutes of hydrogen sulfide addition. A shift of the maximum absorption of the Soret band to 417nm was observed. The Q bands maintained approximately the same absorptions at 540nm, 573nm, and 633nm. The green line spectrum represents the reaction after 30 minutes of hydrogen sulfide addition. The maximum absorption of the Soret band shifted to 421nm, region known for the presence of the ferryl species. The Q bands shifted to 540nm, 575nm, and 633nm. To promote the sulfheme complex formation, hydrogen peroxide

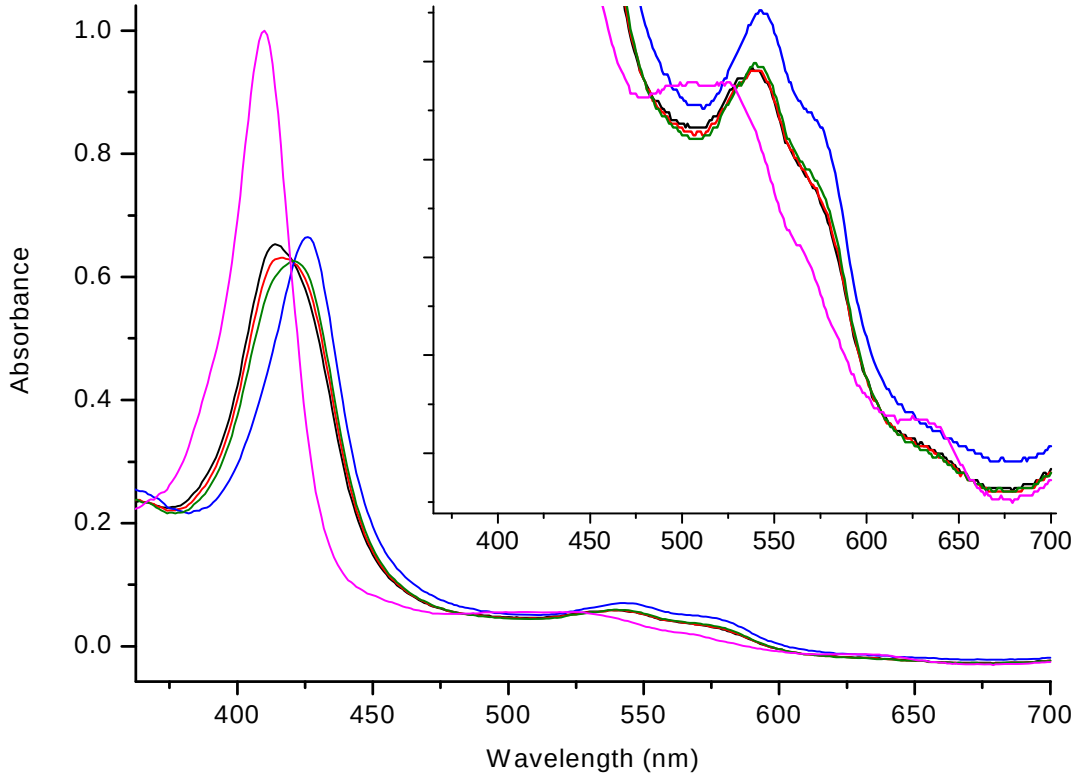

Figure 3.13 UV-Vis Spectra of the reaction for the formation of the sulfheme complex, starting from HbI Phe B10 Val mutant. The pink line spectrum represents the maximum absorption for met-HbI Phe B10 Val mutant. The maximum absorptions after 16 minutes of the reaction between the mutant and hydrogen sulfide, in the presence of dissolved oxygen, are represented by the black line spectrum. The reaction after 20 and 30 minutes are represented by the red and green line spectrum, respectively. The maximum absorptions upon the reaction between the mutant and hydrogen peroxide, in the presence of dissolved oxygen and hydrogen sulfide, are represented by the blue line spectrum. The characteristic sulfheme absorption at 620nm, was not observed at any moment.

was added to the sample. This is represented by the blue line spectrum. The maximum absorption of the Soret band shifted to 426nm, characteristic absorbance of the hydrogen sulfide complex. The unique green color or the characteristic 620nm sulfheme absorption band were not observed at any moment. In Table 3.10, the optical absorptions for the chemical reactions between HbI PheB10Val mutant, hydrogen peroxide, and hydrogen sulfide are summarized.

The HbI PheB10Val mutant did not form the sulfheme complex in the presence of hydrogen peroxide and hydrogen sulfide. Therefore, the reduction behavior of this mutant in the presence of hydrogen sulfide excess had no significant part in the formation of the sulfheme complex. This result confirmed previous suggestion in that His in the E7 position is essential for the sulfheme complex formation. Table 3.11 summarizes the proteins that formed the sulfheme complex.

In summary, the only proteins that formed the sulfheme derivative were the hemeproteins that had the histidine residue in the active site, exclusively in the E7 position. However, in order to further test the hypothesis, and prove that HisE7 is crucial for the sulfheme formation, it was imperative to prove that the HbI GlnE7His mutant should also form the suflheme complex under the same conditions that Mb forms the sulfheme complex. For that reason, the chemical reactions of the met and oxy complexes of HbI GlnE7His mutant with hydrogen sulfide were performed, in the presence of oxygen and absence of hydrogen peroxide.

Table 3.10 Absorption wavelengths (nm) of the UV-Vis Spectra upon the reaction between HbI PheB10Val mutant, hydrogen peroxide and hydrogen sulfide, in the presence of dissolved oxygen.

Description	**Soret**	**Q**	**Q**	**Q**	**Sulf-complex**
Met HbI PheB10Val	410_{vs}	$491\text{-}528_{vw}$	$563\text{-}567_{vw}$	633_{w}	-
Met HbI PheB10Val + H_2S - 16 min	415_{s}	538_{w}	573_{w}	633_{vw}	No
Met HbI PheB10Val + H_2S - 20 min	417_{s}	540_{w}	573_{w}	633_{vw}	No
Met HbI PheB10Val + H_2S - 30 min	421_{s}	540_{w}	575_{w}	633_{vw}	No
Met HbI PheB10Val + H_2S - 30 min + H_2O_2	426_{s}	543_{w}	576_{w}	No	No

The vs, s, w, and vw letters present in the table represent the absorption behavior of each band: vs = very strong, s = strong, w = weak, and vw = very weak. The (–) line indicates that the band is not applicable. The (No) implies that the band was not detectable. Units are in nanometer (nm).

Table 3.11 Summary of the proteins that formed the sulfheme complex, with their correspondent amino acid residue.

Protein	Residue Positions			Sulfheme
	E7	B10	E11	
wt-horse heart Mb	His	Leu	Val	X
wt-human Hb	His	Leu	Val	X
wt-HbI	Gln	Phe	Phe	
wt-HbII/HbIII	Gln	Tyr	Phe	
PheE11Val	Gln	Tyr	Val	
GlnE7His	His	Phe	Phe	X
PheB10His	Gln	His	Phe	
PheB10Val	Gln	Val	Phe	

The (X) indicate that the complex was observed.

As a consequence, Figure 3.14 shows UV-Vis Spectra of the reaction between met-Mb with hydrogen sulfide in the presence of oxygen, for the formation of the sulfmyoglobin complex. The pink line spectrum represents the maximum absorptions for met-Mb complex, where the Soret band is at 410nm and the Q bands are at 504nm and 633nm. The black line spectrum represents the absorptions when 1.86μL of hydrogen sulfide were added to the sample, in the presence of dissolved oxygen and a third oxygen injection. The Soret band remained the same, but two new Q bands were observed at 544nm and 581nm. The 633nm absorption band disappeared while the 505nm absorption band remained present. The characteristic sulfheme absorption was observed at 625nm. An additional 1.64μL of hydrogen sulfide and an oxygen injection was added to the sample to promote the complete formation of the sulfheme complex, which is represented by the red line spectrum. The Soret and Q bands presented absorptions at 410nm, 505nm, 542nm, and 581nm, respectively. The sulfheme absorption shifted to 623nm. The green line spectrum represents the absorption on the next day. The Soret and Q bands maintained practically the same optical absorptions at 411nm, 503nm, 542nm, and 581nm, respectively. The sulfheme absorption was present and stable, at 620nm after 24 hours. The unique green color was never seen; instead the sample maintained a red color at all times. In Table 3.12, the optical absorption shifts upon the chemical reaction between met-Mb with hydrogen sulfide, in the presence of oxygen, are summarized. The chemical reaction between met-Mb, hydrogen sulfide and oxygen, in the absence of hydrogen peroxide, shows the formation of the sulfheme.

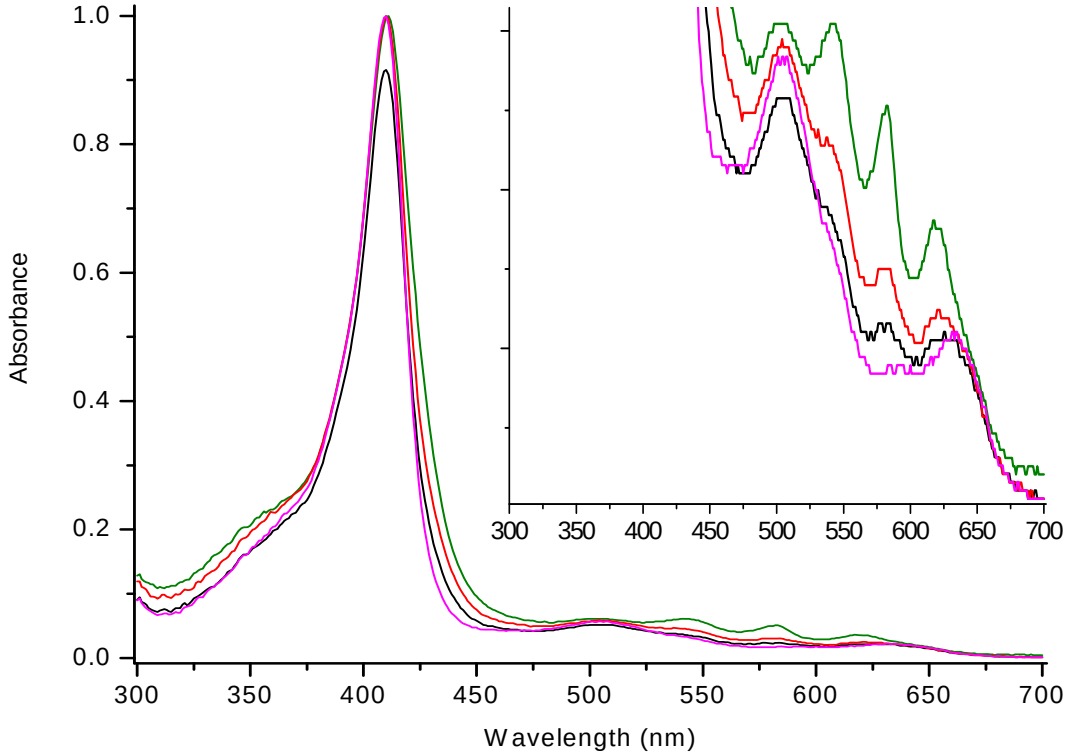

Figure 3.14 UV-Vis Spectra of the reaction for the formation of the sulfmyoglobin complex, starting from met-Mb. The pink line spectrum represents the maximum absorption for met-Mb. The maximum absorptions shifts when 1.86µL of hydrogen sulfide were added to the sample, in presence of dissolved oxygen and a third injection of oxygen, are represented by the black line spectrum. The red line represents the absorption when adding an additional 1.64µL of hydrogen sulfide and oxygen injection. The green line spectrum represents the absorptions observed the next day. The sulfheme complex was observed at 620nm.

Table 3.12 Absorptions wavelength (nm) of the UV-Vis Spectra of the Sulfmyoglobin complex formation upon reaction between horse heart myoglobin with hydrogen sulfide, in the presence of dissolved oxygen.

Description	**Soret**	**Q**	**Q**	**Q**	**Q**	**Sulf-complex (color)**
Met Mb + dO_2	410_{vs}	504_{s}	No	No	633_{w}	-
Met Mb + dO_2 + 1.86uL H_2S 1M + 3^{rd} $O_{2\ inj}$	410_{vs}	505_{s}	544_{vw}	581_{vw}	No	$625_{w\ (red)}$
Met Mb + dO_2 + 3.5uL H_2S 1M + 4^{th} $O_{2\ inj}$	410_{vs}	505_{s}	542_{w}	581_{w}	No	$623_{w\ (red)}$
Met Mb + dO_2 + 3.5uL H_2S 1M + 4^{th} $O_{2\ inj}$ at next day	411_{vs}	503_{s}	542_{s}	581_{s}	No	$620_{s\ (red)}$

The vs, s, w, and vw letters present in the table represent the absorption behavior of each band: vs = very strong, s = strong, w = weak, and vw = very weak. The (–) line indicates that the band is not applicable. The (No) implies that the band was not detectable. Units are in nanometer (nm).

Likewise, Figure 3.15 shows the UV-Vis Spectra of the reaction between met-HbI GlnE7His mutant and hydrogen sulfide, in the presence of dissolved oxygen. The pink line represents the maximum absorption for met-HbI GlnE7His mutant. The Soret band was at 408nm and the Q bands at 500nm, 570nm, and 633nm. The black line represents the maximum absorption after purging the sample with an injection filled with oxygen and adding 1.6μL more of hydrogen sulfide. Immediately, a shift in the maximum absorption of the Soret band was observed at 411nm. The 500nm and 633nm Q bands decreased in intensity while two new Q bands were observed at 539nm and 574nm. However, the characteristic sulfheme absorption was not present. After some time, a shift of the Soret band to 416nm, region known for the presence of the ferryl species, specifically the ferryl compound I, was observed. The Q bands shifted to 542nm, 574nm, and 630nm, while the 500nm band disappeared. This was represented by the red line spectrum. The green line spectrum represents the maximum absorption when the sample was injected for a second time with oxygen and 0.8μL of hydrogen sulfide, in order to promote the formation of the sulfheme complex. The Soret band maintained the same maximum absorption at 416nm, and only one Q band displayed a shift from 574nm to 576nm. The characteristic sulfheme absorption was observed by a very weak band at 626nm. The unique green color was never observed during the reaction, instead it maintiained a red color. In Table 3.13, the absorption shifts upon the chemical reaction between HbI GlnE7His and hydrogen sulfide, in the presence of oxygen, are summarized. Given that the HbI GlnE7His mutant formed the sulfheme complex upon the reaction with hydrogen sulfide and oxygen, in the absence of hydrogen peroxide as in Mb, reinforces the hypothesis that HisE7 is crucial for the formation of the sulfheme complex.

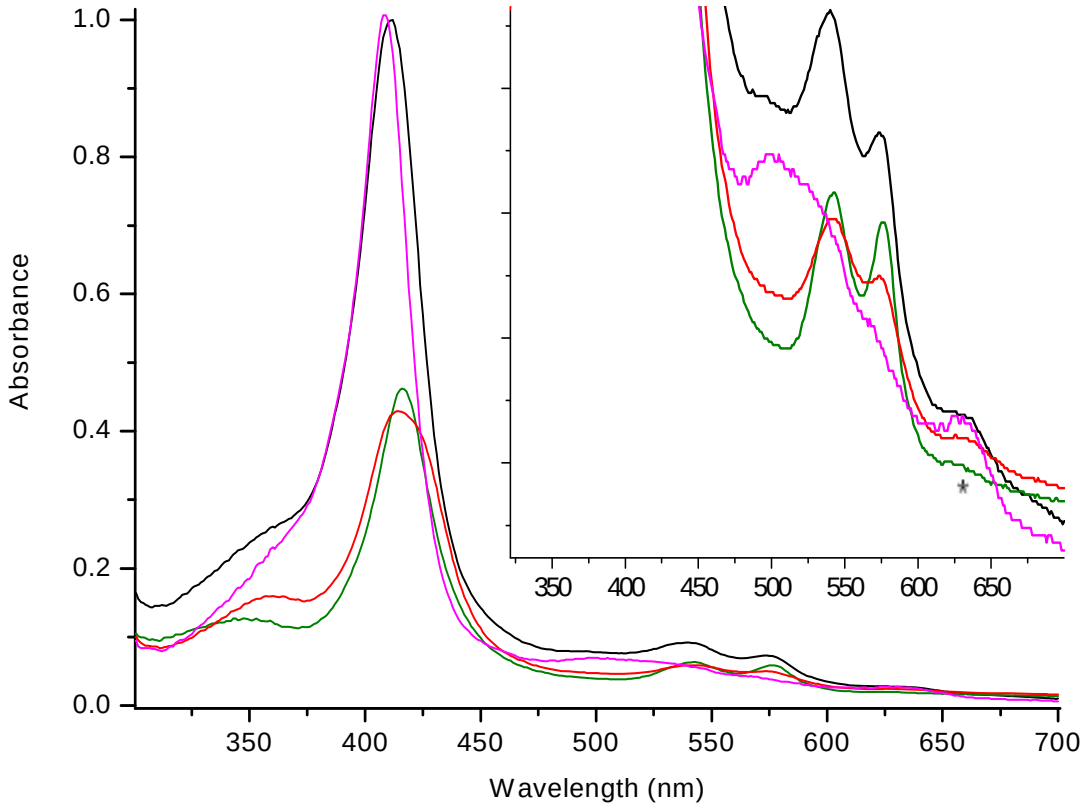

Figure 3.15 UV-Vis Spectra of the formation reaction of sulfhemoglobin, starting from HbI Gln E7 His mutant. The pink line spectrum represents the maximum absorption for met-HbI GlnE7His mutant. The shifts of the maximum absorptions when 1.6µL of hydrogen sulfide is added to the sample, in presence of dissolved oxygen and an injection of oxygen, are represented by the black line spectrum. The red line spectrum represents the absorption after 20 minutes. The green line spectrum shows the absorption after 0.8µL of hydrogen sulfide and a second injection of oxygen, where the presence of the characteristic band of the sulfheme complex at 626nm can be observe.

Table 3.13 Absorption wavelengths (nm) of the UV-Vis Spectra for the Sulfhemoglobin complex formation upon the reaction between HbI GlnE7His with hydrogen sulfide, in the presence of dissolved oxygen.

Description	**Soret**	**Q**	**Q**	**Q**	**Q**	**Sulf-complex (color)**
Met HbI GlnE7His	408	500	No	570	633	-
Met HbI GlnE7His + 1st $O_{2\ inj}$ + 1.6uL H_2S 1M	411_{vs}	500_{vw}	539_{s}	574_{s}	633_{w}	No
Met HbI GlnE7His + 1st $O_{2\ inj}$ + 1.6uL H_2S 1M	416_{w}	No	542_{s}	574_{s}	630_{w}	No
Met HbI GlnE7His + 2nd $O_{2\ inj}$ + 2.4uL H_2S 1M	416_{w}	No	542_{s}	576_{s}	No	$626_{vw\ (red)}$

The vs, s, w, and vw letters present in the table represent the absorption behavior of each band: vs = very strong, s = strong, w = weak, and vw = very weak. The (–) line indicates that the band is not applicable. The (No) implies that the band was not detectable. Units are in nanometer (nm).

Similarly, Figure 3.16 shows the UV-Vis Spectra of the reaction between oxy-Mb and hydrogen sulfide, in presence of dissolved oxygen. The pink line represents the maximum absorption of oxy-Mb. The Soret band was at 417nm and the Q bands were at 503nm, 544nm and 581nm. The black line spectrum represents the maximum absorption when hydrogen sulfide is added to the sample. The Soret and Q bands maintained the same absorption, but the 503nm band disappeared. The characteristic sulfheme band was observed as a very weak 623nm band. The red line spectrum shows the absorption after 75 minutes of the addition of hydrogen sulfide. The Soret band shifted to 412nm, but the Q bands maintained the same absorption at 544nm and 581nm. The 505nm band reappeared while the sulfheme band shifted to 620nm, remaining present and stable after 75 minutes. The unique green color was never observed, instead the sample maintained a red color.

In Table 3.14, the absorption shifts of oxy Mb upon the chemical reaction with hydrogen sulfide and oxygen are summarized, in the absence of hydrogen peroxide. Regarding this, Figure 3.17 shows the UV-Vis Spectra of the reaction between hydrogen sulfide and the oxy-HbI GlnE7His mutant in the presence of dissolved oxygen. The pink line represents the maximum absorption for oxy-HbI GlnE7His mutant. The Soret band is at 417nm and the Q bands are at 542nm and 576nm. The black line represents the maximum absorption after 20 minutes of the addition of 1μL of hydrogen sulfide. Only, a decrease in the maximum absorption of the Soret and Q bands was observed. Since no change was observed after 40 minutes, in order to promote the formation of the sulfheme

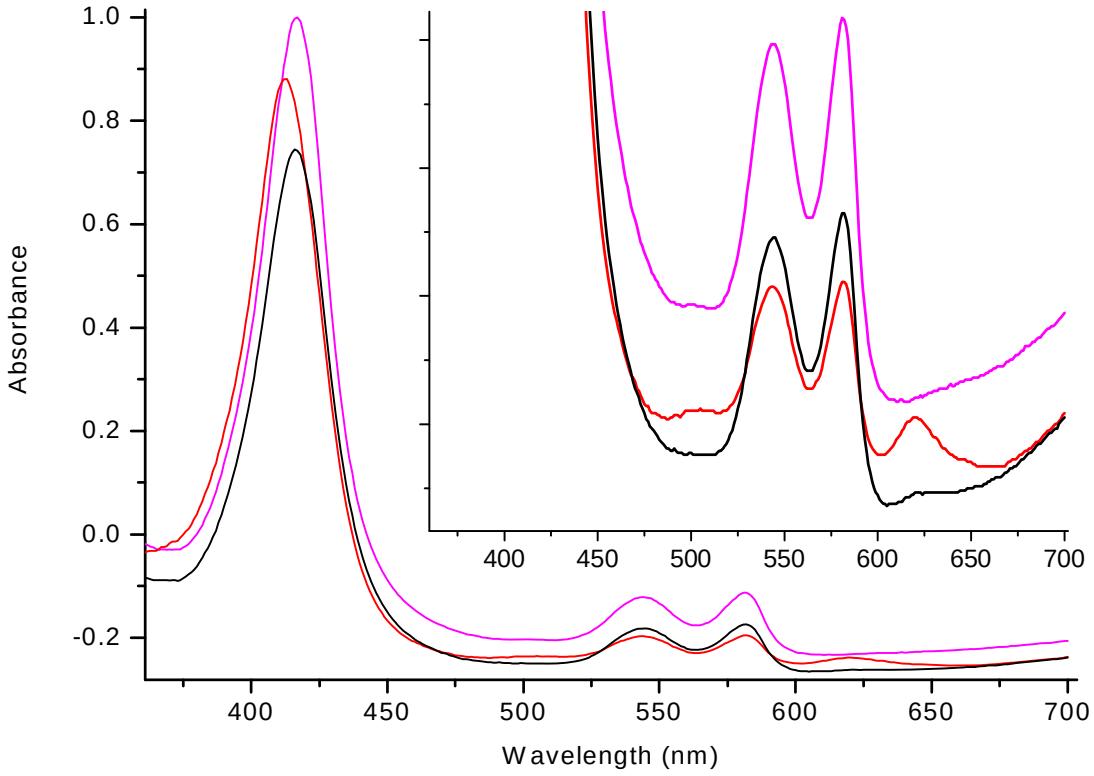

Figure 3.16 UV-Vis Spectra of the reaction for the formation of the sulfmyoglobin complex, starting from oxy Mb. The pink line spectrum represents the maximum absorption for oxy Mb. The black line spectrum shows the optical absorptions shifts when hydrogen sulfide is added to the sample, in presence of dissolved oxygen. The red line spectrum represents the absorption displacements after 75 minutes of addition of hydrogen sulfide. The characteristic sulfheme band can be observed at 620nm.

Table 3.14 Absorption wavelength (nm) of the UV-Vis Spectra for the Sulfmyoglobin complex formation upon reaction between horse heart myoglobin with hydrogen sulfide, in the presence of dissolved oxygen.

Description	**Soret**	**Q**	**Q**	**Q**	**Sulf-complex (color)**
Oxy Mb	417_{vs}	503_{vw}	544_{s}	581_{s}	-
Oxy Mb + dO_2 + H_2S	417_{vs}	No	544_{s}	581_{s}	$623_{vw\ (red)}$
Oxy Mb + dO_2 + H_2S - 30 min	414_{vs}	505_{vw}	544_{s}	581_{s}	$620_{w\ (red)}$
Oxy Mb + dO_2 + H_2S - 75 min	412_{vs}	505_{vw}	544_{s}	581_{s}	$620_{w\ (red)}$

The vs, s, w, and vw letters present in the table represent the absorption behavior of each band: vs = very strong, s = strong, w = weak, and vw = very weak. The (–) line indicates that the band is not applicable. The (No) implies that the band was not detectable. Units are in nanometer (nm).

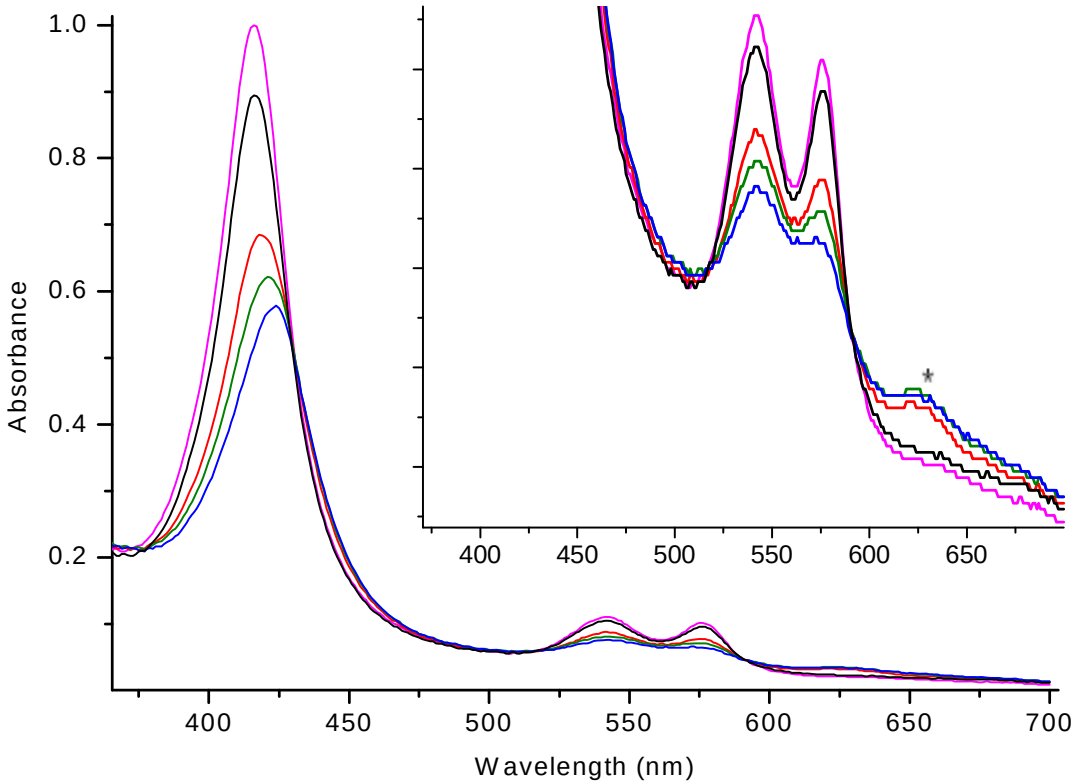

Figure 3.17 UV-Vis Spectra of the formation reaction of sulfhemoglobin, starting from oxy- HbI GlnE7His mutant. The pink line spectrum represents the maximum absorption for oxy- HbI GlnE7His mutant. The maximum absorptions when 1uL of hydrogen sulfide is added to the sample in presence of dissolved oxygen are represented by the black line spectrum. The red line spectrum represents the absorption displacements after 20 minutes of adding 2uL of hydrogen sulfide, where one can already observe the presence of the characteristic band of the sulfheme complex at 624nm. The green line spectrum represents the absorptions after 60 minutes of the addition of hydrogen sulfide. The blue line spectrum represents the absorptions after 95 minutes of the addition of hydrogen sulfide.

complex, an additional μL of hydrogen sulfide was added to the sample. This is represented by the red line. Immediately, the presence of the characteristic sulfheme complex band at 626nm was observed. A decrease and a shift in the maximum absorption of the Soret band to 419nm, region known for the presence of the ferryl species, was also observed. The maximum absorption of the Q bands decreased as well. The green line represents the shifts after 60 minutes. The maximum absorption of the Soret band was observed at 421nm, a region known for the presence of the ferryl compound II. The Q bands shifted to 543nm and 574nm. The characteristic sulfheme band shifted to 624nm. The blue line represents the absorptions after 95 minutes. There, the Soret band was observed at 424nm, a region still known as the presence of the ferryl compound II. The Q bands maintained exactly the same wavelength maxima, with a slight decrease in their absorption. As for the characteristic sulfheme band, it was still present and stable at 625nm. The unique green color was never observed; the sample maintained the initial red color.

In Table 3.15, the absorption shifts upon the reaction of oxy-HbI GlnE7His mutant with hydrogen sulfide, in the presence of oxygen, are summarized. Given that the oxy-HbI GlnE7His mutant formed the sulfheme complex upon the reaction with hydrogen sulfide and oxygen, in the absence of hydrogen peroxide does oxy-Mb, it strengthened the hypothesis that HisE7 is crucial for the formation of the sulfheme complex. The data clearly shows that the HbI GlnE7His mutant forms the sulfheme complex under the same conditions as Mb forms the sulfheme complex. Table 3.16 summarizes the reactions of Mb versus HbI GlnE7His mutant, under the same conditions.

Table 3.15 Absorptions wavelengths (nm) of the UV-Vis Spectra for the Sulfhemoglobin complex formation upon the reaction between HbI GlnE7His mutant with hydrogen sulfide, in the presence of dissolved oxygen.

Description	**Soret**	**Q**	**Q**	**Sulf-Complex (color)**
Oxy HbI GlnE7His	417_{vs}	542_{vs}	576_{vs}	-
Oxy HbI GlnE7His + 1uL H_2S + dO_2 - 20min	417_{vs}	542_{vs}	577_{vs}	No
Oxy HbI GlnE7His + 2uL H_2S + dO_2 - 40min	419_{s}	542_{s}	575_{s}	$626_{vw\ (red)}$
Oxy HbI GlnE7His + 2uL H_2S + dO_2 - 60min	421_{s}	543_{s}	574_{s}	$624_{vw\ (red)}$
Oxy HbI GlnE7His + 2uL H_2S + dO_2 - 95min	424_{s}	543_{s}	574_{s}	$625_{vw\ (red)}$

The vs, s, w, and vw letters present in the table represent the absorption behavior of each band: vs = very strong, s = strong, w = weak, and vw = very weak. The (–) line indicates that the band is not applicable. The (No) implies that the band was not detectable. Units are in nanometer (nm).

Table 3.16 Summary of Mb reactions versus HbI GlnE7His mutant reactions for the formation of the sulfheme coplex.

Protein	Reaction	Residues			Sufheme
		E7	B10	E11	
met-horse heart Mb	dissolved O_2 + H_2S	His	Leu	Val	X
met-GlnE7His HbI	dissolved O_2 + H_2S	His	Phe	Phe	X
oxy-horse heart Mb	dissolved O_2 + H_2S	His	Leu	Val	X
oxy-GlnE7His HbI	dissolved O_2 + H_2S	His	Phe	Phe	X

The (X) indicates that the complex was observed.

The fact that the sulfheme complex was observed using the HbI GlnE7His mutant, no matter the oxidation state of the heme iron or ligand, confirms and reassures the fact that His in the E7 position is responsible for the sulfheme formation. Furthermore, the fact that in the absence of hydrogen peroxide, the characteristic sulfheme band was observed but not the distinctly green color of this sulfheme derivative, in both Mb and HbI GlnE7His mutant, suggests that the green color could be produced by the degradation of the protein upon the reaction with hydrogen peroxide and not to the attributed β-β bond, since the green color was only observed when using hydrogen peroxide.

3.3 Chemical Structure of the heme center in sulfMb and sulfHbI GlnE7His mutant.

The reaction of the heme proteins with H_2S and H_2O_2 presented in the previous sections induced spectral changes characteristic of the known oxy, H_2S, metaquo, and ferryl complexes of the hemoglobins, as shown in Table 3.8. For instance, the final absorptions displacements of met-HbI, met-HbI PheE11Val mutant, and met-HbI PheB10Val mutant, upon the reaction with hydrogen peroxide and hydrogen sulfide in the presence of oxygen, suggest the formation of the heme-H_2S complex. On the other hand, the met-HbI GlnE7His mutant final spectrum, obtained from the reaction with hydrogen sulfide in the presence of oxygen and absence of hydrogen peroxide, suggest a reduction of the hemeprotein to the oxy complex with the coexistence of the sulfheme complex as the final product. However, the final absorption s of the met-human Hb, met-HbII/HbIII mixture, met-HbI GlnE7His mutant, and met-PheB10His mutant, upon the reaction with hydrogen peroxide and hydrogen sulfide in the presence of oxygen, suggest a possible mixture of the oxy and heme-H_2S complexes or the formation of one of the both. For met-human Hb and met-HbI GlnE7His mutant, the final complex, that results from this reaction coexist, with the sulfheme complex. Similarly, the final absorptions of the chemical reaction between oxy-HbI GlnE7His mutant and hydrogen sulfide, in the presence of oxygen, suggest the formation of a possible mixture of the oxy and hydrogen sulfide complexes or the formation of one of the both with the sulfheme derivative, as the final product. However, all final absorptions displacements of the chemical reaction with horse heart Mb, do not show similar Soret and Q bands of the known heme complexes, suggesting the possible formation of any of the oxy, hydrogen sulfide, and heme-ferryl

Table 3.17 Summary of optical absorptions of the hemeproteins with their corresponding possible final complex.

Protein	Soret	Q	Q	Q	Q	Sulfheme Complex	Possible Complex Product Formed		
							Oxy	H_2S	Comp II
Met-horse heart Mb	420	506	548	586	No	620	X	X	X
Met-human Hb	421	505	541	574	No	620	X	X	
Met-HbI	426	No	544	575	No	No		X	
Met-HbII/HbIII	422	No	543	576	No	No	X	X	
Met-HbI PheE11Val	426	No	544	575	633	No		X	
Met-HbI GlnE7His	419-414	No	542	575	No	622-626	X	X	
Met-HbI PheB10His	424	No	542	575	No	No	X	X	
Met-HbI PheB10Val	426	No	543	576	No	No		X	
Met-horse heart Mb, absence of H_2O_2	411	503	542	581	No	620	X	X	X
Oxy-horse heart Mb, absence of H_2O_2	412	505	544	581	No	620	X	X	X
Met-HbI GlnE7His, absence of H_2O_2	416	No	542	576	No	626	X		
Oxy-HbI GlnE7His, absence of H_2O_2	424	No	543	574	No	625	X	X	

The (No) implies that the band was not detectable. The (X) represents the possible complexes. Units are in nanometer (nm).

Table 3.18 Characteristic optical absorptions displacements of Compound II, Oxy HbI, Met HbI, and H_2S HbI complexes.

Complex	**Soret**	**Q**	**Q**	**Q**	**Q**
Compound II-Mb	418-424	-	540	581	-
Oxy-HbI	416	-	541	576	-
Met-HbI	407	502	-	-	633
H_2S-HbI	426	-	544	574	-

The (–) line indicates were a band is not applicable. Units are in nanometer (nm).

complexes or the formation of other complex. For example, the Soret and Q bands of the SMb upon the reaction with hydrogen peroxide and hydrogen sulfide, in the presence of oxygen, are at 420nm, 506nm, 548nm, 586nm and 620nm. The characteristic maximum absorption of the Soret band for the met, oxy, heme-H_2S, and ferryl compound II heme proteins complexes are 407nm, 416nm, 426nm, and 420nm. Hence, the 420nm absorption in SMb suggest the presence of the heme-ferryl compound II in coexistence with the sulfheme derivative. However, the 548nm and 586nm absorptions are not similar to 540nm and 581nm, which are characteristics of the heme-ferryl compound II complex or with the 541nm and 576nm, characteristic of the oxy complex, which suggest that the heme-ferryl compound II and the oxy complexes do not co-exists with the sulfheme complex. The 506nm absorbance is similar to the 502nm characteristic for the met complex, nonetheless, the other characteristic absorbance at 407nm and 633nm were not observed. These suggest that the met-complex does not co-exist as a final product with the sulfheme derivative. Therefore, the formation of another complex or any mixture between the oxy, hydrogen sulfide, and heme-ferryl complexes could co-exist with the sulfheme derivative as the final product.

It is important to study the structural, oxidation and ligand variation of theese sulfheme derivatives produced by the formation of the sulfheme species because they generate sulfhemoglobinemia. The isomeric sulfMb derivatives are found to behave different in their ligand affinity and chemical stability properties. Therefore, their reactivity patterns are different. Ligand affinities differ substantially among the isomeric sulfMbs in the order of SAMb<SBMb<SCMb<Mb. Little information exists on the source of this altered reactivity. The chemical properties are affected by steric

perturbations by distal amino acids in the side chains, electronic perturbations by peripheral heme interactions, proximal axial interactions via the ligated histidyl imidazole or whichever mixtures of these effects (Chatfield et al, 1987).

The chemical reaction between met-horse heart Mb with hydrogen sulfide at a pH of 6.5, in the presence of oxygen, leads to a sample with ^{1}H NMR Spectrum as shown in Figure 3.18, taken with a spectral window of 200ppm and increasing temperature ranging from 278˚K to 303˚K. The downfield of the SMb spectrum, from 278 to 303˚K, is showed in Figure 3.19, where the changes in intensity and displacements of the real peaks are clearly observed. As a result the peak can be distinguished from the baseline noise and peaks that are cover up by other peaks may be observed. For example, with increase in temperature from 278˚K to 303˚K the marked peak shifts (labeled *) from 92.22ppm to 82.72 ppm at the same time that it increases in intensity, respectively.

Regarding this, Table 3.19 summarizes the overall results of the shifts, with change in temperature from 278˚K to 303˚K, of the 200ppm spectral window. To have a more clear downfield and upfield view, Figure 3.20 shows the SMb ^{1}H NMR spectrum, with a spectral window of 34 ppm. Figure 3.21 and 3.22 shows the downfield and upfield of the SMb ^{1}H NMR Spectrum with a spectral window of 34 ppm. In the downfield spectrum, the marked peak with changes in temperature, from 278˚K to 303˚K, shifts from more than 20.63ppm to 18.81ppm with increasing intensity. Similarly, in the upfield spectrum, the marked peak shifts with changes in temperature from more than -5.11ppm to -3.87ppm, with increasing intensity.

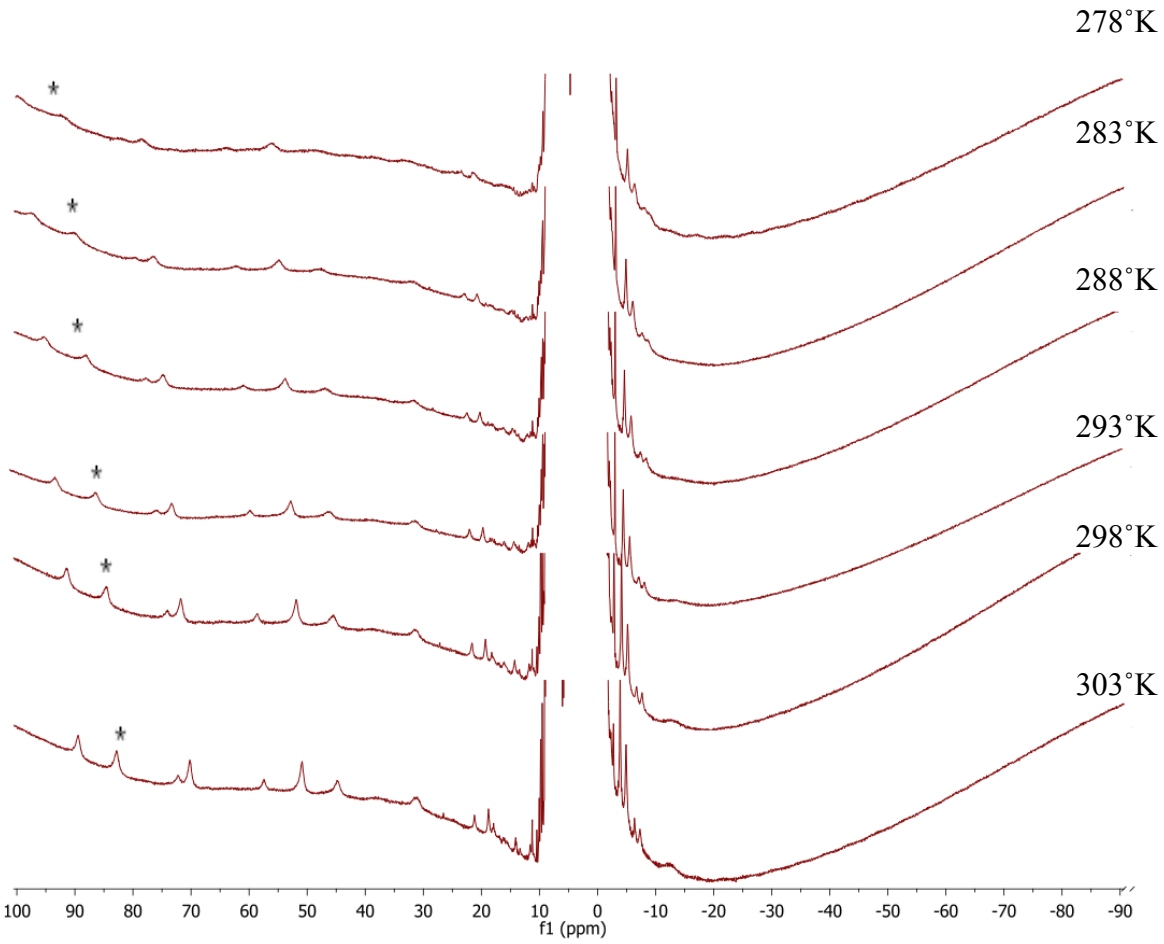

Figure 3.18 shows the shifts at a 200ppm spectral window of the 1H NMR spectrum, with changes in temperature from 303˚K to 278˚K, of the SMb sample formed upon the reaction of the hemeprotein with hydrogen sulfide, in the presence of oxygen, as a function of temperature. The shift and increase in intensity of the marked peak from 92.22ppm to 82.72ppm with changes in temperature from 278˚K to 303˚K is observed.

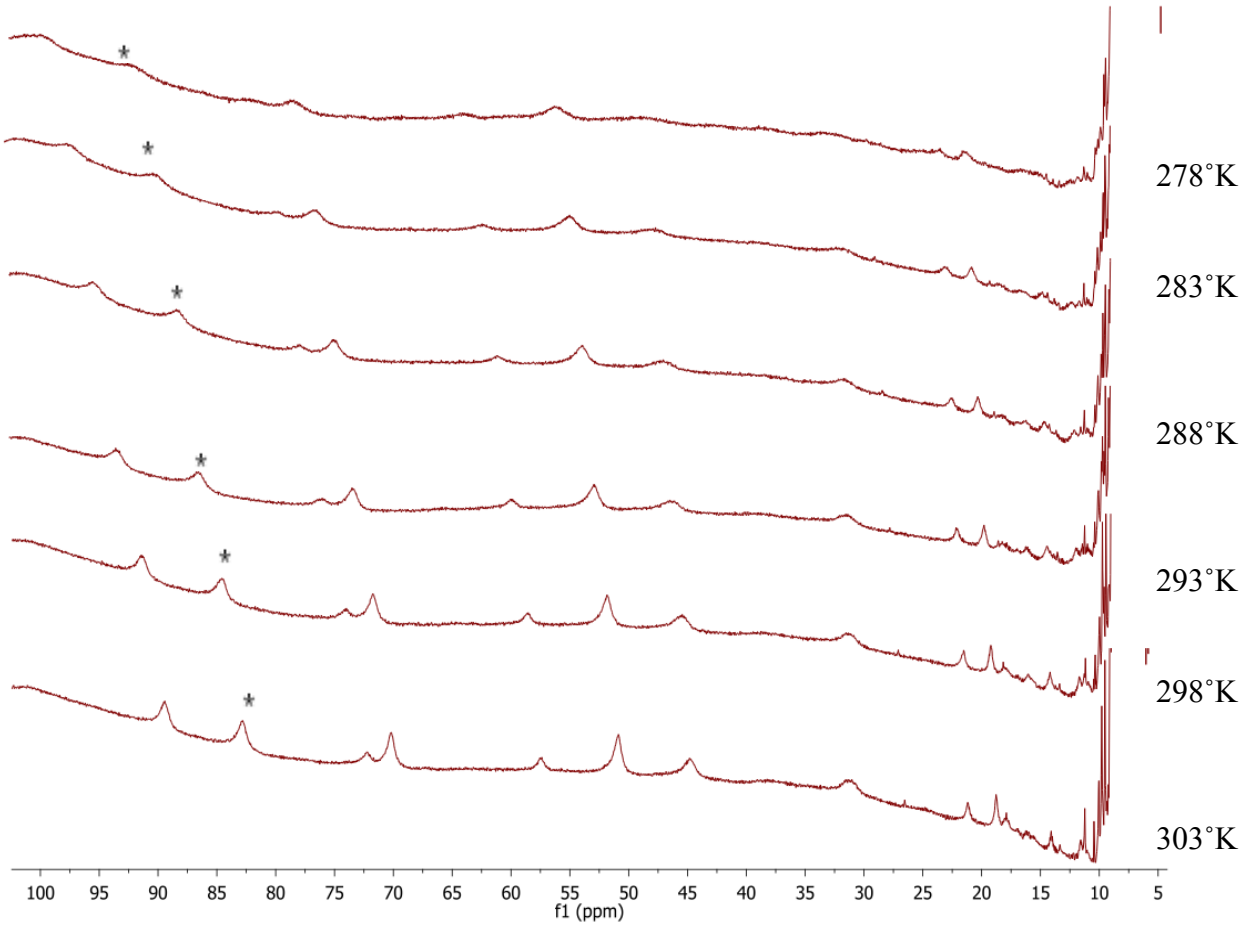

Figure 3.19 shows the downfield shifts at a 200ppm spectral window of the 1H NMR spectrum, with changes in temperature from 303˚K to 278˚K, of the SMb sample formed upon the reaction of the hemeprotein with hydrogen sulfide, in the presence of oxygen, as a function of temperature. For example, with increase in temperature from 278˚K to 303˚K the marked peak shifted from 92.22ppm to 82.72 ppm at the same time that it increases in intensity, respectively.

Table 3.19 Summarizes the downfield shifts (ppm) at a 200ppm spectral window of the 1H NMR spectrum, with changes in temperature from 303˚K to 278˚K, of the SMb sample formed upon reaction of the hemeprotein with hydrogen sulfide, in the presence of oxygen.

Downfield-^{1}H NMR Shifts, spectral window of 200ppm	
Chemical Shift of the Sulfmyoglobin Complex	
From 303˚K	**To 278˚K**
17.79	19.69
18.79	21.35
21.14	23.30
26.42	29.71
31.15	32.90
37.70	38.60
44.79	48.73
51.03	56.11
57.42	64.01
63.39	↓
70.21	78.48
72.17	81.94
82.72	92.22
89.39	100.00

The (-) indicates that it has not been assigned. The (↓) indicate that the peak decrease in intensity until it was no longer observed.

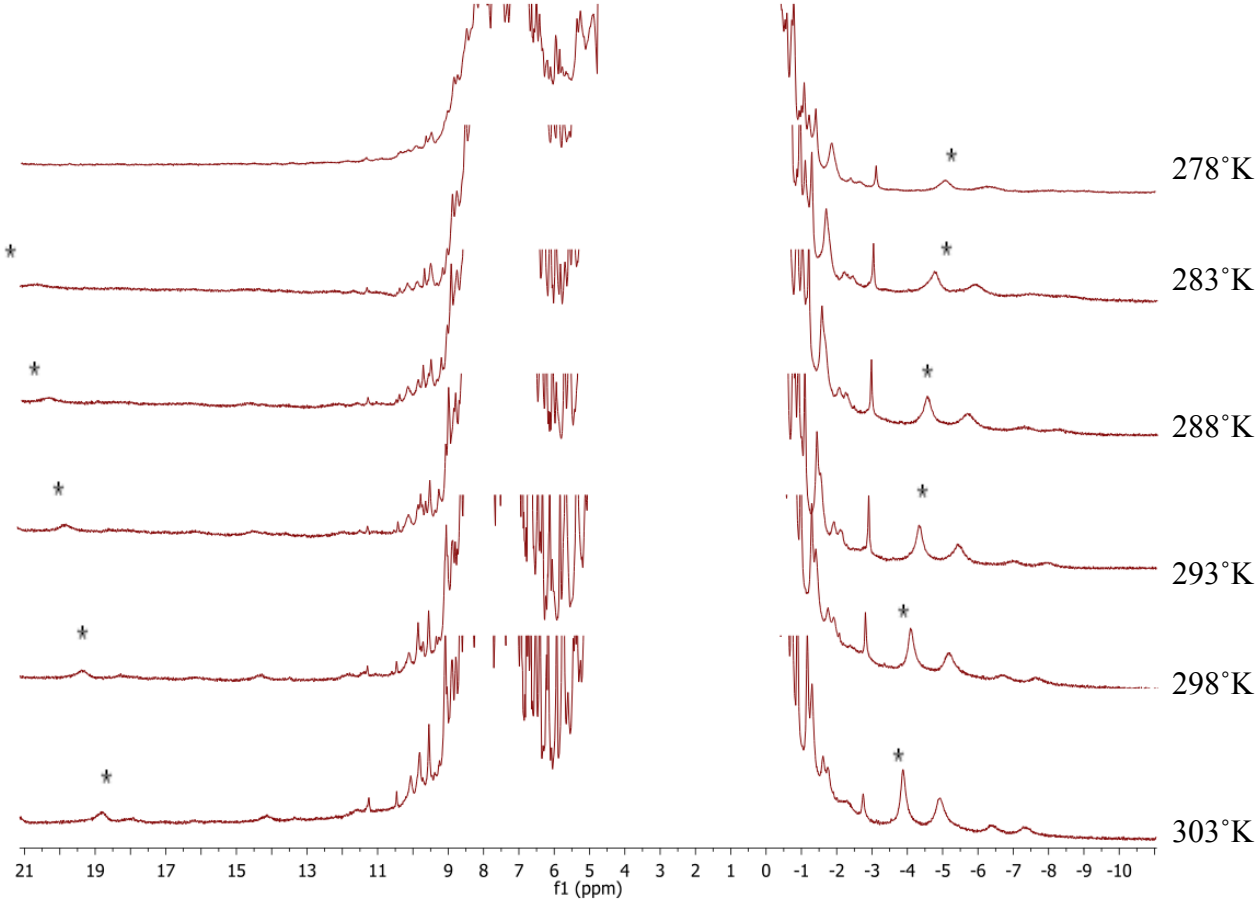

Figure 3.20 shifts at a 34ppm spectral window of the 1H NMR spectrum, with changes in temperature from 303˚K to 278˚K, of the SMb sample formed upon reaction of the hemeprotein with hydrogen sulfide, in the presence of oxygen. For example, with increasing temperature from 278˚K to 303˚K the downfield marked peak shifted from more than 20.63ppm to 18.81 ppm at the same time that it increased in intensity, respectively. The upfield marked peak shifted from -5.11ppm to -3.87 ppm at the same time that it increased in intensity with changes in temperature, respectively.

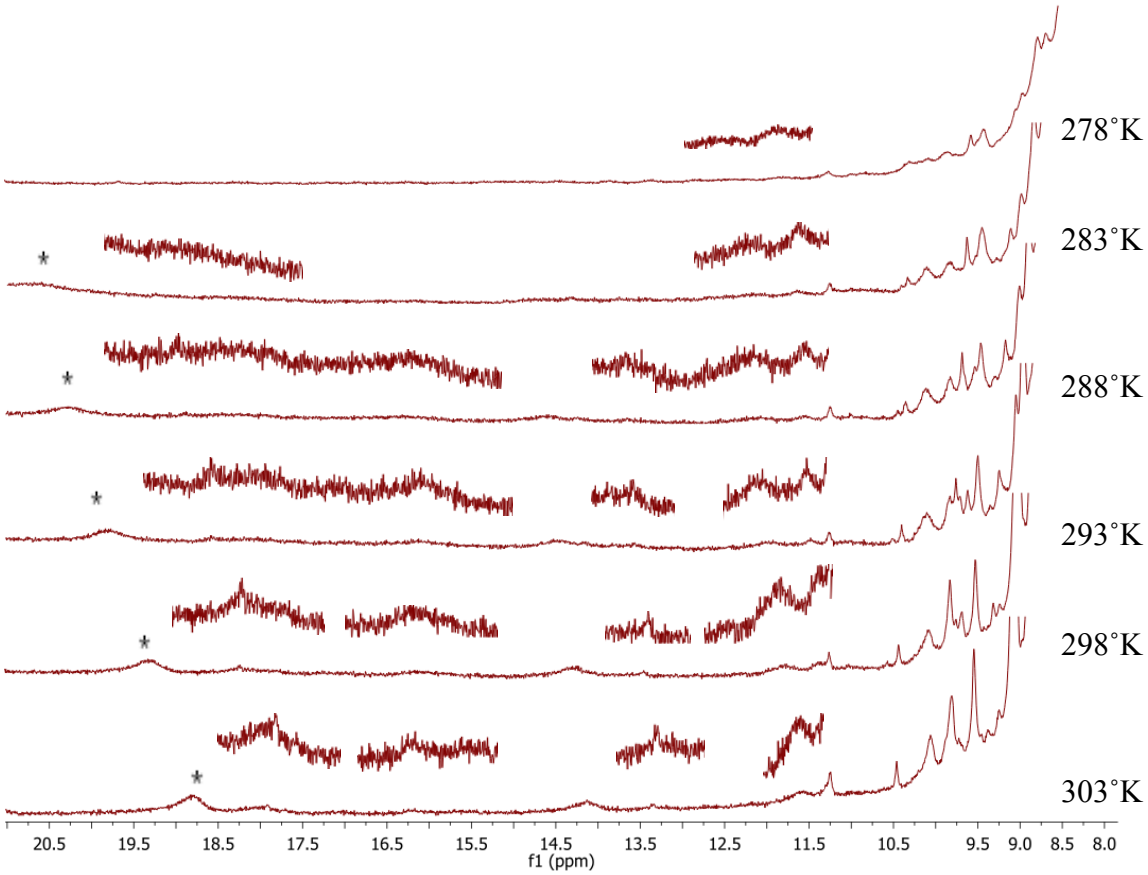

Figure 3.21 Downfield shifts at a 34ppm spectral window of the 1H NMR spectrum, with changes in temperature from 303˚K to 278˚K, of the SMb sample formed upon reaction of the hemeprotein with hydrogen sulfide, in the presence of oxygen. For example, with increasing temperature from 278˚K to 303˚K the downfield marked peak shifted from more than 20.63ppm to 18.81 ppm at the same time that it increased in intensity, respectively. The peaks with low intensity are expanded.

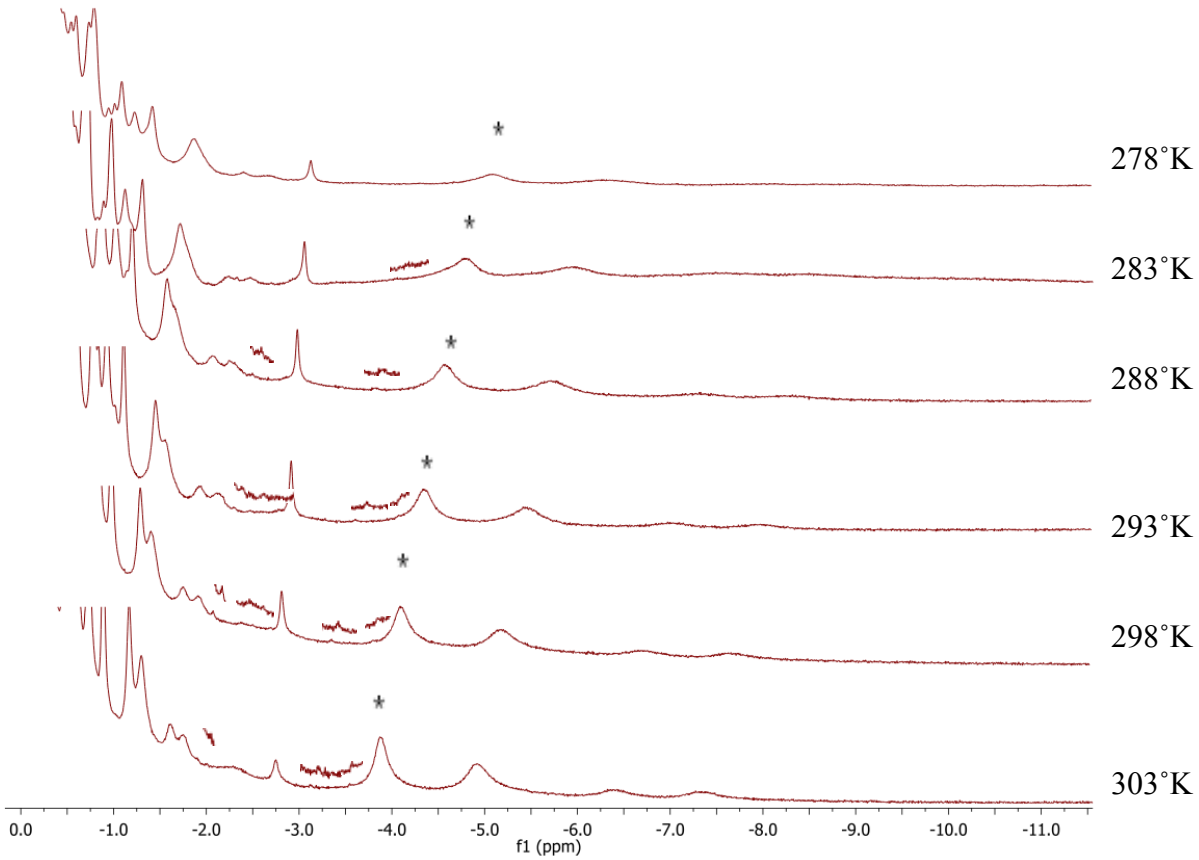

Figure 3.22 Upfield shifts at a 34ppm spectral window of the ^{1}H NMR spectrum, with changes in temperature from 303˚K to 278˚K, of the SMb sample formed upon reaction of the hemeprotein with hydrogen sulfide, in the presence of oxygen. The upfield marked peak shifted from -5.11ppm to -3.87 ppm at the same time that it increased in intensity with changes in temperature from 278˚K to 303˚K, respectively. The peaks with low intensity are expanded.

Table 3.20 and Table 3.21 summarizes the changes in intensity and displacements of the peaks for the SMb sample for the downfield and upfield ^{1}H NMR Spectrum with a spectral window of 34 ppm, respectively.

The peaks of the SMb spectrum, showed in Figure 3.23, allowed a comparison between met-Mb, oxy-Mb, SMb samples ($SMb_{(H2O2)}$), obtained by the reaction of met-Mb with hydrogen peroxide and hydrogen sulfide in the presence of oxygen, and SMb sample ($SMb_{(O2)}$) , obtained by the reaction of met-Mb with hydrogen sulfide in the presence of oxygen. A detailed analysis of the downfield and upfield ^{1}H NMR spectrum of $SMb_{(O2)}$, met-Mb and oxy-Mb at 298˚K and with a spectral window of 200ppm, indicated that the presence of the $SMb_{(O2)}$ was difficult to detect beneath the numerous coincident met-Mb resonances, showed in Figure 3.24 and 3.25, respectively. The upfield resonance of $SMb_{(O2)}$ sample was similar to the met-Mb and specially to the oxy-Mb, which indicated that it had contributions of both complexes. On the other hand, the downfield resonances are almost identical to the met-Mb complex. A characteristic pattern for the sulfheme complex formation in 1H NMR spectrum, is a decrease in intensity of the methyl protons signals due to the distortion of the heme group upon conversion of the native globin to sulfglobin. This decrease in intensity of the methyl protons in observed in the $SMb_{(O2)}$ ^{1}H NMR spectrum when it is compared to the native met-Mb. For example, note the decrease in intensity of the 5-methyl in $SMb_{(O2)}$ at 84.69 compared to 5-methyl proton intensity at 85.41ppm.

Table 3.20 Downfield shifts (ppm) at a 34ppm spectral window of the ^{1}H NMR Spectrum, with changes in temperature from 303˚K to 278˚K, of the SMb sample formed upon reaction of the hemeprotein with hydrogen sulfide, in the presence of oxygen.

Downfield-^{1}H NMR Shifts, spectral window of 34ppm	
Sulfmyoglobin Complex	
From 303˚K	**To 278˚K**
9.82	9.89
10.06	10.09
10.46	10.31
10.46	10.31
11.25	11.26
11.37	11.81
11.58	12.31
13.34	13.85
14.12	14.89
16.09	16.32
17.05	19.67
18.81	>20.63

Table 3.21 Upfield shifts (ppm) at a 34ppm spectral window of the ^{1}H NMR spectrum, with changes in temperature from 303˚K to 278˚K, of the SMb sample formed upon reaction of the hemeprotein with hydrogen sulfide, in the presence of oxygen.

Upfield-^{1}H NMR Shifts, spectral window of 34ppm	
Sulfmyoglobin Complex	
From 303˚K	**To 278˚K**
-7.32	-8.92
-6.36	-8.10
-4.90	-6.34
-3.87	-5.11
-3.14	-4.31
-2.74	-3.15
-2.26	-2.82
-1.99	-2.82
-1.74	-2.70
-1.60	-2.42
-1.29	-1.87
-1.16	-1.87
-0.88	-1.45
-0.73	-1.23

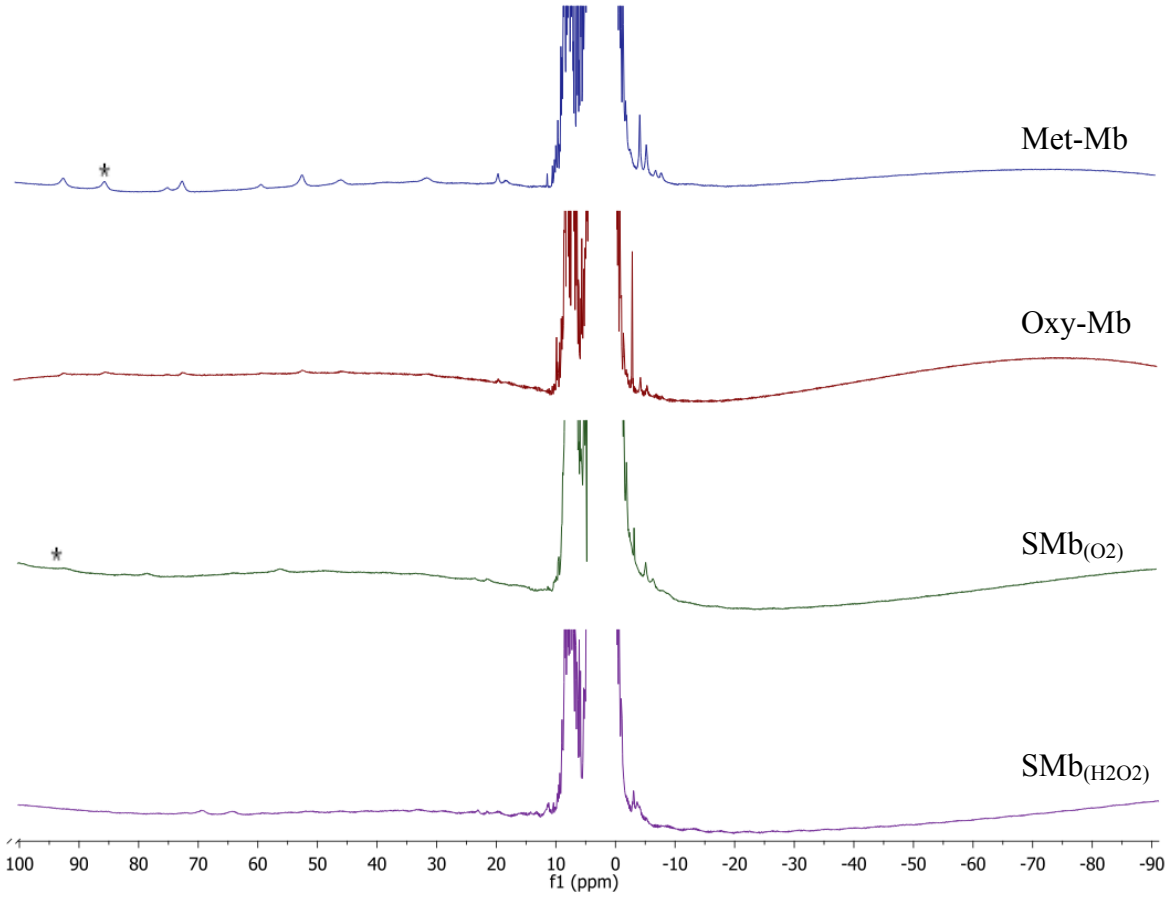

Figure 3.23 Shifts comparison at a 200ppm spectral window of the ^{1}H NMR Spectrum, at 298˚K, of the met-Mb, oxy-Mb, $SMb_{(O2)}$, and $SMb_{(H2O2)}$ samples, represented by the blue, red, green, and purple color spectrum, respectively. Note the decrease in intensity 5-methyl marked peak in met-Mb versus $SMb_{(O2)}$.

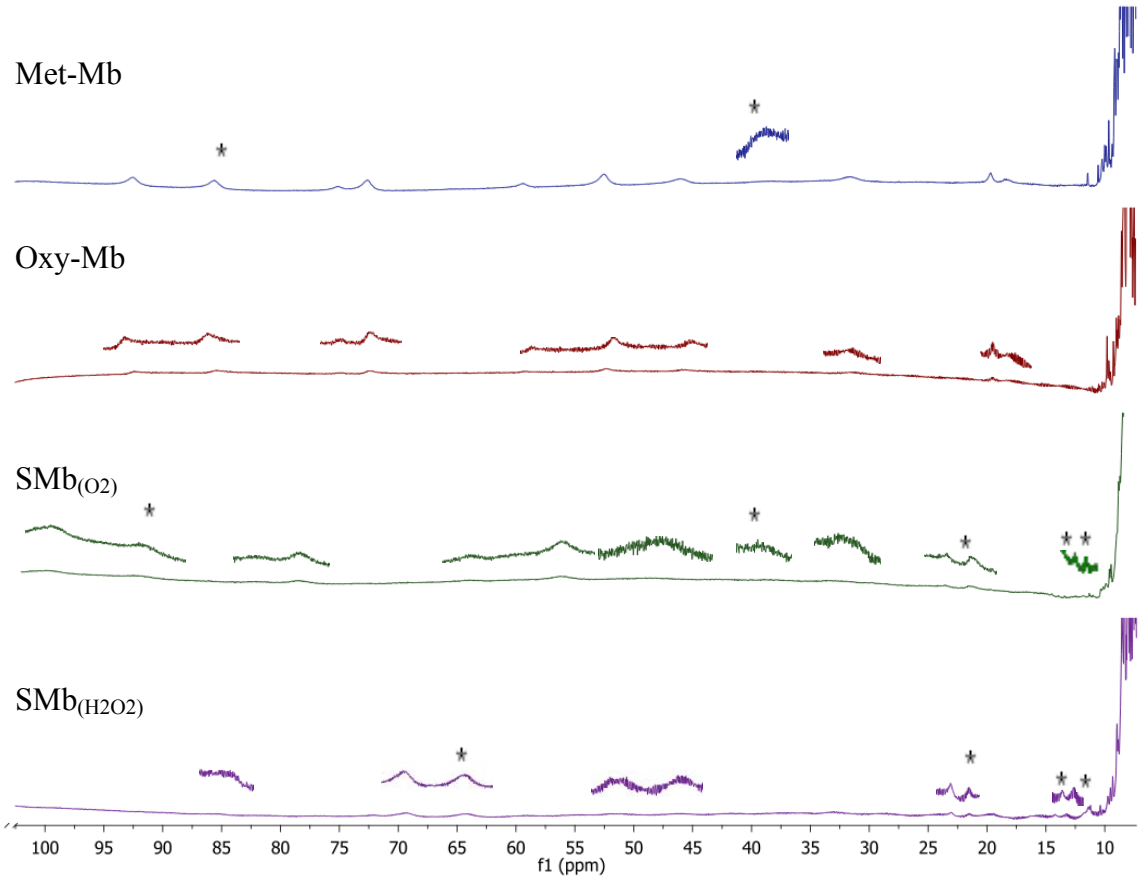

Figure 3.24 Downfield shifts comparison at a 200ppm spectral window of the ^{1}H NMR spectrum, at 298˚K, of the met-Mb, oxy-Mb, $SMb_{(O2)}$, and $SMb_{(H2O2)}$ samples, represented by the blue, red, green, and purple color spectrum, respectively. Note the decrease in intensity of the 5-methyl marked peak in met-Mb versus $SMb_{(O2)}$. The characteristic meso shift representing a six heme iron coordination is marked at 38.34ppm for met-Mb and 38.74ppm for $SMb_{(O2)}$. A peak at approximately 65.00ppm in the SMb(H2O2) spectrum, could suggest the interaction of the amino acid imidazole with the heme iron. In addition, the formation of the sulf heme complex is observed in $SMb_{(O2)}$ and $SMb_{(H2O2)}$ by the presence of the peaks at approximately 21.00ppm, 14.50ppm, and 13.50ppm. The low intensity peaks are expanded.

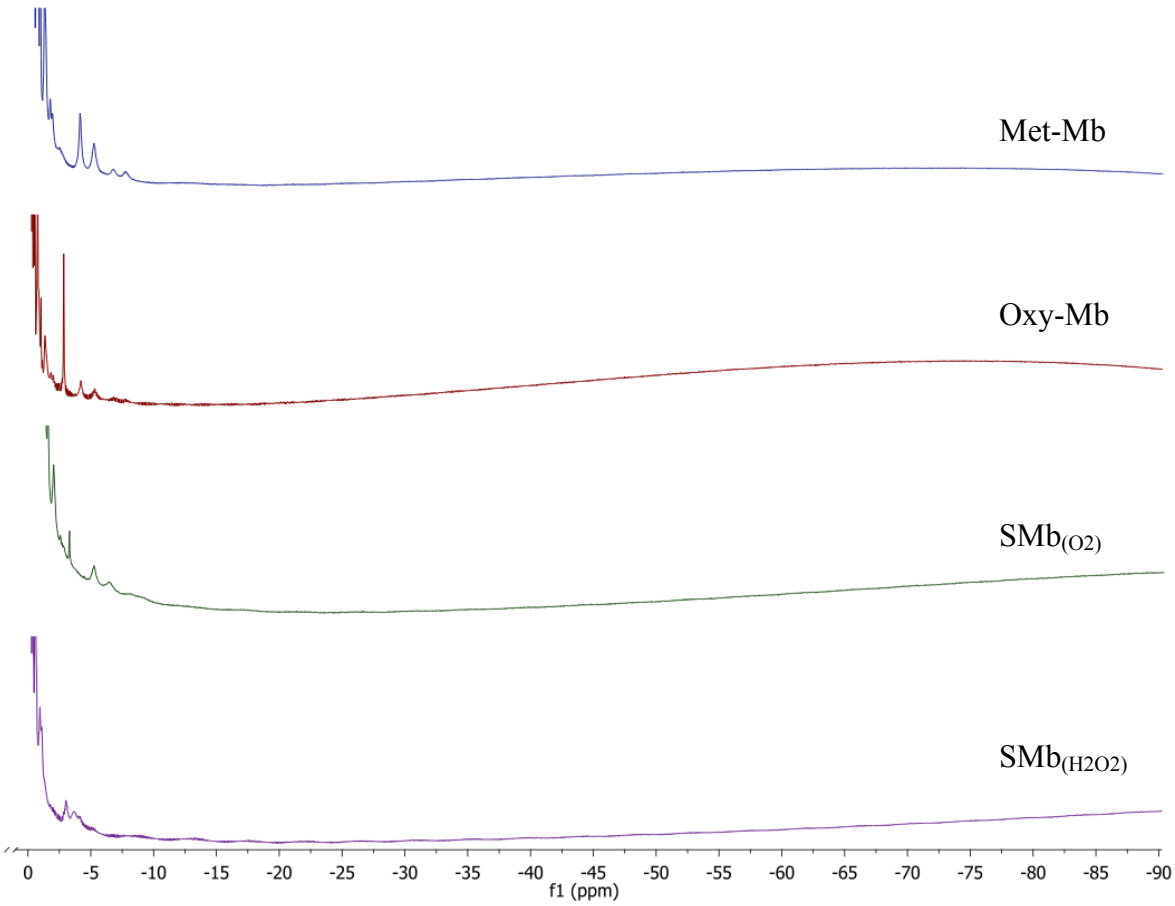

Figure 3.25 Upfield shifts comparison at a 200ppm spectral window of the ^{1}H NMR spectrum, at 298˚K, of the met-Mb, oxy-Mb, $SMb_{(O2)}$, and $SMb_{(H2O2)}$ samples, represented by the blue, red, green, and purple color spectrum, respectively. There was no presence of any peak after -10.00ppm.

In addition, Figure 3.24 shows several unique single-proton resonances, distinct from the oxy and met complexes resonances, which are observed in the downfield region of the spectrum at 21.00ppm, 14.50ppm and 13.50ppm. These shifts are suggested to arise from the formation of SMb in the sample, on the basis of the previously reported met-SMb and met-SMbCN ^{1}H NMR spectrum (Chatfield et al, 1987).

In general, the pattern of proton NMR hyperfine shift of high spin ferric heme proteins provides a wealth of information of the active site electronic and molecular structure. Extensive studies of heme model complexes have revealed an empirical indicator that discriminates between five and six coordinated ferric hemes, which was proposed to serve as a probe for water coordination in met-Mbs and Hbs. This empirical probe involves the characteristic differences in the sign of the heme meso H contact shifts, which are found ~30 to 40 ppm low field in six-coordinated and ~20 to 70 ppm upfield in five coordinated systems. Detailed assignments of heme resonances have shown that the meso H shifts are indeed lowfield ~40ppm in SW met Mb. The direction of the meso H shift correlates with the ligation state in all structurally characterized systems. A peak at 38.34ppm and 38.74ppm observed in native met-Mb and $SMb_{(O2)}$, respectively, which suggest the presence of a six coordinated species for the $SMb_{(O2)}$ complex (Rajarathnam et al, 1991).

The resonance pattern of the $SMb_{(O2)}$ ^{1}H NMR spectrum is characteristic of a high spin state form, as in hydrogen sulfide or specially met, but the optical absorptions of the final high spin $SMb_{(O2)}$ product do not correlates completely with any of the met or hydrogen sulfide high spin state characteristic optical absorptions. Therefore, none of the known high spin state complexes could be distinguished from this spectrum. The

possibility of a new high spin complex, with optical absorption around 409-420, 540, and 581, is in consideration.

When analyzing the $SMb_{(H2O2)}$ ^1H NMR and optical spectra, the fast degradation of the protein through the reaction with hydrogen peroxide is evident. The characteristic peaks for the presence of the sulfheme complex are observed at 21.37ppm and 14.20ppm. The labile ring proton of the proximal histidine in high-spin heme has been demonstrated to serve as a sensitive indicator of iron-imidazole bonding. This resonance has been reported at 66ppm for deoxy-sperm whale SMb, while in $SMb_{(H2O2)}$, a clear peak at 64.22 was observed. This could suggest the interaction of the HisE7 imidazole with the heme iron. Further studies of this protein are complicated by the instability of the protein, which makes the results obscure. Table 3.22 summarizes the downfield shifts of the 20ppm spectral window for the met-Mb, oxy-Mb, $SMb_{(O2)}$ and $SMb_{(H2O2)}$ complexes (Chatfield et al, 1987).

The possibility of the presence of compound II as a ligand in co-existence with the sulfheme derivative, as the final product for some heme proteins, is represented in Table 3.17. NMR studies of the ferryl species, under cryogenic conditions, have been made over the years. Characteristics proton peaks at 16.14ppm, 14.83ppm, 10.22ppm, and -6.20ppm have been attributed to the presence of the ferryl compound II presence (La Mar et al, 1983). Regarding this, Figure 3.26 shows the 34ppm spectral window of the ^1H NMR spectrum for met-mb, oxy-Mb, $SMb_{(O2)}$ and $SMb_{(H2O2)}$ complexes. The downfield and upfield ^1H NMR spectrum of met-Mb, oxy-Mb, $SMb_{(O2)}$ and $SMb_{(H2O2)}$ complexes are showed in Figure 3.27 and 3.28, respectively. In the downfield spectrum the peaks at 14.20ppm and 13.29ppm for $SMb_{(H2O2)}$ and at 14.31ppm and 13.45ppm for

Table 3.22 Downfield shifts comparison at a 200ppm spectral window of the ^{1}H NMR spectrum, at 298˚K, of the met-Mb, oxy-Mb, $SMb_{(O2)}$, and $SMb_{(H2O2)}$ samples.

Downfield - ^{1}H NMR Shifts, spectral window of 200ppm				
Assign	***Complex***			
	Met Mb	**Oxy Mb**	**SMb (H_2O_2)**	**SMb (O_2)**
8-M	92.39	92.20	No	92.18
5-M	85.41	85.24	85.12	84.69
7-H_α Prop	74.94	74.94	No	74.14
3-M	72.41	72.27	72.23	71.79
-	No	No	69.40	No
-	65.31	No	64.22	64.83
6-H_α Prop	59.26	59.15	59.17	58.74
1-M	52.27	52.33	51.36	51.93
6-H_α Prop	45.84	45.66	46.06	45.54
Meso	38.34	No	No	38.74
2-H_α	31.64	31.20	33.02	31.07
-	No	No	No	27.33
-	25.33	No	22.87	No
Sulf-complex	No	No	21.37	21.65
7-$C_\beta H$ Prop	19.57	19.45	19.55	19.31
$C_\beta H$-HisF8	18.23	17.97	No	No

The (-) indicates that it has not been assigned. The (No) indicate were a shift was not observed.

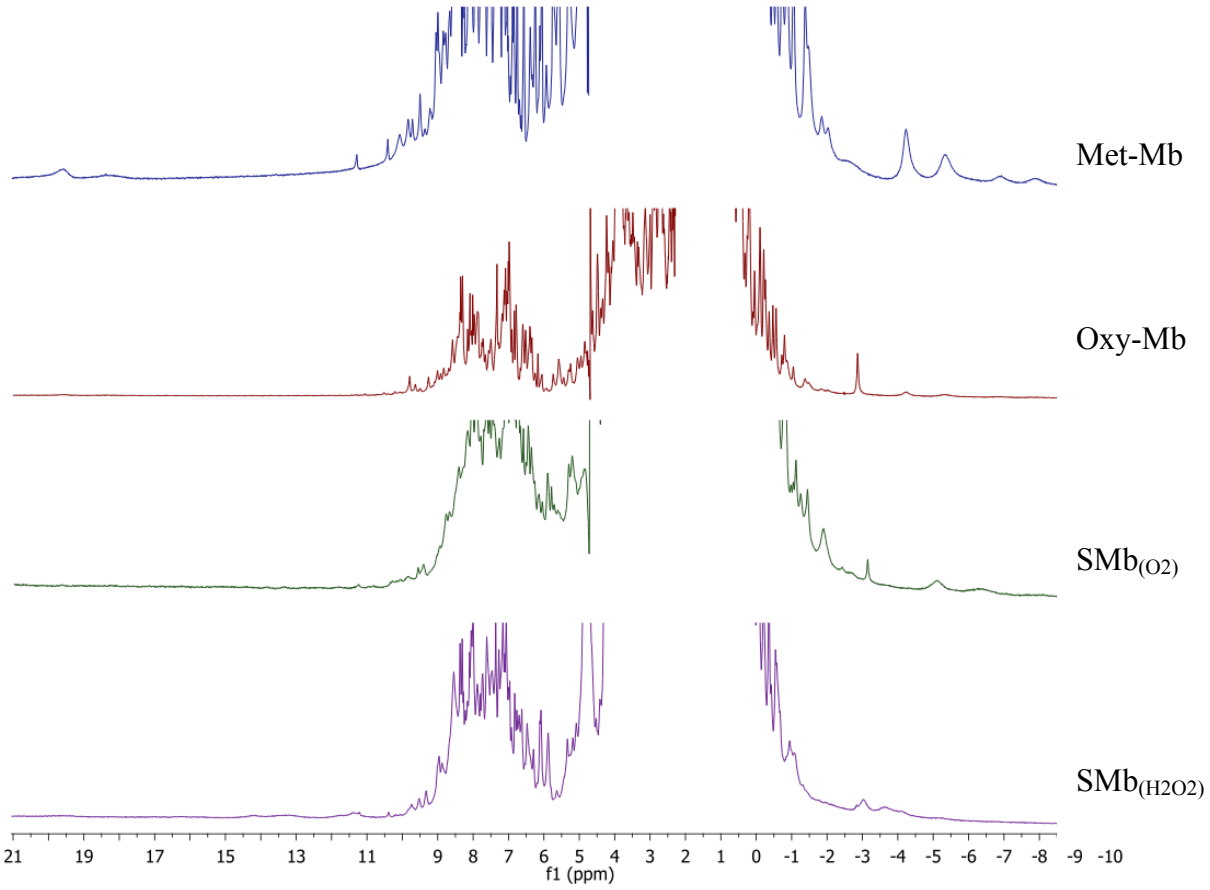

Figure 3.26 ^{1}H NMR Spectrum of the met-Mb, oxy-Mb, $SMb_{(O2)}$, and $SMb_{(H2O2)}$ samples, represented by the blue, red, green, and purple color spectrum, respectively, 34ppm spectral window at 298˚K .

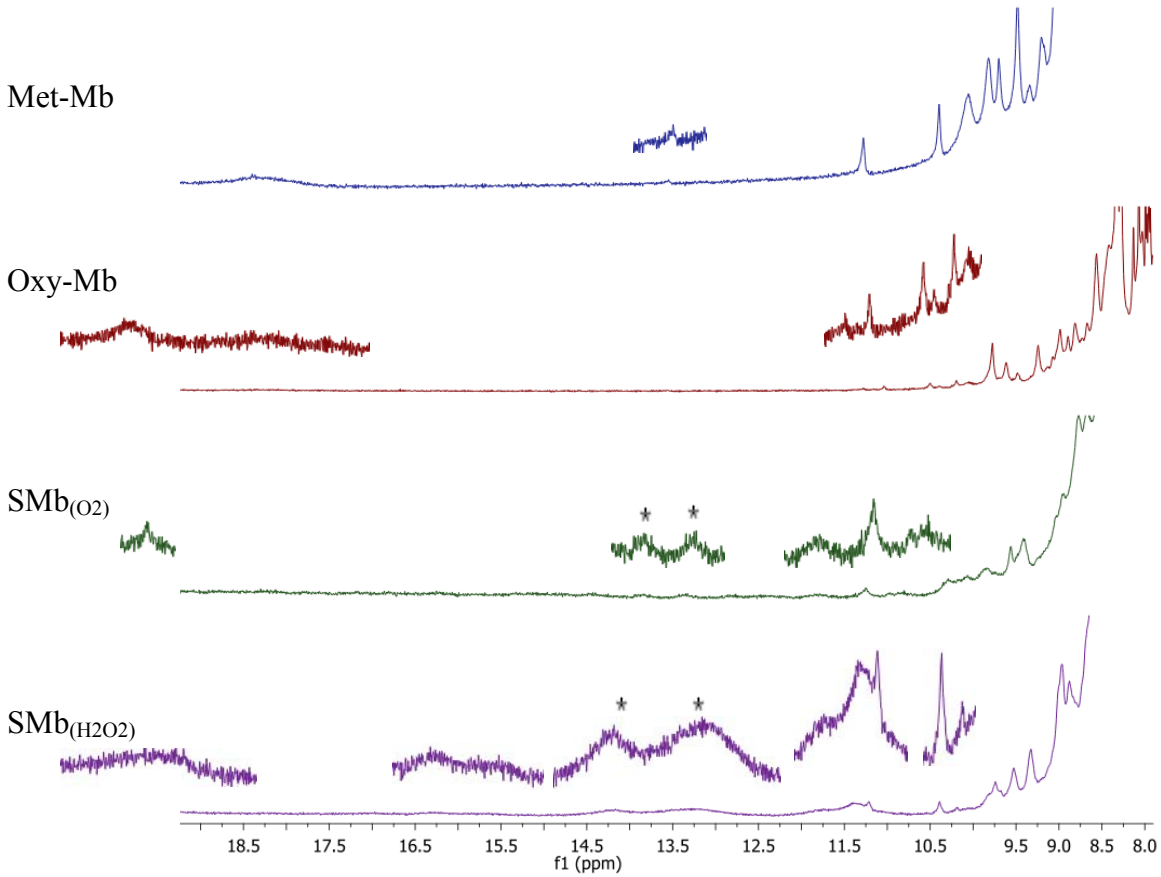

Figure 3.27 Chemical shifts comparison at a 34ppm spectral window of the ^{1}H NMR Spectrum, at 298˚K, of the met-Mb, oxy-Mb, $SMb_{(O2)}$, and $SMb_{(H2O2)}$ samples, represented by the blue, red, green, and purple color spectrum, respectively. The characteristic peaks for the sulfheme formation are marked. In the $SMb_{(H2O2)}$ spectrum the characteristic sulfheme peaks are at 14.20ppm and 13.29ppm. In the $SMb_{(O2)}$ spectrum the characteristic sulfheme peaks are at 14.31ppm and 13.45ppm. The low intensity peaks are expanded.

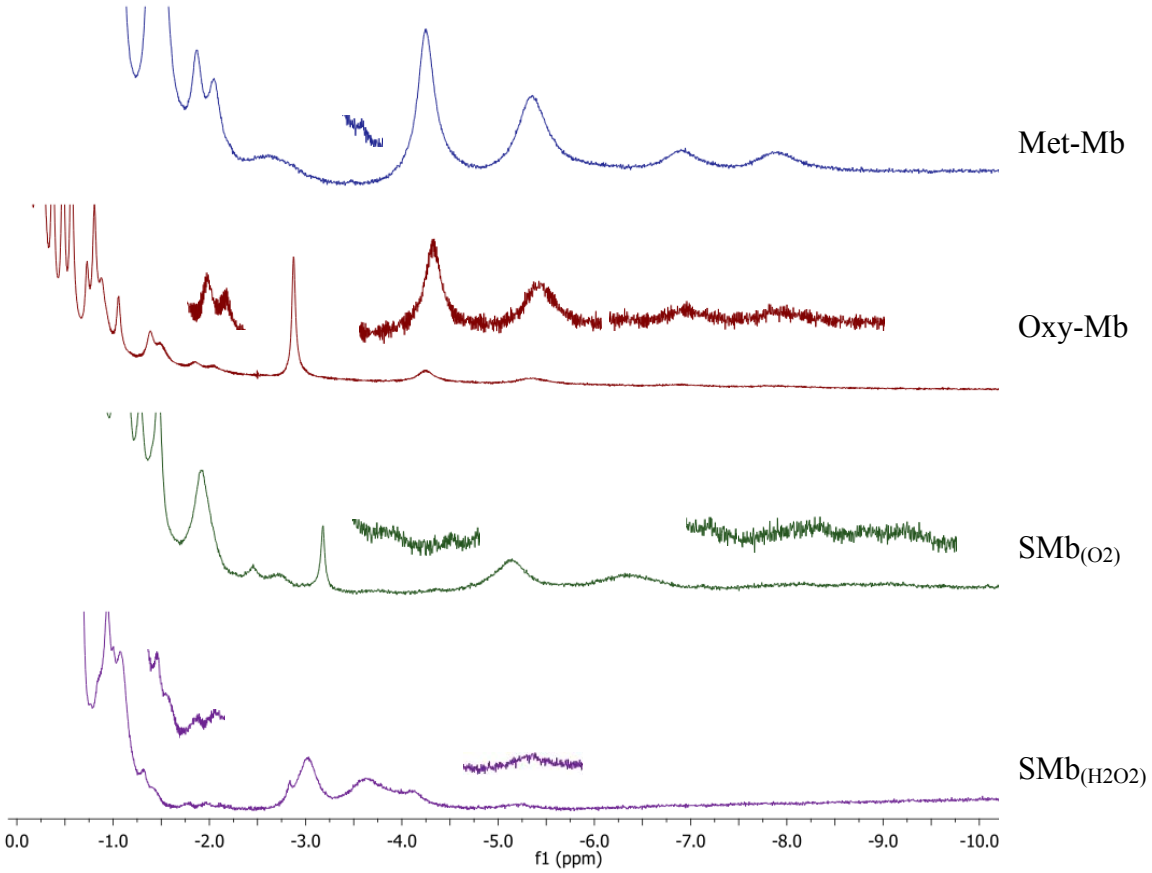

Figure 3.28 Upfield shifts comparison at a 34ppm spectral window of the ^{1}H NMR spectrum, at 298˚K, of the met-Mb, oxy-Mb, $SMb_{(O2)}$, and $SMb_{(H2O2)}$ samples, represented by the blue, red, green, and purple color spectrum, respectively. The low intensity peaks are expanded.

$SMb_{(H2O2)}$ and 14.31ppm and 13.45ppm for $SMb_{(O2)}$,characteristic for the sulfheme complex formation, are clearly observed. The resonances of the $SMb_{(O2)}$ and $SMb_{(H2O2)}$ final products reveals no evidence for the presence of the ferryl species, since the characteristics peaks of the ferryl compound II are also present in met and oxy native Mb. Table 3.23 and 3.24 summarizes the shifts at a 34ppm spectral window for the ^1H NMR spectrum of met-Mb, oxy-Mb, $SMb_{(O2)}$ and $SMb_{(H2O2)}$ complexes.

On the other hand, the optical absorption spectra of the SHbI GlnE7His mutant revealed an instantly natural interconversion of the oxidation and ligand states, from the metaquo state to the oxy state, with the immediate addition of hydrogen peroxide and hydrogen sulfide for the sulfheme complex formation. However, in the presence of oxygen and hydrogen sulfide, the characteristic optical absorptions for the oxy complex are observed right away, but the presence of the 620nm band, characteristic for the sulfheme formation, was gradual. Therefore, the inability to detect downfield and upfield resonances characteristic of the sulfheme complex in the 1H NMR spectrum of met-Mb, oxy-Mb, $SMb(O_2)$, and SHbI GlnE7His mutant, shown in Figure 3.29, is not surprising since the final product of the natural inter conversion may be oxy-SHbI GlnE7His mutant. Note that the downfield resonances in Figure 3.30, 3.31, and 3.32 of the SHbI GlnE7His mutant complex exhibit an unusual downfield shift peak at 15.21, which could be attributed to the NH proton of the proximal His F8, as reported for theCO-SMb complex. A peak at 14.49 was observed, which could be attributed to the sulfheme derivative formation (Chatfield et al, 1987). The upfield SHbI GlnE7His mutant complex resonances are showed in Figure 3.33. The characteristic sulfheme absorption for the CO-SMbc isomer is at 626nm, as in our SHbI GlnE7His mutant. Another similar

Table 3.23 Downfield shifts (ppm) comparison at a 34ppm spectral window of the ^{1}H NMR spectrum, at 298˚K, for the met-Mb, oxy-Mb, $SMb_{(O2)}$, and $SMb_{(H2O2)}$ samples.

Downfield - ^{1}H NMR Shifts, spectral window of 34ppm				
Assign	***Complex***			
	Met Mb	**Oxy Mb**	**SMb (H_2O_2)**	**SMb (O_2)**
-	9.84	9.84	9.51	9.85
-	10.08	10.10	No	10.08
-	No	10.23	10.18	No
-	10.42	10.43	10.38	10.42
-	No	10.55	No	10.56
-	No	No	No	No
-	No	11.08	11.21	No
-	11.30	11.31	11.38	11.27
-	No	No	11.74	11.37
-	No	No	No	11.78
4-$H_{\beta c}$	13.56	No	13.29	13.45
4-$H_{\beta c}$	No	No	14.20	14.31
$C_{\beta}H$-HisF8	No	No	No	No
-	No	No	16.26	16.09
$C_{\beta}H$-HisF8	18.38	18.30	No	18.25
7-$C_{\beta}H$	19.60	19.61	19.55	19.31

The (-) indicates that the peaks are not assigned. The (No) indicates that the peak was not observed.

Table 3.24 Upfield shifts (ppm) comparison at a 34ppm spectral window of the ^{1}H NMR spectrum, at 298˚K, for the met-Mb, oxy-Mb, $SMb_{(O2)}$, and $SMb_{(H2O2)}$ samples.

Upfield - ^{1}H NMR Shifts, spectral window of 34ppm				
Assign	***Complex***			
	Met Mb	**Oxy Mb**	**SMb (H_2O_2)**	**SMb (O_2)**
-	-7.84	-7.84	-5.23	-7.63
-	-6.89	-6.89	-4.14	-6.71
-	-5.34	-5.32	-3.65	-5.20
-	-4.23	-4.23	-3.02	-4.11
-	-3.44	No	No	-3.37
-	No	-2.86	-2.85	-2.84
-	-2.63	No	No	-2.41
-	-2.02	-2.02	-1.96	-2.08
-	-1.84	-1.84	-1.77	-1.77
-	No	No	No	-1.89
-	-1.48	No	-1.44	-1.42
-	-1.38	No	-1.31	-1.33
-	No	No	-1.18	No
-	-1.05	No	-1.01	-1.00
-	No	No	-0.95	-0.88

The (-) indicates that the peaks are not assigned. The (No) indicates that the peak was not observed.

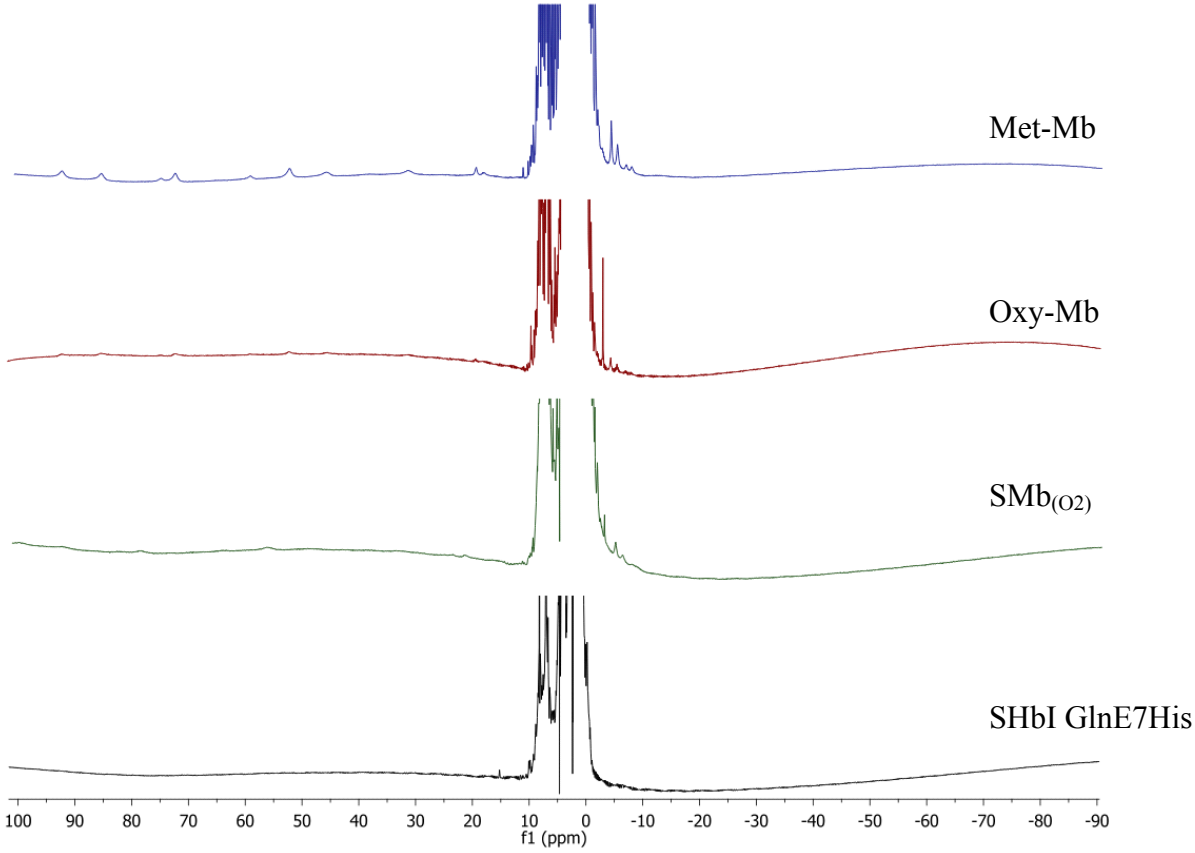

Figure 3.29 Chemical shifts comparison at a 200ppm spectral window of the ^{1}H NMR spectrum, at 298˚K, for the met-Mb, oxy-Mb, $SMb_{(O2)}$, and SHbI GlnE7His mutant samples, represented by the blue, red, green, and black color spectrum, respectively.

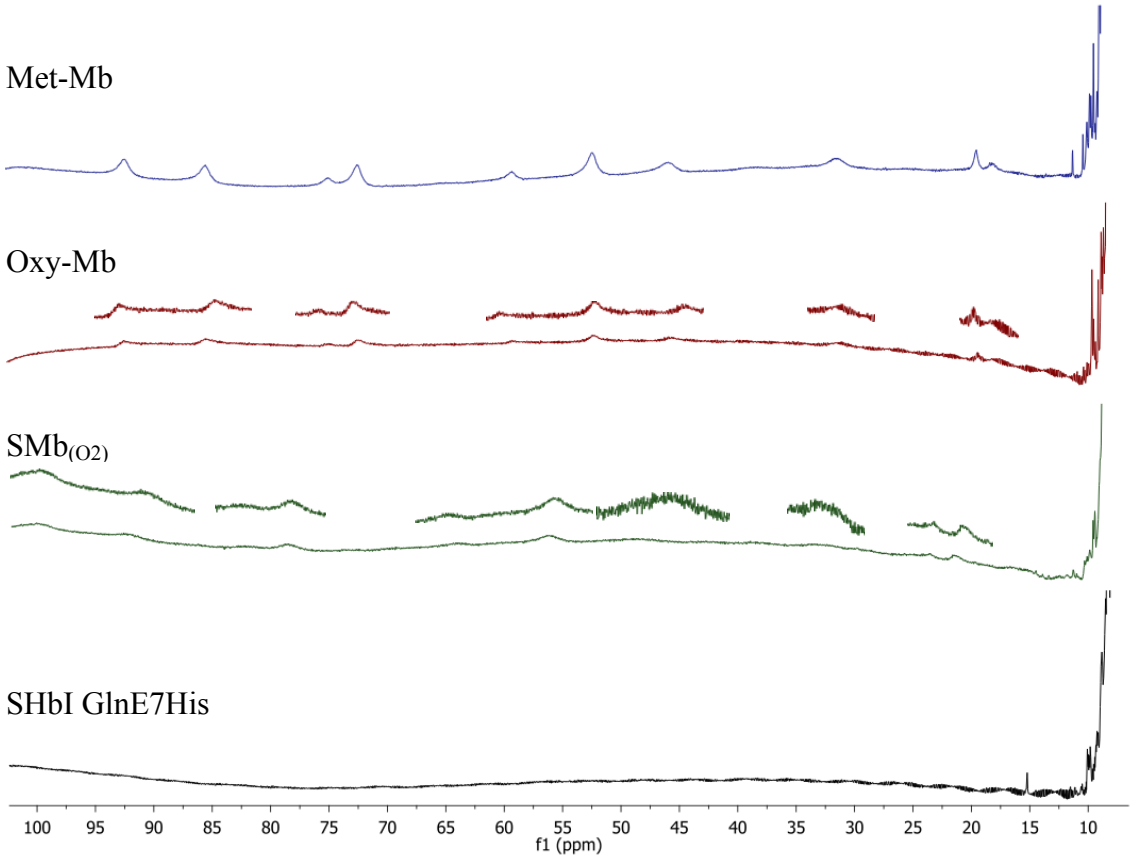

Figure 3.30 Downfield shifts comparison at a 200ppm spectral window of the ^{1}H NMR spectrum, at 298˚K, for the met-Mb, oxy-Mb, $SMb_{(O2)}$, and SHbI GlnE7His mutant samples, represented by the blue, red, green, and black color spectrum, respectively. The low intensity peaks are expanded.

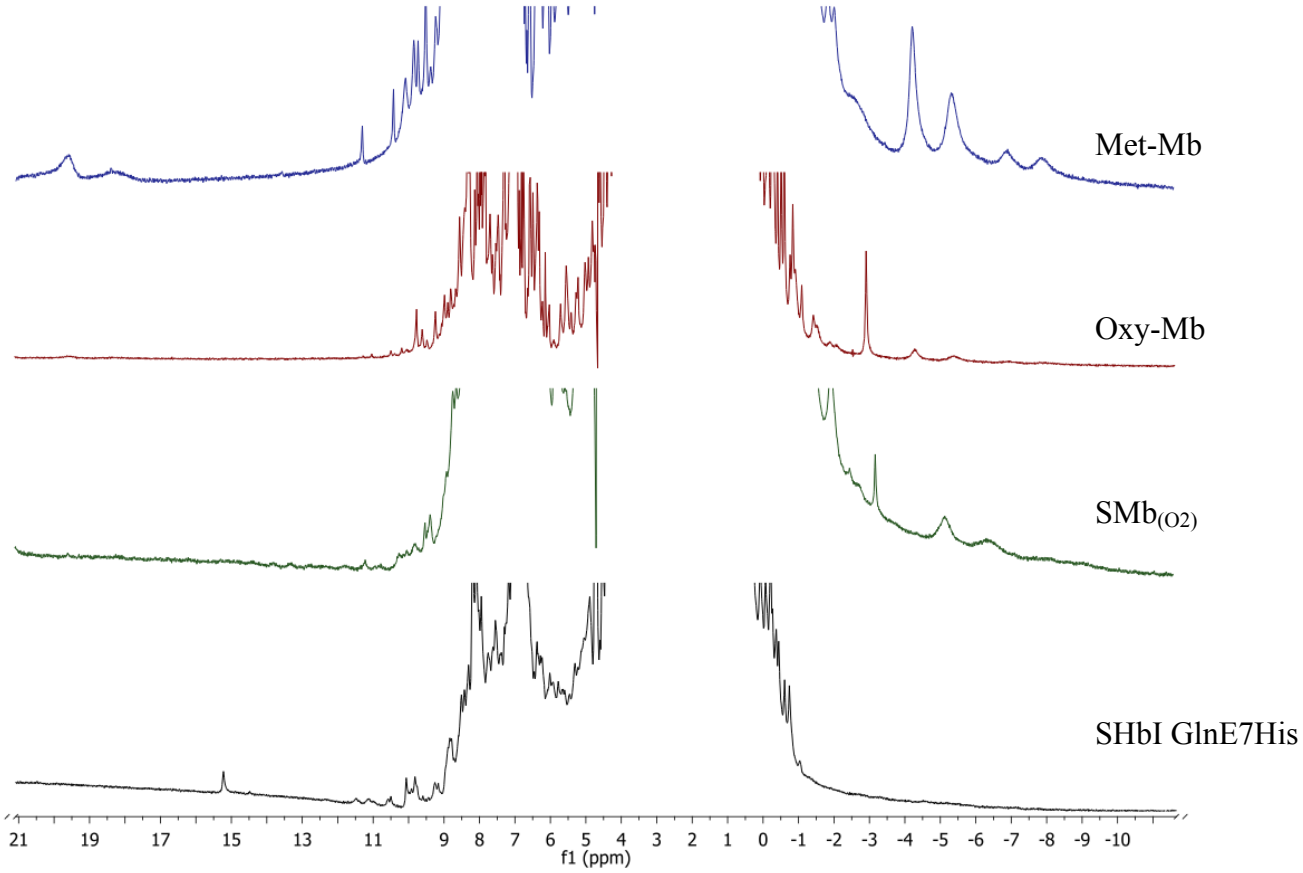

Figure 3.31 Chemcal shifts comparison at a 34ppm spectral window of the ^{1}H NMR spectrum, at 298˚K, for the met-Mb, oxy-Mb, $SMb_{(O2)}$, and SHbI GlnE7His mutant samples, represented by the blue, red, green, and black color spectrum, respectively.

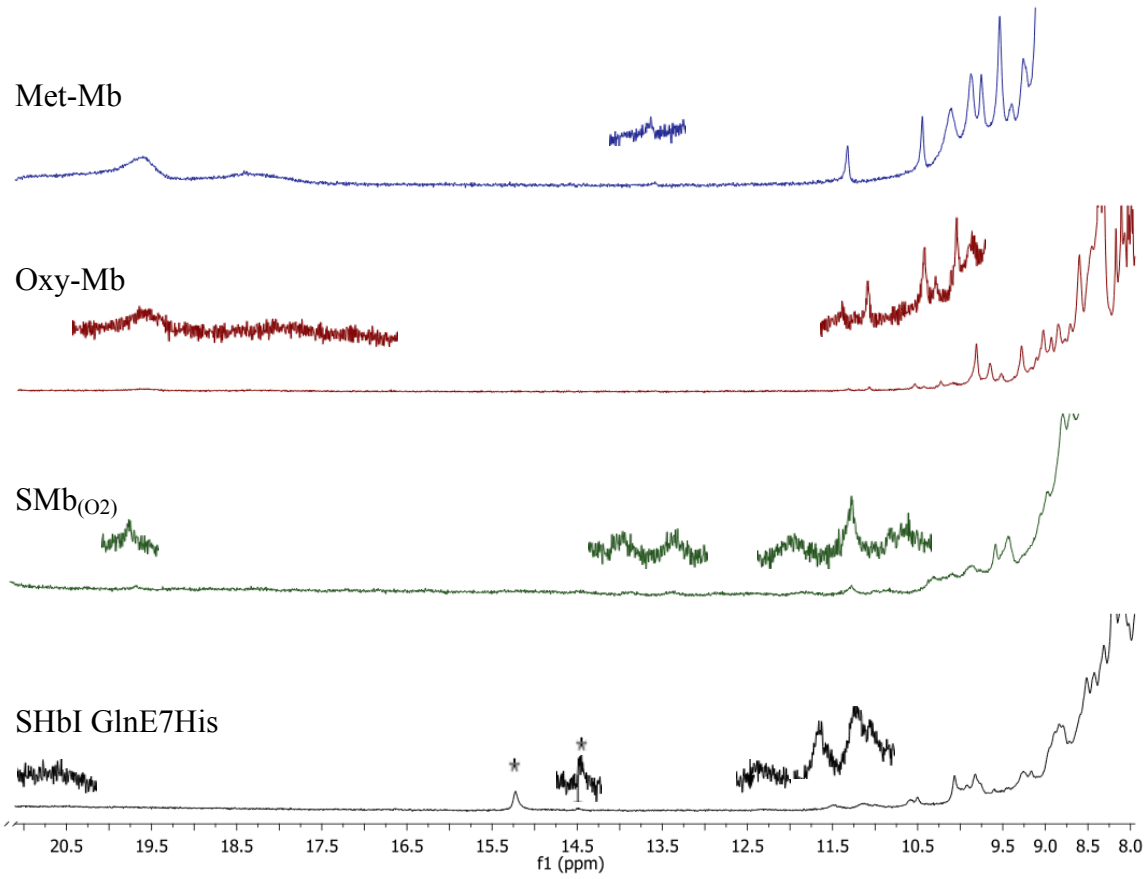

Figure 3.32 Downfield shifts comparison at a 34ppm spectral window of the ^{1}H NMR spectrum, at 298˚K, for the met-Mb, oxy-Mb, SMb(O_2), and SHbI GlnE7His mutant samples, represented by the blue, red, green, and black color spectrum, respectively. The marked 15.21ppm peak in the SHbI GlnE7His mutant spectrum could be attributed to the NH proton of the proximal histidine. Low intensity peak are expanded.

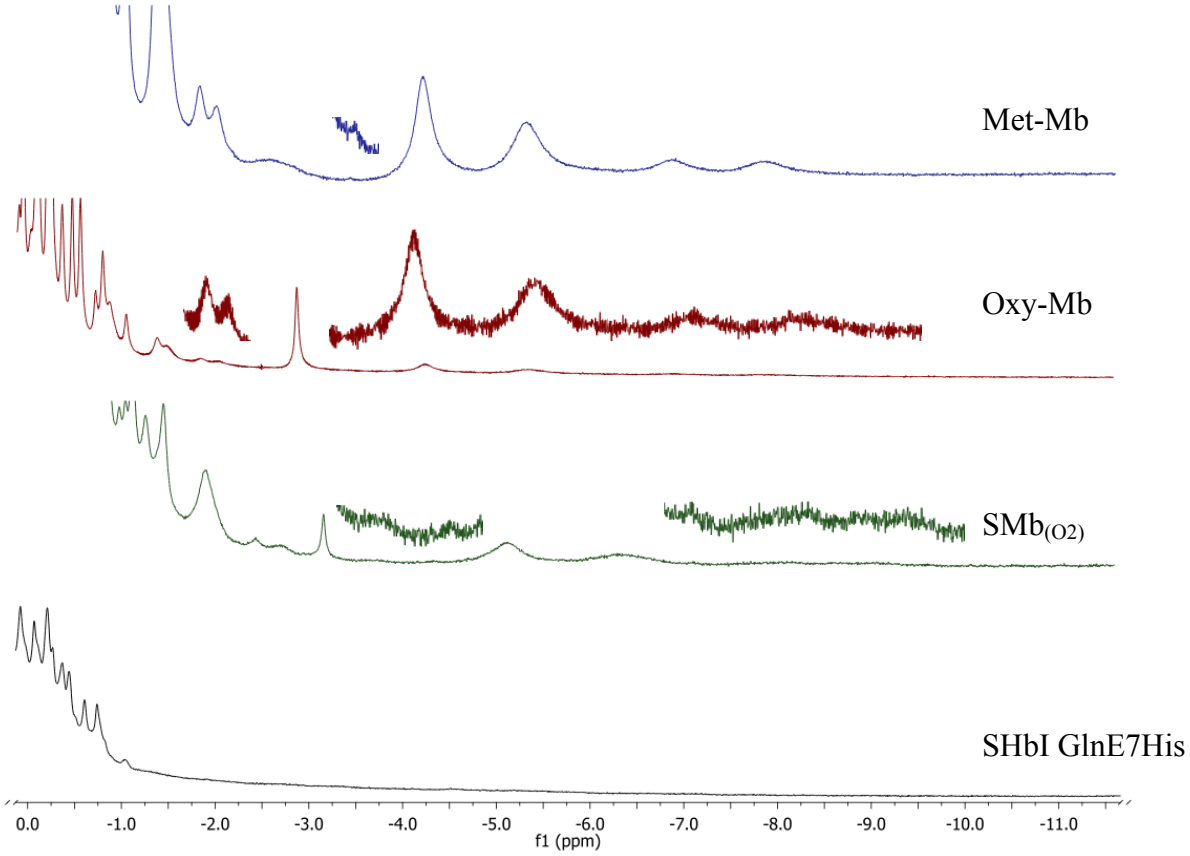

Figure 3.33 Upfield shifts comparison at a 34ppm spectral window of the ^{1}H NMR spectrum, at 298˚K, for the met-Mb, oxy-Mb, $SMb_{(O2)}$, and SHbI GlnE7His mutant samples, represented by the blue, red, green, and black color spectrum, respectively. No peaks were observed in the upfield SHbI GlnE7His mutant spectrum. Low intensity peaks are expanded.

behavior is the greater CO affinity of that sulfheme isomer and for the SHbI GlnE7His mutant complex a greater O_2 affinity was observed. There is a possibility that the isomer present in our SHb His E7 mutant may be the sulfHbc. In Tables 3.25, 3.26, and 3.27, the shifts for the met-Mb, oxy-Mb, $SMb_{(O2)}$, and SHbI GlnE7His mutant with spectral window at 200ppm downfield, 34ppm downfield, and 34ppm upfield, respectively of the ^1H NMR spectrum. The variation in behavior between $SMb_{(O2)}$ and SHbI GlnE7His mutant that leads to the different final product of the chemical reaction with hydrogen sulfide, in the presence of dissolved oxygen, may be attributed to the dissimilar amino acid residue in their active site that they still have.

3.4 Mechanism of the Sulfheme Formation

It has been shown that His in the E7 position is crucial for the sulfheme protein formation. Paulos and Kraus proposed a specific mechanism for the formation of the ferryl species, which involved the heme iron, hydrogen peroxide, and histidine, as showed in Figure 3.34 (Shintaku et al, 2005). Since histidine is so important for the sulfheme formation, then the same mechanism is proposed here for the formation of the sulfheme proteins. First, the coordination of the hydrogen peroxide to the iron occurs. Then, the transition state of the O-O bond heterolysis is proposed. The structure is unstable because of the doubly protonated His. The deprotonation fo the distal His causes the stabilization of the iron hydroperoxide complex. Water is immediately liberated, and the formation of the radical cation compound I is observed. An electron is provide to the compound I from somewhere in the protein moiety. Finally, the formation of the stable compound II is observed. It has been proposed the importance of a ferryl

Table 3.25 Downfield shifts (ppm) comparison at a 200ppm spectral window of the ^{1}H NMR spectrum, at 298˚K, for the met-Mb, oxy-Mb, $SMb_{(O2)}$, and SHbI GlnE7His mutant samples.

Downfield - ^{1}H NMR Shifts, spectral window of 200ppm				
Assign	***Complex***			
	Met Mb	**Oxy Mb**	**SMb (O_2)**	**SHbI GlnE7His**
8-M	92.39	92.20	92.18	No
5-M	85.41	85.24	84.69	No
7-H_α Prop	74.94	74.94	74.14	No
3-M	72.41	72.27	71.79	No
-	No	No	No	No
-	65.31	No	64.83	No
6-H_α Prop	59.26	59.15	58.74	No
1-M	52.27	52.33	51.93	No
6-H_α Prop	45.84	45.66	45.54	No
Meso	38.34	No	38.74	No
2-H_α	31.64	31.20	31.07	No
-	No	No	27.33	No
-	25.33	No	No	No
Sulf-complex	No	No	21.65	No
7-$C_\beta H$ Prop	19.57	19.45	19.31	No
$C_\beta H$-HisF8	18.23	17.97	No	No

The (-) indicate that it has not been assigned. The (No) indicates that a shift was not observed.

Table 3.26 Downfield shifts (ppm) comparison at a 34ppm spectral window of the ^{1}H NMR spectrum, at 298˚K, for the met-Mb, oxy-Mb, $SMb_{(O2)}$, and SHbI GlnE7His mutant samples.

Downfield - ^{1}H NMR Shifts, spectral window of 34ppm				
Assign	***Complex***			
	Met Mb	**Oxy Mb**	**SMb (O_2)**	**SHbI GlnE7His**
-	9.84	9.84	9.85	9.82
-	10.08	10.10	10.08	9.93
-	No	10.23	No	10.06
-	10.42	10.43	10.42	10.50
-	No	10.55	10.56	10.54
-	No	No	No	10.99
-	No	11.08	No	11.12
-	11.30	11.31	11.27	11.47
-	No	No	11.37	No
-	No	No	11.78	12.32
4-$H_{\beta c}$	13.56	No	13.45	No
4-$H_{\beta c}$	No	No	14.31	14.49
$C_{\beta}H$-HisF8	No	No	No	15.21
-	No	No	16.09	No
$C_{\beta}H$-HisF8	18.38	18.30	18.25	No
7-$C_{\beta}H$	19.60	19.61	19.31	No

The (-) indicate that it has not been assigned. The (No) indicates were a shift was not observed.

Table 3.27 Upfield shifts comparison at a 34ppm spectral window of the ^{1}H NMR spectrum, at 298˚K, for the met-Mb, oxy-Mb, $SMb_{(O2)}$, and SHbI GlnE7His mutant samples.

Upfield - ^{1}H NMR Shifts, spectral window of 34ppm				
Assign	***Complex***			
	Met Mb	**Oxy Mb**	**SMb (O_2)**	**SHbI GlnE7His**
-	-7.84	-7.84	-7.63	-5.23
-	-6.89	-6.89	-6.71	-4.14
-	-5.34	-5.32	-5.20	-3.63
-	-4.23	-4.23	-4.11	No
-	-3.44	No	-3.37	No
-	No	-2.86	-2.84	No
-	-2.63	No	-2.41	No
-	-2.02	-2.02	-2.08	No
-	-1.84	-1.84	-1.77	No
-	No	No	-1.89	No
-	-1.48	No	-1.42	No
-	-1.38	No	-1.33	No
-	No	No	No	No
-	-1.05	No	-1.00	-1.05
-	No	No	-0.88	No

The (-) indicate that it has not been assigned. The (No) indicates were a shift was not observed.

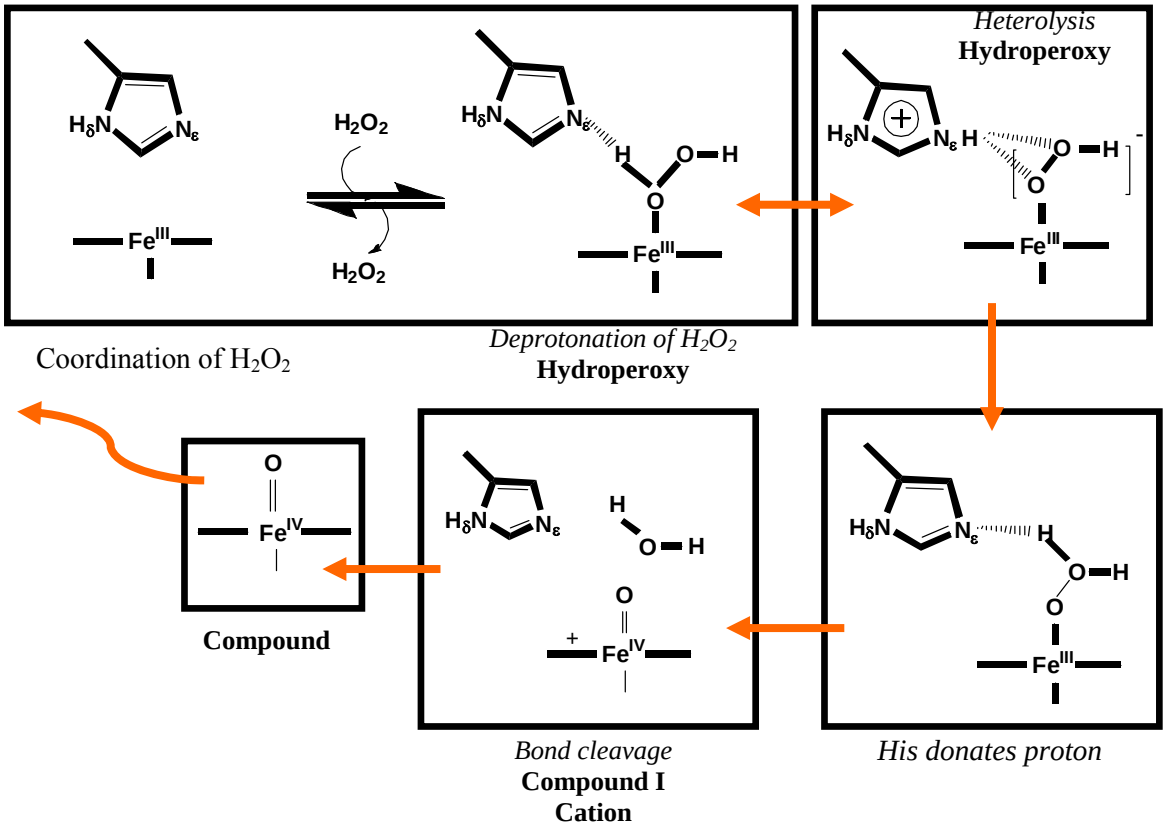

Figure 3.34 Proposed chemical mechanism for the formation of the sulfheme proteins.

species for the sulfheme derivative formation. The research presented here has showed that compound I and compound II do not play a significant role in the suflheme formation. Given that HisE7 is extremely important for the sulfheme complex formation, it is suggested that if a ferryl species is essential for the sulfheme complex formation, it is the one where His has a direct interaction, as in the heme hydroperoxy complex.

CHAPTER 4
Conclusion

The experimental data along with site-directed mutagenesis allow us to elucidate the role of the histidine in the E7 position of the heme proteins, using HbI from *Lucina Pectinata*. UV-Vis spectroscopic analyses were made of human Hb, HbI, HbII/HbIII, HbI PheE11Val, HbI GlnE7His, HbI PheB10His, HbI PheB10Val mutants upon the reaction with hydrogen sulfide and hydrogen peroxide, using horse heart Mb as the control. Surprisingly, the only mutant to form the sulfheme complex was the HbI GlnE7His mutant, as judged by the formation of the 626nm band. These studies revealed that only the heme proteins with histidine in the specific E7 position form the unique sulfheme derivative. However, the $sulfMb_{(O2)}$ final product may co-exist with a six coordinated high spin species while the SHbI GlnE7His final product could co-exist with a low spin oxy complex, as shown by Optical and ^{1}H NMR Spectroscopies. In addition, the results indicated that neither compound I nor compound II play a significant role in the formation of the sulfheme derivative given that the hemeproteins HbI and HbII/HbIII, with a stable compound I and compound II, respectively, did not form the derivative. Since HisE7 is necessary for the sulfheme formation, if a ferryl species plays an important role during the formation to the sulfheme derivative, it is the one were His in the E7 position has a direct interaction, as seen in the hydroperoxy complex.

Future Works

To better understand the sulfheme complex formation, the following studies are proposed: (1) Kinetics experiments with different hemeproteins, hydrogen sulfide, oxygen, and hydrogen peroxide concentrations to verify the mechanism of sulfheme complex association and dissociation; (2) Resonance Raman could offer information about the chemical interactions that lead, to the unknown optical absorptions; (3) Crystallography may provide data that may answer the uncertain final ligand/sulfheme final complex; (4) Optical studies of double and triple HbI mutants upon the reaction with hydrogen peroxide and hydrogen sulfide to give information about the sulfheme complex chemical reactivity and stability; (5) Two dimensional NMR experiments to verify the structure and interactions of the sulfheme final product.

References

Alayash, A.I., Ryan, B.A.; Eich, R.F., Olson, J.S., Cashon, R.E. (1999). Reactions of sperm whale myoglobin with hydrogen peroxide. Effects of distal pocket mutations on the formation and stability of the ferryl intermediate. *J. Biol. Chem.*, 274, 2029-2037.

Andersson, L.A., Loehr, T.M., Lim, A.R., Mauk, A.G. (1984) Sulfmyoglobin. Resonance Raman spectroscopic evidence for an iron-chlorin prosthetic group. *J. Biol. Chem*. 259, 15340-9.

Antommattei, F. M., Rosado-Ruiz T., Cadilla C. L., López-Garriga J. (1999). The cDNA-Derived Amino Acid Sequence of Hemoglobin I from *Lucina pectinata*, *J. Protein Chem*. 18, 831-836.

Berzofsky, J.A., Peisach, J., Blumberg, W.E. (1971) Sulfheme proteins. I. Optical and magnetic properties of sulfmyoglobin and its derivatives. *J. Biol. Chem.* 246, 3367-77.

Berzofsky, J.A., Peisach, J., Alben, J.O. (1972) Sulfheme proteins. 3. Carboxysulfmyoglobin : relation between electron withdrawal from iron and ligand binding. *J. Biol. Chem*. 247, 3774-82.

Berzofsky, J.A., Peisach, J., Horecker, B.L. (1972) Sulfheme proteins IV. Stoichiometry of sulfur incorporation and the isolation of sulfhemin, the prosthetic group of sulfmyoglobin. *J. Biol. Chem.* 247, 3783-91.

Brittain, T., Baker, A. R., Butler, C.S., Little, R.H., Lowe, D.J., Greenwood, C., Watmough, N.J. (1997). Reaction of variant sperm whale myoglobins with hydrogen peroxide: the effects of mutating a histidine residue in the haem distal pocket, *Biochem. J*., 326, 109-115.

Cerda J., Echevarría Y., Morales E., López-Garriga J. (1999). Resonance Raman studies of the heme-ligand active site of hemoglobin I from *Lucina pectinata*. *Biospectroscopy* 5, 289-301.

Chatfield, M.J., La Mar, G.N. (1992). ^{1}H nuclear magnetic resonance study of the prosthetic group in sulfhemoglobin. *Arch Biochem Biophys.* 295, 289-296.

Chatfield, M.J., La Mar, G.N., Smith, K.M., Leung, H.K., Pandey, R.K. (1988) Identification of the altered pyrrole in the isomeric sulfmyoglobins: hyperfine shift patterns as indicators of ring saturation in ferric chlorins. *Biochemistry.* 27, 1500-7.

Chatfield, M.J., La Mar, G.N., Kauten, R.J. (1987). Proton NMR characterization of isomeric sulfmyoglobins: preparation, interconversion, reactivity patterns, and structural features. *Biochemistry* 26, 6939-6950.

De Jesus, W.; Cortes, J, and López-Garriga J. (2001). Formation of Compounds I and Compound II Ferryl Species in the Reactions of Hemoglobin I from *Lucina pectinata* with Hydrogen Peroxide. *Arch. Biochem. Biophys*. 390, 304-308.

De Jesús, W., Cruz, A., Cerda, J., Bacelo, D., Cadilla, C., López-Garriga, J. (2006) Hydrogen bonding conformations of Tyrosine B10 tailor the hemeprotein reactivity of ferryl species. *J. Biol. Inorg. Chem.* 11(3):334-42.

De Jesus-Bonilla, W., Jia, Y., Alayash, A.I., and Lopez-Garriga, J. (2007) The Heme Pocket Geometry of *Lucina pectinata* Hemoglobin II Restricts Nitric Oxide and Peroxide Entry: Model of Ligand Control for the Design of a Stable Oxygen Carrier. *Biochemistry.* 46, 10451-60.

De Jesús, W., Ramírez, E., Cerda, J. López-Garriga, J. (2002). Evidence for a Nonhydrogen Bonded Compound II in the Cyclic Reaction of Hemoglobin I from *Lucina pectinata* with Hydrogen Peroxide. *Biopolymers (Biospectroscopy)* 62, 176-185.

Dominy, J.E., Stipanuk, M.H. (2004). New roles for cysteine and transsulfuration enzymes: production of H2S, a neuromodulator and smooth muscle relaxant. *Nutr Rev.* 62, 348-53.

Egawa, T., Shimada, H., Ishimura, Y. (2000). Formation of compound I in the reaction of native myoglobins with hydrogen peroxide," *J. Biol. Chem*., 275, 34858-34866.

Eto, K., Asada, T., Arima, K., Makifuchi, T, Kimura, H. (2002). Brain hydrogen sulfide is severely decreased in Alzheimer's disease. *Biochem. Biophys. Res. Commun*. 293, 1485-8.

Eto, K., Kimura, H. (2002). A novel enhancing mechanism for hydrogen sulfide-producing activity of cystathionine beta-synthase. *J. Biol. Chem*. 277, 42680-5

Evans S.V., Sishta, B.P., Mauk, A.G., Brayer, G.D. (1994) Three-dimensional structure of cyanomet-sulfmyoglobin C. *Proc. Natl. Acad. Sci.* U S A. 91, 4723-6.

Gavira, J.A., Camara-Artigas, A., De Jesus-Bonilla, W., Lopez-Garriga, J., Lewis, A., Pietri, R., Syun-Ru, Y., Cadilla, C.L., Garcia-Ruiz, J.M. (2008) Structure and Ligand Selection of Hemogobin II from *Lucina pectinata. J. Biol. Chem.* 283, 9414-23.

Guidotti, T.L. (1994). Occupational exposure to H_2S in the sour gas industry: some unresolved issues. *Int. Arch.Occup. Environ. Health.* 66, 153-160.

Hayes, L. C. (1999). Control of hydrogen sulfide emissions associated with wastewater treatment plants. *Practice Periodical of Hazardous, Toxic, and Radioactive Waste Management*. 3, 35-38.

Hershman, J.M., Berg, L. (1997) Pitfalls in Discriminating sulfhemoglobin and Methemoglobin. *Clin. Chem.* 43, 1098-9.

Hoppe-Seyler, F. (1862). Ueber das Verhalten des Blutfarbstoffs im Spectrum des Sonnenlichts. *Archiv für pathologische Anatomie und Physiologie und für klinische Medicin* 23, 446-449.

Hoppe-Seyler, F. (1863). Einwirkung des Schwefelwasserstoffgases auf das Blut. *Centralblatt für die medicinischen Wissenschaften* 28, 433.

Kashiba, M., Kajimura, M., Goda, N., Suematsu, M. (2002). From O_2 to H_2S: a landscape view of gas biology *Keio J Med*. 51, 1-10.

Kimura, H. (2002). Hydrogen sulfide as a neuromodulator. *Mol Neurobiol*. 26, 13-9.
Kitagawa, M., T. Ochi and S. Tanaka. (1998). Study on hydrogen sulfide generation rate pressure mains. *Wat. Sci. Tech*. 37, 77-85.

Kraus, D.W. and Wittenberg, J.B. (1990). Hemoglobins of the *Lucina pectinata*/Bacteria Symbiosis I. *J. Biol. Chem*. 265, 16043-16053.

Kraus, D.W.,Wittenberg, J. B., Jing-Fen, L. Peisach, J. (1990). Hemoglobins of the *Lucina pectinata* Bacteria Symbiosis II. *J. Biol. Chem*. 265, 16054-16059.

Krishnakumar, R., La Mar, G.N., Chiu, M.L., Sligar, S.G., Singh, J.P., Smith, K.M. (1991) ^{1}H NMR hyperfine shift pattern as a probe for ligation state in high-spin ferric hemoproteins: water binding in metmyoglobin mutants. *J. Am. Chem. Soc.* 113, 7886-92.

La Mar, G.N., de Ropp, J.S., Latos-Grazynski, L., Balch, A.L., Johnson, R.B., Smith, K.M., Parish, D.W., Cheng, R. (1983) Proton NMR characterization of the ferryl group in model heme Complexes and hemoproteins: Evidence for the FeIV=O group in ferryl myoglobin and compound II of horseradish peroxidase. *J. Am. Chem. Soc.* 105, 782-7.

La Mar, G.N., Satterlee, J.D., De Ropp, J.S. (2000) Nuclear magnetic resonance of hemoproteins. *The Porphyrin Handbook*. 5, 185-298.

Leon R., Munier, H., Barzu O., Baudin., V., Pietri R., Lopez-Garriga J., Cadilla C. L. (2004). High-level production of recombinant sulfide-reactive hemoglobin I from *Lucina pectinata* in *Escherichia coli*: High yields of fully functional holoprotein synthesis in the BLi5 E. coli strain. *Protein Expr. Purif.* 38, 184-195.

Lewis A., Arbelo H., Pietri R., Li D., Leon R.G., López-Garriga J., Yeh S.R., Cadilla C. (2006) Conformational changes in hemoglobin I from *Lucina pectinata*: Probe for the flexibility in the heme-ligand moiety. *J. Biol. Chem.* (manuscript in preparation).

Magliozzo, R.S., Peisach, J.A. (1986). Proton nuclear magnetic resonance study of sulfmyoglobin cyanide. *Biochim Biophys Acta*. 872, 158-62.

Matsui, T., Ozaki. S., Liong, E., Phillips Jr., G.N. Watanabe, Y. (1999). Effects of the location of distal histidine in the reaction of myoglobin with hydrogen peroxide. *J. Biol. Chem*., 274, 2838-2844 (1999).

Matsui, T., Ozaki. S., Watanabe, Y. (1997). On the formation and reactivity of compound I of the His-64 myoglobin mutants, *J. Biol. Chem*., 272, 32735-32738.

Michel, H.O. (1938). A study of Sulfhemoglobin. *J. Biol. Chem.* 126, 323-348.

Navarro A.M., Maldonado M., González-Lagoa J., López-Mejía R., López-Garriga J., Colón J.L. (1996). Control of carbon monoxide binding status and dynamics in hemoglobin I of *Lucina pectinata* by nearby aromatic residues. *Inorganica Chimica Acta* 243, 161-166.

Nagababu, E., and Rifkin, J.M. (2000). Reaction of hydrogen peroxide with ferrylhemoglobin: Superoxide production and heme degradation. *Biochemistry*, 39, 12503-12511.

Pietri, R., Leon, R.G., Kiger, L., Marden, M.C., Granell, L.B., Cadilla, C.L., Lopez-Garriga, J. (2006) Hemoglobin I from *Lucina pectinata*: A model for distal heme-ligand control. *Bioch. et Bioph. Acta*. 1764, 758-65.

Parker, W.O. Jr., Chatfield, M.J., La Mar, G.N. (1989). Determination of the chirality of the saturated pyrrole in sulfmyoglobin using the nuclear Overhauser effect. *Biochemistry.* 28, 1517-1525

Rajarathman, K., La Mar, G.N., Chiu, M.L., Sligar, J.P., Smith, K.M. (1991). 1H NMR Hyperfine Shift Pattern as a Probe for Ligation State in High-Spin Ferric Hemoproteins: Water Binding in Metmyoglobin Mutants. *J. Am. Chem. Soc.*113, 7886-92.

Rizzi, M.,Wittenberg, J. B., Coda, A., Fasno, M., Ascenzi, P. Bolognesi, M. (1996). Structural Base for Sulfide Recognition in *Lucina pectinata* Hemoglobin I. *J. Mol. Biol*. 258, 1-5.

Rizzi, M., Wittenberg, J. B.; Coda, A. Fasno, M.; Ascenzi, P. Bolognesi, M. (1994). Structure of the Sulfide-reactive Hemoglobin from the Clam Lucina pectinata. *J. Mol. Biol.* 244, 86-99.

Rosado T., Antommattei F., Cadilla C.L., López-Garriga J. (2001). Expression and Purification of Recombinant Hemoglobin I from *Lucina pectinata*. *J. Protein. Chem*. 20, 311-31.

Silfa, E., Almeida, M., Cerda, J., Wu, S., Lopez-Garriga, J. (1998) Orientation of the Heme Vinyl Groups in the Hydrogen Sulfide-Binding Hemoglobin I from *Lucina pectinata*. *Biospectroscopy.* 4, 311-26.

Tangerman, A., Bongaerts, G., Agbeko, R., Semmekrot, B., Severijnen, R. (2002). The origin of hydrogen sulfide in a newborn with sulfhaemoglobin induced cyanosis. *J. Clin. Pathol*. 55, 631-3.

Wu, C., Kenny, M.A.. (1997) A case of sulfhemoglobinemia and emergency measurement of sulfhemoglobin with as OSM3 CO-oximeter. *Clin. Chem*. 43, 162-6.